3 Ecological studies on permafrost soils and landscapes of the central Lena Delta

Dirk Wagner, Lars Kutzbach, Christian Wille, Svenja Kobabe, Oliver Spott, Anna Kurchatova, Mikhail N. Grigoriev, Günther Stoof, Waldemar Schneider, Ekatarina N. Abramova, Hanno Meyer, Svetlana Kuzmina, Sebastian Wetterich, Dmitry Bolshiyanov, Irina Fedórova, Mikhail Tretiakov and Eva-Maria Pfeiffer

Wet tundra environments of the Arctic influence the global climate by the release of methane and other radiatively active trace gases into the atmosphere. Methane contributes to the enhanced greenhouse effect with a portion of approx. 20 % (Wuebbles and Hayhoe, 2002). The world-wide wetland area has a size of about 5.5 x 10^6 km^2 (Aselman and Crutzen, 1989), about half of it is located in high-latitudes of the northern hemisphere (> 50°N). The atmospheric input of methane from tundra soils of this region has been estimated between 20-40 Tg CH_4 yr^{-1} (Christensen et al. 1996), corresponding to about 25 % of the methane emission from natural sources (Fung et al. 1991). However, the strength of tundra environments as a methane source and the sensitivity of permafrost to potential changes in climate are still uncertain.

Approximately 14 % of the global carbon are stored in permafrost soils and sediments (Post et al., 1982). Due to this carbon pool, tundra environments play a major role in the global carbon cycle, even more since current climate models predict significant changes in temperature and precipitation patterns in these regions (Hansen et al., 1988; Kattenberg et al., 1996).

The interdisciplinary soil and microbiological studies are focused on the seasonal variability of the modern carbon fluxes (CH_4, CO_2), the quantification of microbial processes as well as the thermal and hydrological dynamics of permafrost affected soils of the Lena Delta.

During the fifth Lena Delta Expedition the investigations of the methane and carbon dioxide emission from different polygonal tundra sites and tundra lakes could be continued by closed chamber measurements. Furthermore, fluxes of methane, carbon dioxide, water vapour, sensible heat and momentum was analysed on the ecosystem scale by eddy covariance measurements for the first time. The microbial methane production and oxidation of permafrost soils was studied by additional field experiments. For further microbial ecological studies permafrost sediments of late Pleistocene age were drilled and transported in frozen conditions to Germany.

In addition to the investigation of the carbon dynamic, which pertain to an ongoing long-term study of trace gas fluxes from permafrost soils, research to the following topics were carried out during the expedition 2002: recent cryogenesis, botanical diversity, recent insects and freshwater ostracodes, paleo-climate and the hydrology of the central delta.

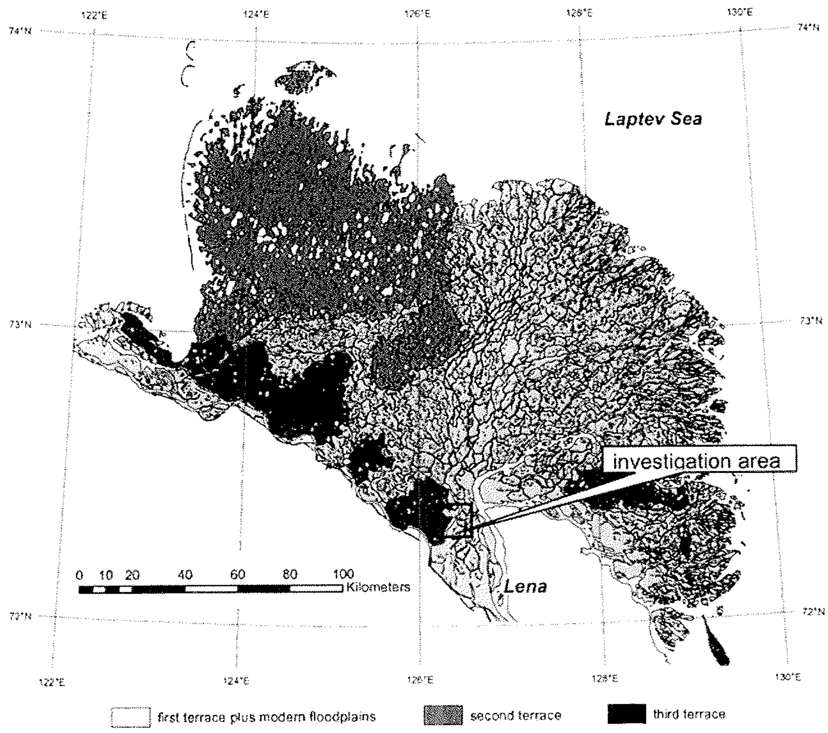

Figure 3-1. Map of the Lena Delta with location of the investigation area Samoylov / Kurungnakh. Geomorphological units are according to Grigoriev (1993).

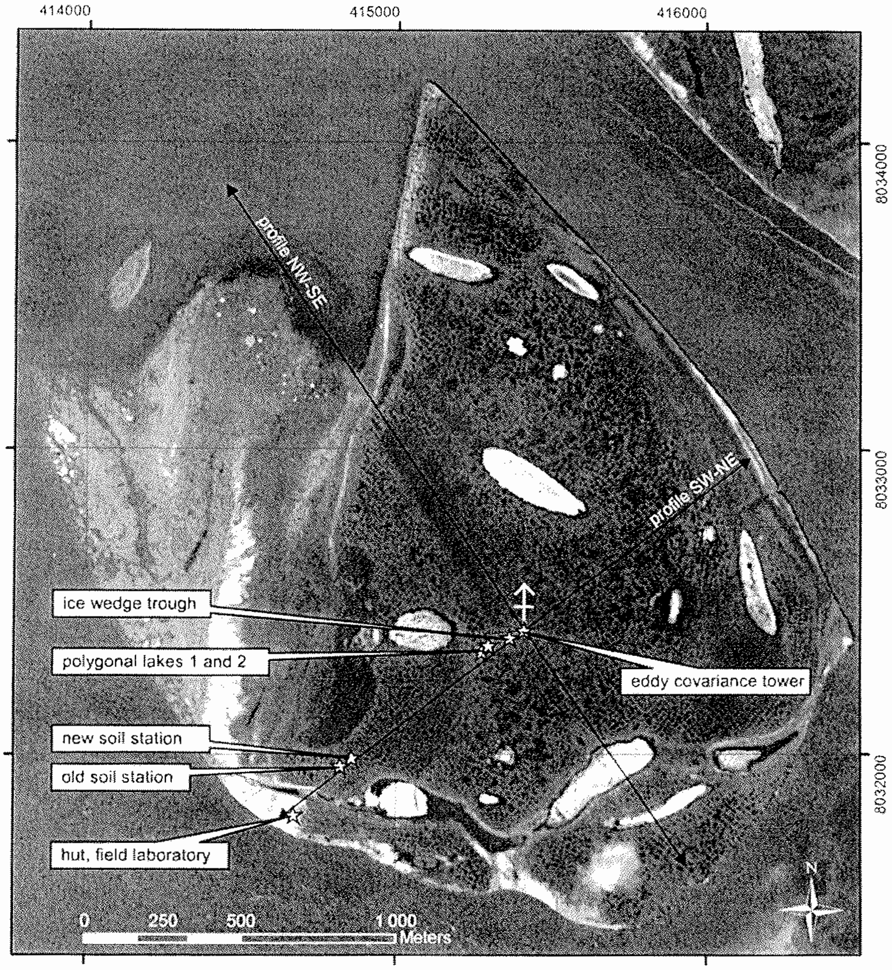

Figure 3-2. Site map Samoylov Island. – Positions of investigation sites, instruments, and geodetic elevation profiles. Coordinate system: UTM Zone 52N, WGS84. Satellite image: CORONA June 22, 1964.

3.1 Heat, water and carbon exchange between arctic tundra and the atmospheric boundary layer – the eddy covariance method

Lars Kutzbach, Christian Wille and Eva-Maria Pfeiffer

3.1.1 Introduction

An eddy covariance measurement system (ECS) was installed in June 2002 on Samoylov Island. The ECS was designed to determine simultaneously the turbulent fluxes of CH_4, CO_2, H_2O, sensible heat, and momentum that are representative on the ecosystem scale. The advantages of the eddy covariance technique are:

(1) It inherently averages the small-scale variability of fluxes over a surface area that increases with measurement height (ha to km^2, ecosystem scale).

(2) Measurements are continuous and in high temporal resolution (intervals of 15 to 30 min).

(3) Fluxes are determined without disturbing the surface being monitored.

(4) Fluxes of carbon, energy, and water are measured parallelly, by the same method, and in the same scale. Thus, a good basis for analysing interactions between the individual fluxes is provided.

Almost all vertical transport of air constituents in the atmospheric boundary layer happens by turbulence. The micrometeorological eddy covariance technique analyses the properties of turbulent moving air parcels - the eddies- to determine the vertical fluxes of air constituents, such as energy, water vapour, CO_2, or CH_4. The eddy flux F_c of any scalar quantity c is computed as the covariance of the density of the scalar quantity ρ_c and the vertical wind velocity w.

$$F_c = \overline{w' \rho_c'}$$

The primes indicate the fluctuation about the mean value, and the overbar represents the mean of the product over a sampling interval.

The spatially extended eddies are leaded past a stationary sensor by the mean horizontal wind u_{mean}. Thus, measurements at one point in space over a time period provide a spatially-integrated flux value, that is representative for a specific footprint area depending on sensor height and micrometeorological conditions.

Because the eddy covariance technique considers the very small fluctuations about the mean, it requires a high resolution of sensors (0.5 % of mean). To resolve the important small-scaled eddies adequately, the frequency response of the ECS has to be high (10 Hz).

3.1.2 Experimental set-up

The ECS tower was established in the centre of the terrace plain in the east part of Samoylov Island at 72°22.44' N, 126°29,80' E (UTM: Zone 52 415417E 8032409N, Figure 3-2). The Holocene river terrace is characterised by wet polygonal tundra with very poor drainage. The macrorelief of the terrace is level with slope gradients less than 0.2 % (Figure 3-3). Only at scarps along ancient river channels, abrupt elevation differences of up to 2.5 m are present. The surface of the terrace is structured by a regular microrelief with elevation differences of about 0.5 m (Figure 3-5), which is caused by the genesis of low-centred ice wedge polygons. The fetch of polygonal tundra, which is considered a homogenous landscape, extended at least 870 m in all directions from the tower, except for the sector from southwest to west. With a typical wind speed for the region of 5 m s^{-1}, more than 90 % of the measured flux originated within this footprint area.

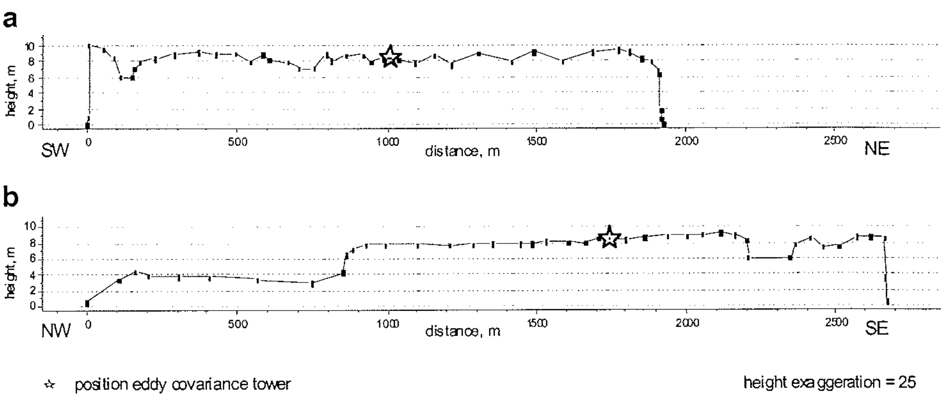

Figure 3-3. Relief of the island Samoylov and position of the eddy covariance tower. – a elevation profile from south-west to north-east, b elevation profile from north-west to south-east. Positions of profiles are shown in Figure 3-2.

To minimise perturbation, instruments were set up in a line to the southwest (Figure 3-4), which is the least frequent wind direction. Data gathered during periods with winds from southwest to west will be excluded from the flux analyses.

Parallelly to the ECS measurements, barometric pressure, air temperature, air humidity, radiation, and soil temperature (at two sites in a polygon adjacent to the ECS tower) were recorded automatically. Complementary meteorological data was provided by the automatic meteorological station on Samoylov Island (see Chapter 3.2).

In addition to the automatic measurements, active layer depth, water level depth, soil moisture, and soil temperature profiles were measured manually in intervals of 1 to 3 days at a transect of 14 soil survey sites. At three of these sites (S1, S2, S7), CH_4 emission was determined daily by a closed-chamber technique for comparison between methods. For characterisation of the vegetation at the investigation site, the species composition was studied at 5 vegetation survey sites. The spatial arrangement of instruments, soil and vegetation survey sites, and elevation profiles is shown in Figure 3-4. A short characterisation of soil survey sites is given in Table 3-2.

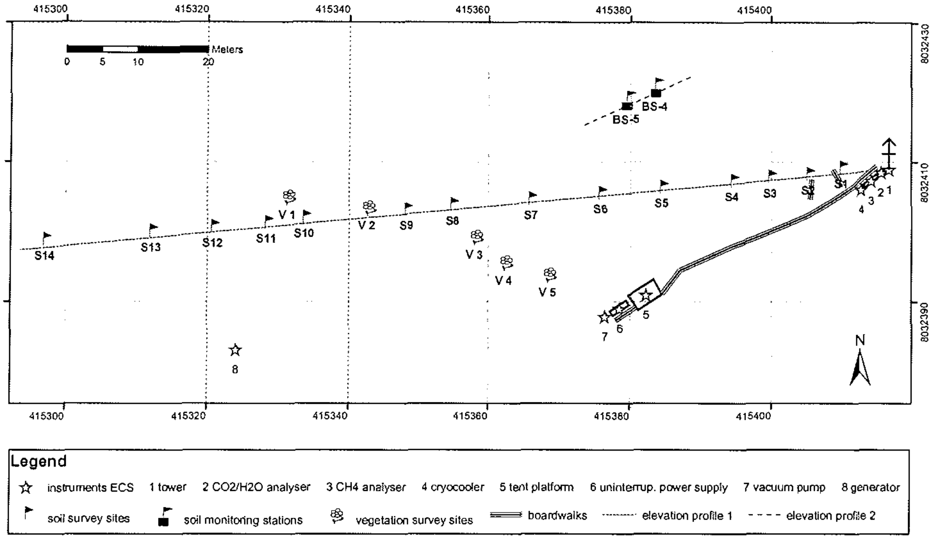

Figure 3-4. Site map eddy covariance measurement system. – Positions of instruments, soil survey sites, soil monitoring stations, vegetation survey sites, and elevation profiles. Coordinate system: UTM Zone 52N, WGS84.

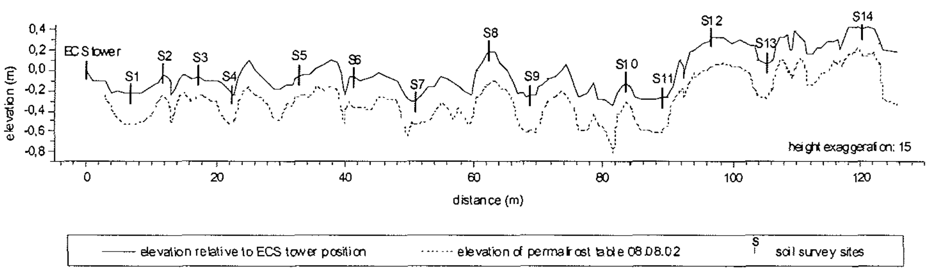

Figure 3-5. Elevation profile 1 with positions of soil survey sites S1 to S14. – The straight line indicates the soil surface, the dashed line indicates the permafrost table. Distances and elevations are measured relative to the soil surface position at the ECS tower.

The ECS was composed of commercially available instruments assembled according to our objectives (Fig. 3-6, Fig. 3-7). The technical set-up included a three-axis sonic anemometer, an infrared CO_2/H_2O analyser, and a CH_4 analyser based on tuneable laser infrared spectroscopy. Both gas analysers were closed-path instruments and were arranged in series in the sample gas line. Accuracy of concentration measurements was 20 ppm for H_2O, 0.3 ppm for CO_2, and 0.007 ppm for CH_4. The anemometer and the sample air intake were mounted on a 3.6 m high tower while the gas analysers were installed at the base of the tower. Sample air was drawn through the system by a vacuum pump with a flow rate of 19 slpm. Various filters and needle valves provided a pressure drop inside the system. Pressure was 820...850 hPa inside the CO_2/H_2O analyser and 75 hPa inside the CH_4 analyser. All signals were digitised at 10 Hz by the anemometer. Data were logged and processed by the software EdiSol running on a portable PC. Autonomous and continuous operation was ensured by a generator and an uninterruptible power supply. Further information on instruments is given in Table 3-1.

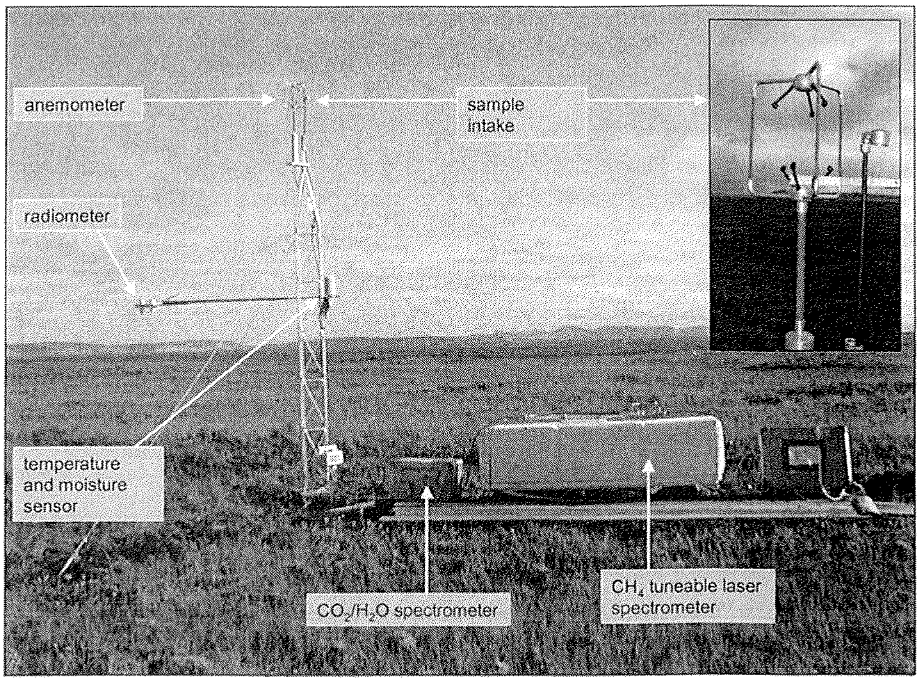

Figure 3-6. Photograph of the ECS in the field.

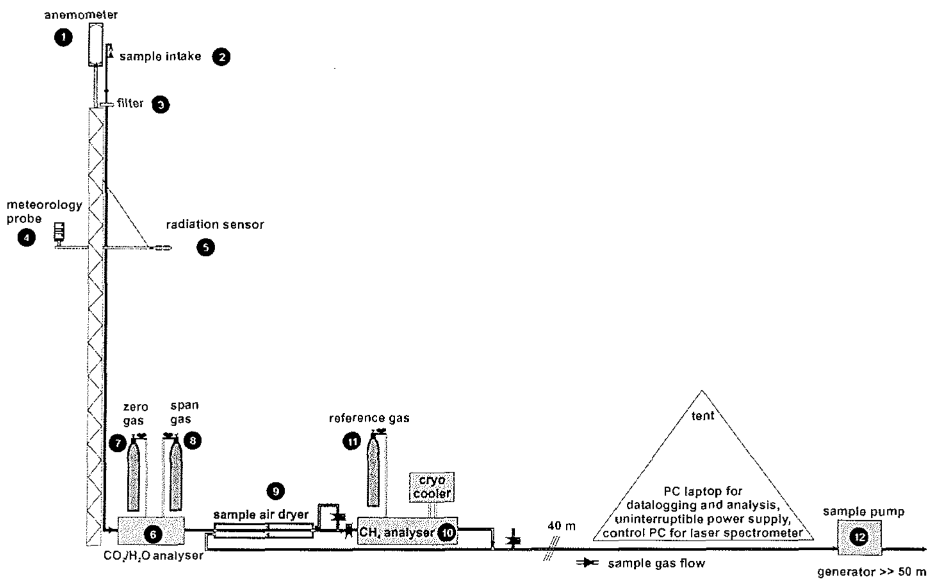

Figure 3-7. Technical set-up of the ECS.

Table 3-1. Components of ECS and related measurements. – Positions 1-12 are numbered according to Figure 3-7. Positions 13 and 14: sensors used for automatic measurements; positions 15 and 16: instruments used for manual measurements.

Pos.	Sensor Type
1	Gill Instruments Ltd., Ultrasonic anemometer 1210 R3
2	PE tubing 3/8" OD 1/4" ID
3	Schleicher & Schuell, Membranfilter 1µm TE 37
4	Rotronic Meßgeräte GmbH, Meteorological probe for humidity and temperature MP103A
5	Kipp & Zonen B.V., Net radiometer CNR 1
6	LI-COR LI-7000, Differential infrared CO_2/H_2O analyzer
7	Zero gas: pure N_2
8	Span gas: 480ppm CO_2 in N_2
9	Perma Pure Inc., Gas dryer PD-200T-48 SS
10	Campbell Scientific Inc., Tunable diode laser CH_4 analyzer TGA100
11	Reference gas: 0.5% CH_4 in N_2
12	Busch Inc., Rotary vacuum pump RB0021
13	Druck Messtechnik GmbH, Barometric pressure sensor RPT 410
14	Campbell Scientific Ltd., Thermistor soil temperature probe 107
15	UIT GmbH Dresden, Soil temperature probe ET, Pt 1000
16	Delta-T Devices Ltd., Moisture meter HH2, soil moisture probe ML2, profile soil moisture probe PR1

Table 3-2. Characterisation of soil survey sites adjacent to the ECS.

ID	soil material	soil type	situation in microrelief
S1	complete profile peat	*Typic Fibristel*	polygon centre, wet, swampy
S2	0...11 cm peat; 11...16 cm Sl3; 16...28 cm Slu	*Typic Aquiturbel*	polygon rim, relatively flat, not much elevated
S3	0...6 cm peat; 6...13 cm Sl3; 13...25 cm Slu	*Typic Aquiturbel*	polygon centre, degraded polygon, moist
S4	complete profile peat	*Typic Glacistel*	polygon crack, swampy, vegetated, about 0.6m wide
S5	0...11 cm peat; 11...26 cm Slu	*Typic Aquiturbel*	polygon rim, flat, polygon strongly degraded, drained
S6	0...9 cm peat; 9...15 cm Sl3; 15...36 cm Slu...Lu	*Typic Aquiturbel*	slope of raised polygon rim, direction crack
S7	complete profile peat	*Typic Glacistel*	polygon crack, 1m wide, swampy, vegetated
S8	0..6 cm peat; 6...19 cm Slu; 19...41 cm Lu	*Typic Aquiturbel*	polygon rim, strongly raised, dry
S9	complete profile peat	*Typic Fibristel*	polygon centre, wet, swampy
S10	0...11 cm peat; 11...25 cm Slu	*Typic Aquiturbel*	polygon rim, relatively flat, not much raised
S11	complete profile peat	*Typic Fibristel*	polygon centre, wet, swampy
S12	0...7 cm peat; 7...15 cm Slu; 15...35 cm Lu	*Typic Aquiturbel*	polygon rim, strongly raised
S13	complete profile peat	*Typic Fibristel*	polygon centre, wet, swampy
S14	0...5 cm peat; 5...14 cm Sl3; 14...23 cm Lu; 23...30 cm Lu	*Typic Aquiturbel*	polygon rim, strongly raised, dry

3.1.3 First Results

Some exemplary datasets of the eddy covariance flux calculations and the supporting soil and meteorological measurements are shown in Figure 3-9 and Figure 3-8, respectively.

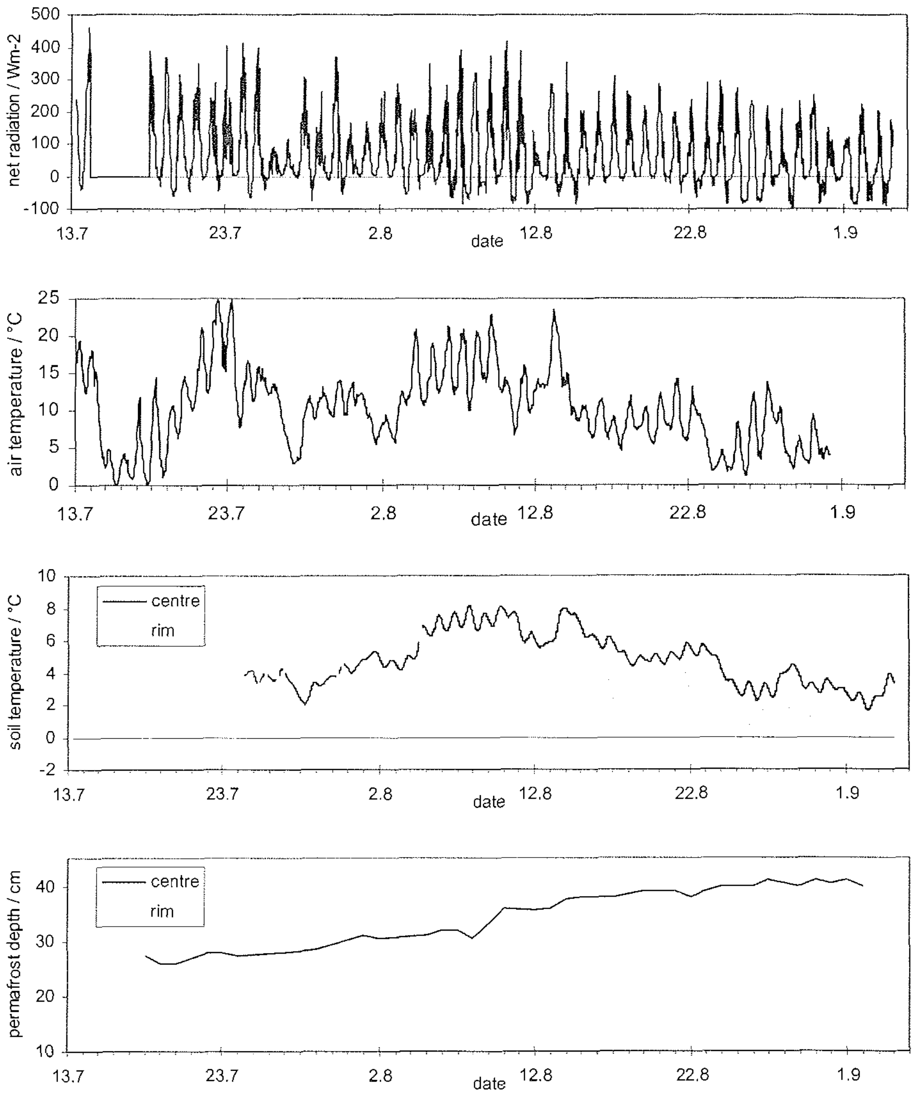

Figure 3-8. Results of ECS supporting measurements. – From top to bottom: net radiation, air temperature 0.5 m above ground (data from meteorological station), soil temperature at 10 cm below surface and depth of the permafrost table. Soil temperature and permafrost depth were measured in the centre and the rim of a polygon adjacent to the ECS tower.

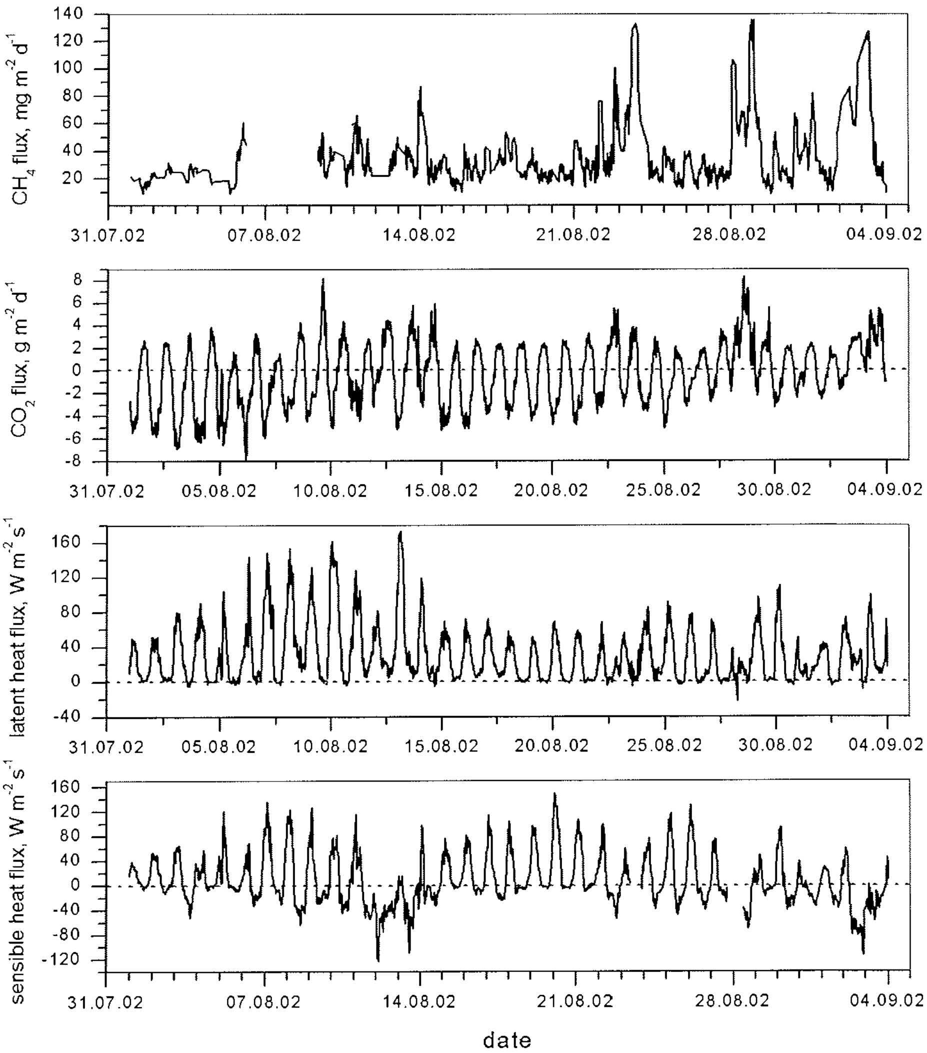

Figure 3-9. Preliminary calculations of eddy covariance fluxes August 2002. – From top to bottom: fluxes of methane, carbon dioxide, latent heat, sensible heat.

3.1.4 Perspectives

The presented measurement campaign will make available the first data of ecosystem-representative CH_4 and CO_2 fluxes for permafrost landscapes of the Siberian Arctic. The experimental set-up provides data sets that allow the coupling of the water and energy budget of permafrost soils with the carbon exchange processes between permafrost soils, tundra vegetation, and the atmospheric boundary layer. This kind of data is necessary for the improvement of soil-vegetation-atmosphere models able to assess the impact of climatic change on arctic ecosystems.

Based on the experiences made during these expeditions, the option of using the ECS during further campaigns in cooperation with other working groups will be evaluated. Due to its rugged and autonomous design, the ECS can be used in remote areas and under severe climatic conditions. Most interesting would be the installation on aircrafts or research vessels to investigate spatial variability of trace gas fluxes on the large scale.

3.2 Energy and water budget of permafrost soils – long time soil survey station on Samoylov Island

Christian Wille, Svenja Kobabe and Lars Kutzbach

3.2.1 Survey station 1998...2002

The automatic soil and meteorology measurement station on Samoylov Island was installed in July of 1998. It was situated in direct vicinity to the emission measurement site on the first terrace about 150 meters northeast of the Lena Delta reserve station building. The data recorded by the measurement station are as shown Table 3-3.

Table. 3-3. Data and sensors of Samoylov measurement station 1998...2002.

Pos.	Data Measured	Sensor Type
1	Air Temperature and Relative Humidity	Rotronic Meßgeräte GmbH Meteorological Probe for Humidity and Temperature MP340
2	Wind Speed & Direction	R M Young Company Anemometer 05103
3	Net Radiation	Kipp & Zonen B.V. Net Radiometer NR-Lite
4	Precipitation (liquid, i.e. Rain)	R M Young Company Tipping Bucket Rain Gauge 52203
5	Snow Height	Campbell Scientific Ltd. Sonic Ranging Sensor SR 50
6	Soil Temperature	Campbell Scientific Ltd. Thermistor Soil Temperature Probe 107
7	Soil Bulk Electrical Conductivity	Campbell Scientific Ltd. TDR Soil Moisture System
8	Soil Volumetric Water Content	Campbell Scientific Ltd. TDR Soil Moisture System
9	Heat Flux out of / into Soil	Hukseflux Thermal Sensors Heat Flux Sensor HFP01SC

Measurements of air temperature and relative humidity were made at 0.5 and 2.0 meters above ground. The measurement of soil bulk electrical conductivity and soil water content were made by time domain reflectometry (TDR). Soil temperature and TDR measurements were carried out along two vertical profiles in the polygon centre and the polygon rim respectively. Soil heat flux was recorded at two different depths in the polygon rim.

Due to technical problems there exist several gaps in the data. Table 3-4 shows the time periods during which data was collected by the station. As an example, Figure 3-10 shows a one year period of soil temperature data collected at the polygon rim site together with air temperature (0.5 m above ground) data from the same time period.

Table 3-4. Existing data series 1998...2002.

Data	Existing Data Series
Meteorological Data (Pos. 1-4 of Table 3-3)	28.07.98...10.05.00 17.08.00...20.10.00 18.03.01...25.08.02
Soil Data (Pos. 5-9 of Table 3-3)	30.07.98...18.12.99 06.02.00...25.05.00 25.07.00...12.11.00 14.02.01...05.06.01 22.07.01...25.08.02

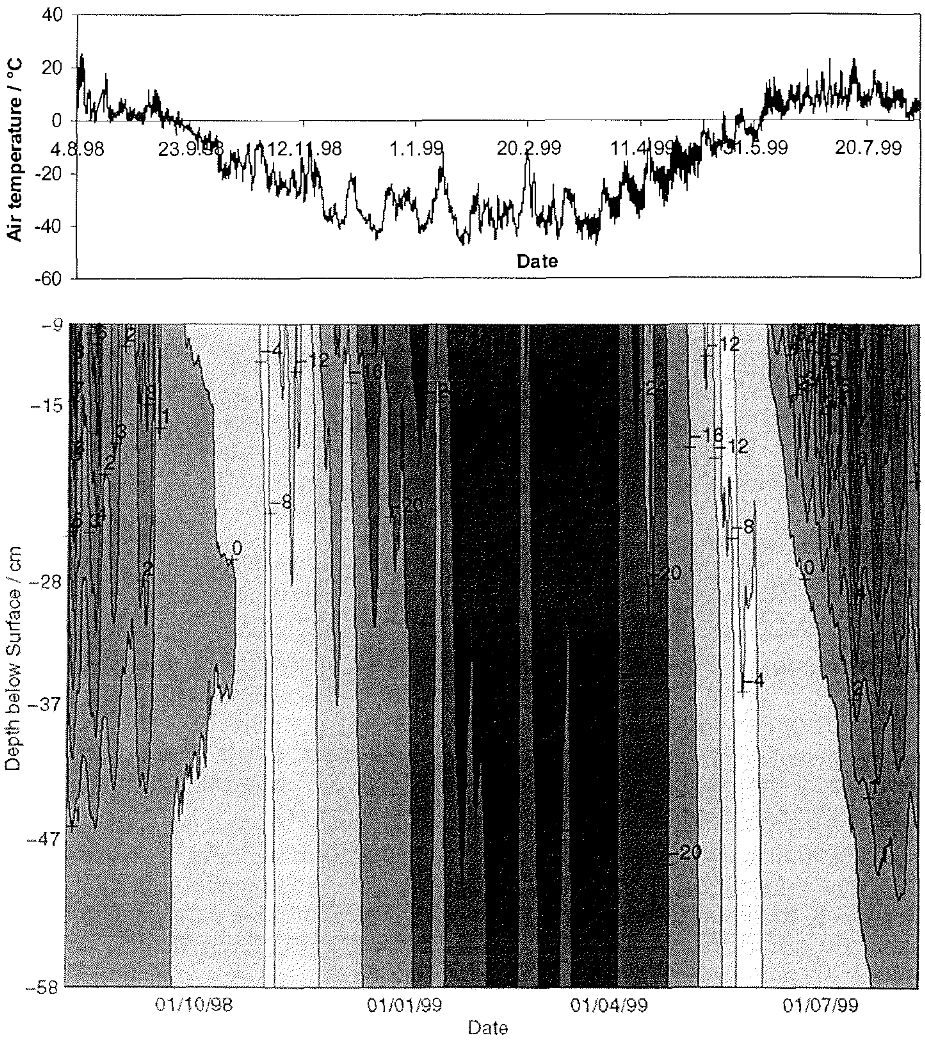

Figure 3-10. Air temperature at 0.5 m above ground (top) and Soil temperature profile from polygon rim (bottom) during period 04.08.98...12.08.99. Depth labels in soil temperature chart indicate position of sensors.

3.2.2 New long time survey station

During the Lena 2002 expedition two new measurement stations were set up on Samoylov Island. The first station which serves as the new permanent meteorology and soil survey station is situated about 30 m northeast of the old measurement site as shown in Figure 3-11. The station was put in operation in August of 2002.

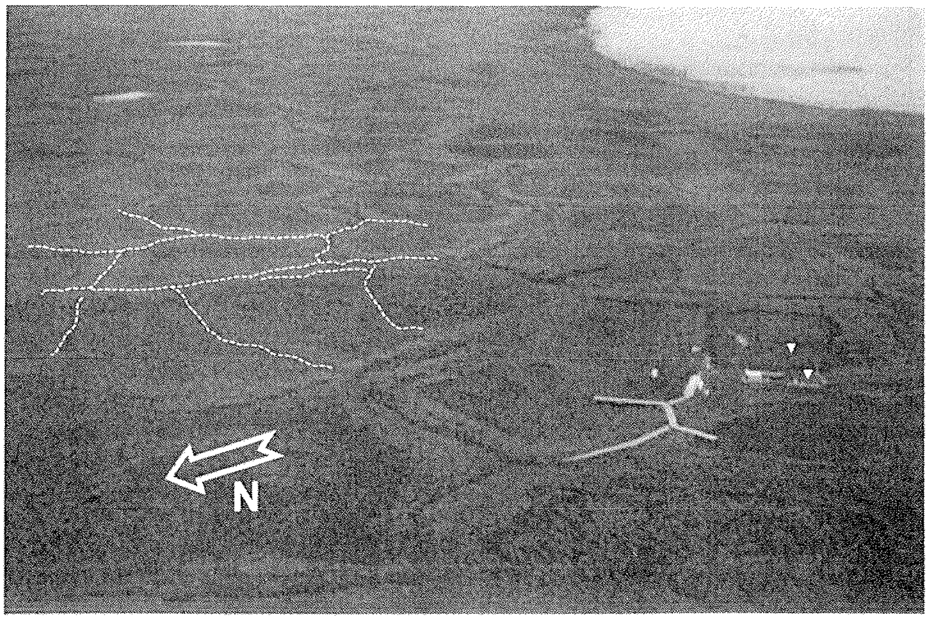

Figure 3-11. Arial view of the old measurement station in 2001. The white triangles indicate the position of the old soil measurement profiles. The dashed line encircles the polygon in which the new soil profiles were installed.

For the new measurement station 3 profile pits were dug through the active layer and into the permafrost at the summit and the slope of the elevated polygon rim (BS-1, BS-2) and in the depressed centre (BS-3) of the designated polygon. Figure 3-12 shows a 3D-model of the polygon and the position of the profiles.

Soils were described and classified according to *Soil Taxonomy* (USDA1998, 8^{th} edition) and the German field book for describing soils *Bodenkundliche Kartieranleitung* (AG Boden 1994, 4^{th} edition). Additionally, soils were classified according to the *World Reference Base for Soil Resources* (FAO 1998) and the Russian system of Elovskaya (1987). The soil descriptions are given in Tables 3-5...3-7. Three different sample types were collected from each horizon: moist and deep frozen samples for microbiological analyses, air-dried bulk samples to investigate soil chemistry, and undisturbed soil density cores to analyze soil physics. A complete sample list is provided in Appendix 3-1.

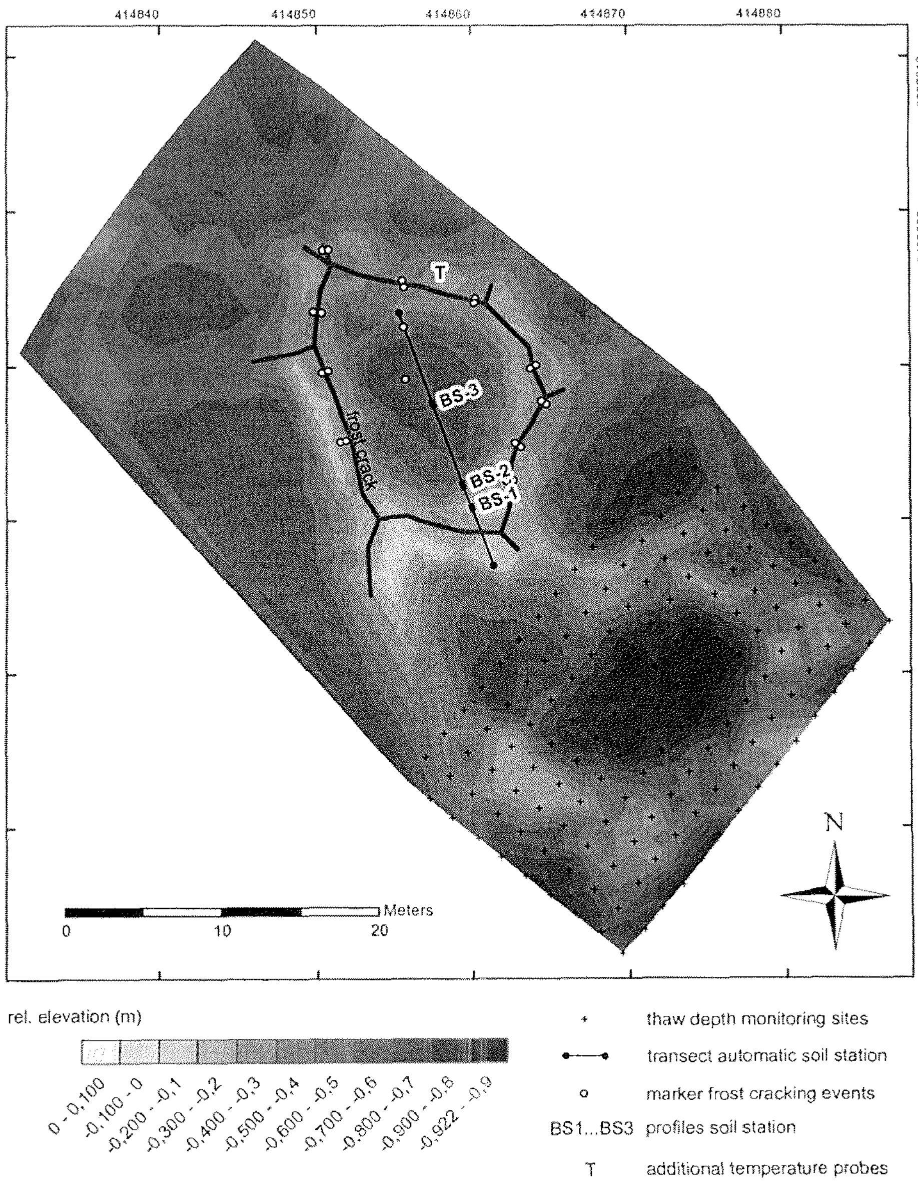

Figure 3-12. Site map new longtime soil survey station. – Positions of thaw depth monitoring sites (manual measurements), polygon transect (see Figure 3-13), markers for frost cracking events, soil profiles BS-1...BS-3, and additional temperature probes. The 3D-model is based on a triangulated irregular network (TIN; 482 measuring points). Elevation values are measured relatively to the heighest point. Coordinate system: UTM Zone 52N, WGS84.

Table 3-5. Description of soil profile BS-1 (summit of polygon rim).

profile ID: **LD02-BS-1** location: Samoylov, Lena-Delta date: 16.08.02
altitude a.s.l.: 12.0 m UTM: Zone 52, 414860E, 8031981N

relief situation: 1. main delta terrace, summit of elevated polygon rim
substrate: fluviatile (+aeolian) stratified sands and loams, peat layers

profile depth: 100 cm permafrost depth: 40 cm water level depth: --

vegetation: mosses total 95%, height 1...2 cm, *Hylocomium splendens* 90%; lichens 1%; vascular plants total 25%, height 20 cm, *Carex aquatilis* 15%, *Dryas octopetala* 4%, *Astragalus frigidus* 3%, *Hedysarum hedysaroides* 3%, *Lagotis glauca* r, *Valeriana capitata* r, *Saxifraga punctata* r

depth (cm)	horizon[1] (cm)	sample ID LD02-	properties
0...3	Oi	6983	organic material, slightly decomposed moss fibers, >30% org. matter, few fine roots, 7.5YR2/2, inclusions of aeolian sand
3...7	Ajj1	6984	loamy sand, granular to single grain, 2...4% org. matter, many fine roots, 10YR3/2
7...15	Ajj2	6985	sandy loam, subangular blocky to coherent, 2...4% org. matter, many fine roots, 10YR3/2
15...23	Bjjg1	6986	sandy loam, granular to coherent (compressed), 2...4% org. matter, common fine roots, very many dead fine roots (fossil A horizon), 2.5YR4/1, irregular band of redoximorphic concretions: 30...40% (7.5YR4/4)
23...29	Bjjg2	6987	silt loam, platy to coherent, stratified, peat layers, 4...8% org. matter, common fine roots, 2.5Y4/2, peat: root residues, sedge leave sheaths, wood
29...34	Bjjg3	6988	sand, coherent, <1% org. matter, very few fine roots, 2.5Y4/2, α,α-dipyridyl reaction positive
34...40	Bjjg4	6989	sandy loam/silt loam, coherent, stratified, peat layers, 8...15% org. matter. no roots, 10YR2/2, α,α-dipyridyl reaction positive
40...55	Bjjgf1	6990	permafrost, alternating peat and sediment layers, peat layers narrow (<0.5cm), horizontal ice veins, high ice content in peat layers
55...65	Bjjgf2	6991	similar to Bjjgf1
65...100	Bjjgf3	6992	similar to Bjjgf1

remarks: sediments stratified; wavy to irregular horizon boundaries: cryoturbation

Soil Taxonomy: **Typic Aquiturbel**
World Reference Base for Soil Resources: **Gleyi-Turbic Cryosol (Fluvic)**
Russian Classification (Elovskaya): **Permafrost Turfness Gley**

1) symbols according to Soil Taxonomy 8th edition (USDA 1998)

Table 3-6. Description of soil profile BS-2 (slope of polygon rim).

profile ID: **LD02-BS-2** location: Samoylov, Lena-Delta date: 20.08.02
altitude a.s.l.: 11.8 m UTM: Zone 52, 414859E, 8031982N

relief situation: 1. main delta terrace, slope of elevated polygon rim
substrate: shallow moss and sedge peat above fluviatile stratified sands and loams, peat layers

profile depth: 50 cm permafrost depth: 17 cm water level depth: --

vegetation: mosses total 98%, height 3...4 cm, Hylocomium splendens 80%; vascular plants total 20% height 25 cm, *Carex aquatilis* 10%, *Salix glauca* 10%, *Dryas octopetala* r, *Pyrola secunda* r, *Polygonum viviparum* r

depth (cm)	horizon[1] (cm)	sample ID LD02-	Properties
0...10	Oi1	7002	organic material, peat, slightly decomposed moss fibers, >30% org. matter, many fine roots, 10YR2/3, inclusions of aeolian sands
10...17	Oi2	7003	organic material, peat, slightly decomposed moss fibers, >30% org. matter, many fine roots, 10YR1.7/1, inclusions of aeolian sands, common *Carex* rhizomes and coarse roots of *Salix*
17...25	Bjjgf1	7004	permafrost, sand, 2...4% org. matter, 10YR3/1, sand layers alternating with slightly decomposed peat layers; at 25cm fossil root horizon; in peat layers high ice content; at 18cm: horizontal crack 0.5...1cm wide, α,α-dipyridyl reaction positive
25...50	Bjjgf2	7005	permafrost, loamy sand, 2...4% org. matter, 10YR2/2, sand layers alternating with very narrow peat layers, along peat layers thin ice layers

remarks: sediments stratified; wavy horizon boundaries: cryoturbation

Soil Taxonomy: Typic Aquiturbel
World Reference Base for Soil Resources: **Turbi-Histic Cryosol (GleyicFluvic)**
Russian Classification (Elovskaya): **Permafrost Peatish Gley**

1) symbols according to Soil Taxonomy 8th edition (USDA 1998)

Table 3-7. Description of soil profile BS-3 (polygon centre).

profile ID: **LD02-BS-3** location: Samoylov, Lena-Delta date: 20.08.02
altitude a.s.l.: 11.5 m UTM: Zone 52, 414853E, 8031988N

relief situation: 1. main delta terrace, depressed centre of polygon
substrate: moss and sedge peat above fluviatile sands

profile depth: 50 cm permafrost depth: 34 cm water level depth: 6 cm

vegetation: mosses total 95%, height 1...5 cm; vascular plants total 40%, height 30 cm, *Carex aquatilis* 40%, *Saxifraga cernua* r, *Caltha palustris* r, *Pedicularis sudetica* r

depth (cm)	horizon[1] (cm)	sample ID LD02-	Properties
0...15	Oi1	7007	organic material, peat, slightly decomposed moss and sedge fibers, >30% org. matter, very many fine roots, 10YR2/3, common *Carex* rhizomes
15...34	Oi2	7008	organic material, peat, slightly decomposed moss and sedge fibers, >30% org. matter, many fine roots, 2.5Y4/4, inclusions of sand layers, more dense than Oi1, α,α-dipyridyl reaction positive
34...50	Bgf	7009	permafrost, sand, 2...4% org. matter, 7.5YR5/1, sand layers alternating with medium-decomposed peat layers (moss + dead roots), α,α-dipyridyl reaction positive

remarks: no cryoturbation

Soil Taxonomy: Typic Historthel
World Reference Base for Soil Resources: **Gleyi-Histic Cryosol (Fluvic Fibric)**
Russian Classification (Elovskaya): **Permafrost Peat Gley**

1) symbols according to Soil Taxonomy 8th edition (USDA 1998)

Temperature and TDR sensors were installed in pairs to measure vertical profiles of soil temperature and soil volumetric water content. In every profile sensors were installed so as to cover the whole depth range of the profile, i.e. from the very top through the active layer and into the permafrost soil. The positions of the sensors were chosen according to the existing soil horizons so that every horizon in the profile was probed at least once. Additionally, a measurement chain of temperature sensors was installed in the ice wedge down to a depth of 220 cm into the ice. Heat flux sensors were installed at small depths below the surface in the rim and centre profiles. Figure 3-13 and Table 3-8 show the configuration of the new measurement station in graphical and Table form respectively.

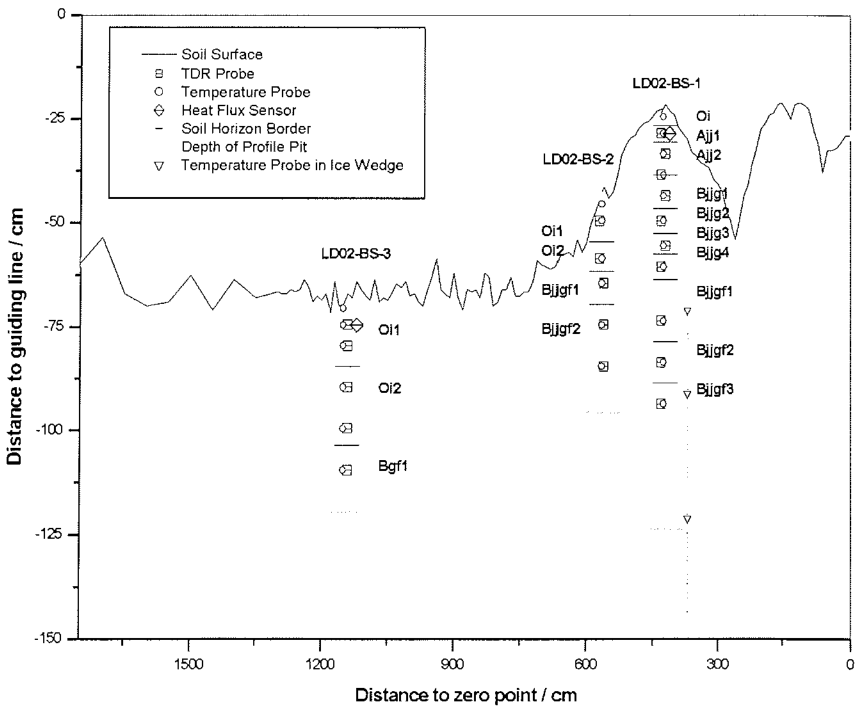

Figure 3-13. Transect of the polygon with the new measurement station. The solid line shows the surface profile of the polygon along the line connecting the measurement profiles. The markers indicate the position of sensors. The chain of temperature probes in the ice wedge continues below the depth range shown.

Table 3-8. Configuration of the measurement profiles. Depth of temperature sensors in ice wedge is given in cm below top surface of ice wedge shoulder.

Profile ID / Description	BS-1 / Polygon Rim										
Depth (cm)	1	5	10	15	20	26	32	37	50	60	70
TDR Sensor ID	--	29	28	27	21	26	25	22	10	12	11
Temp. Sensor ID	22	7	6	11	8	13	12	10	29	28	19
Heat Flux Sensor ID	--	550	--	--	--	--	--	--	--	--	--
Profile ID / Description	Ice Wedge										
Depth (cm)	-10	10	40	70	100	130	160	190	220		
Temp. Sensor ID	9	27	26	25	24	20	16	18	17		
Profile ID / Description	BS-2 / Polygon Slope										
Depth (cm)	1	5	14	20	30	40					
TDR-Sensor ID	--	30	24	23	15	6					
Temp.-Sensor ID	21	5	4	3	2	1					
Profile ID / Description	BS-3 / Polygon Centre										
Depth (cm)	1	5	10	20	30	40					
TDR-Sensor ID	--	8	14	16	9	13					
Temp.-Sensor ID	40	30	23	37	38	39					
Heat Flux Sensor ID	--	551	--	--	--	--					

The tower with meteorological instruments, the sonic ranging sensor for measuring snow depth as well as the power supply equipment were moved from the old measurement station and installed at the new site. A new sensor for the measurement of long wave radiation emitted from the ground was installed on the meteorological tower. Table 3-9 lists the data collected by the new measurement station as well as the sensors used. Meteorological data (Pos. 1-5 in Table 3-9) is sampled every 20 seconds and hourly averages are stored. Soil data (Pos. 6-10 in Table 3-9) is sampled and stored once an hour.

Table 3-9. Data and sensors of new permanent measurement station.

Pos.	Data Measured	Sensor Type
1	Air Temperature and Relative Humidity	Rotronic Meßgeräte GmbH Meteorological Probe for Humidity and Temperature MP340
2	Wind Speed & Direction	R M Young Company Anemometer 05103
3	Net Radiation	Kipp & Zonen B.V. Net Radiometer NR-Lite
4	Long wave Radiation	Kipp & Zonen B.V. Pyrgeometer CG1
5	Precipitation (liquid, i.e. Rain)	R M Young Company Tipping Bucket Rain Gauge 52203
6	Snow Height	Campbell Scientific Ltd. Sonic Ranging Sensor SR 50
7	Soil Temperature	Campbell Scientific Ltd. Thermistor Soil Temperature Probe 107
8	Soil Bulk Electrical Conductivity	Campbell Scientific Ltd. TDR 100, Probe CS605
9	Soil Volumetric Water Content	Campbell Scientific Ltd. TDR 100, Probe CS605
10	Heat Flux out of / into Soil	Hukseflux Thermal Sensors Heat Flux Sensor HFP01

3.2.3 Eddy site soil measurement profile

A second measurement station was installed near the Eddy Covariance measurement site. This station consists of two profiles (BS-4, BS-5) of temperature, TDR and heat flux sensors in a degraded polygon about 35 m northwest of the eddy measurement tower. During future campaigns a preassembled data logging system can be connected to the sensors to deliver additional data for the eddy covariance measurements.

As for the permanent measurement station (see previous chapter), profile pits were dug, soils were described and classified, samples were collected, and sensors were installed. The soil descriptions are given in Table 3-10 and 3-11, a complete sample list is provided in Appendix 3-1.

Table 3-10. Description of soil profile BS-4 (polygon rim).

profile ID: **LD02-BS-4** location: Samoylov, Lena-Delta date: 28.08.02
altitude a.s.l.: 11.5 m UTM: Zone 52, 415383E, 8032420N

relief situation: 1. main delta terrace, summit of elevated polygon rim
substrate: fluviatile loams

profile depth: 50 cm permafrost depth: 32 cm water level depth: --

vegetation: mosses total 98%, height 2...4cm; vascular plants total 20%, height 20cm, *Carex aquatilis, Salix reticulata, Salix glauca, Saxifraga punctata, Pyrola secunda, Saxifraga hirculus*

depth (cm)	horizon[1] (cm)	sample ID LD02-	Properties
0...6	Oi	7016	organic material, slightly decomposed moss fibers,>30% org. matter, few fine roots, 10YR2/3
6...20	Ajj	7017	sandy loam, sub angular to angular blocky, 2...4% org. matter, many fine roots, 10YR3/2, at the horizon top band of redoximorphic concretions: 10% (2,5YR4/6), no prominent peat layers
20...32	Bjjg	7018	silt loam, subangular blocky to coherent, 2...4% org. matter, many fine roots, 10YR4/1, no prominent peat layers, α,α-dipyridyl reaction negative
32...50	Bjjgf	7019	permafrost,, 1...2% org. matter, 10YR3/1, no stratification noticeable, ice lense in direction crack 3cm thick

remarks: wavy horizon boundaries: slight cryoturbation

Soil Taxonomy: **Typic Aquiturbel**
World Reference Base for Soil Resources: **Gleyi-Turbic Cryosol**
Russian Classification (Elovskaya): **Permafrost Turfness Gley**

1) symbols according to *Soil Taxonomy* 8th edition (USDA 1998)

Table 3-11. Description of soil profile BS-5 (polygon centre).

profile ID: **LD02-BS-5** location: Samoylov, Lena-Delta date: 29.08.02
altitude a.s.l.: 11.0 m UTM: Zone 52, 415379E, 8032418N

relief situation: 1. main delta terrace, depressed centre of polygon
substrate: moss and sedge peat above fluviatile loams

profile depth: 55 cm permafrost depth: 34 cm water level depth: 4 cm

vegetation: mosses total 98%, height 1...5 cm; vascular plants total 30%, height 30 cm, Carex *aquatilis*, *Potentilla palustris*, *Pedicularis sudetica*

depth (cm)	horizon[1] (cm)	sample ID LD02-	Properties
0...10	Oi1	7020	organic material, slightly to medium decomposed moss peat,>30% org. matter, very many fine roots, 10YR1.7/1 + 7.5YR3/4, few aeolian sand
10...26	Oi2	7021	organic material, slightly to medium decomposed moss peat, >30% org. matter, many fine roots, 10YR3/3, few aeolian sand, α,α-dipyridyl reaction positive
26...34	Bg	7022	sandy loam, 15...30% org. matter, 10YR4/2, medium-decomposed sedge and moss peat, α,α-dipyridyl reaction positive
34...55	Bgf	7023	permafrost, sandy loam, 15...30% org. matter, 10YR4/1, loam layers alternating with peat layers (medium-decomposed sedge residues), α,α-dipyridyl reaction positive

remarks: no cryoturbation

Soil Taxonomy: **Typic Historthel**
World Reference Base for Soil Resources: **Gleyi-Histic Cryosol (Fibric)**
Russian Classification (Elovskaya): **Permafrost Peat Gley**

1) symbols according to Soil Taxonomy 8th edition (USDA 1998)

Figure 3-14 and Table 3-12 show the configuration of the measurement profiles in graphical and table form respectively.

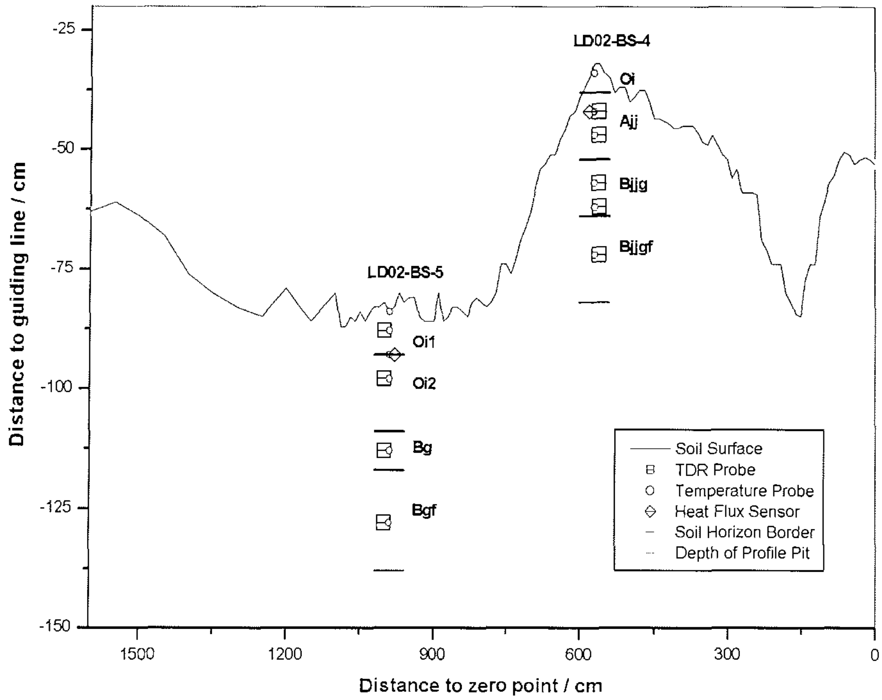

Figure 3-14. Transect of the polygon with the eddy site measurement profiles. The solid line shows the surface profile of the polygon along the line connecting the measurement profiles. The markers indicate the position of sensors. The location of transect is shown in Figure 3-4 (elevation profile-2).

Table 3-12. Configuration of the "Eddy Site" measurement profiles.

Profile ID / Description	BS-4 / Polygon Rim					
Depth (cm)	2	10	15	25	30	40
TDR Sensor ID	--	5	19	2	20	4
Temp. Sensor ID	34	32	33	36	35	31
Heat Flux Sensor ID	--	20	--	--	--	--
Profile ID / Description	BS-5 / Polygon Centre					
Depth (cm)	1	5	10	15	30	45
TDR-Sensor ID	--	3	--	7	17	18
Temp.-Sensor ID	L8	43	L10	44	41	42
Heat Flux Sensor ID	--	--	19	--	--	--

3.3 Studies on recent cryogenesis

Hanno Meyer

3.3.1 Introduction

Samoylov Island is subdivided into four different geomorphologic elements (Akhmadeeva et al. 1999): a lower flood plain, a middle flood plain and a high flood plain in the western part of the island, which are separated by an up to 8 m high cliff from an old river terrace (1st Lena river terrace). The low and middle flood plains are those which are in general annually flooded by Lena river, but for different time spans, whereas the high flood plain is reached by water only during high floods. The 1st Lena river terrace reaches up to 12 m a.s.l. and has been built up since the Middle Holocene. Both, the high flood plain and the 1st Lena river terrace are characterised by polygonal-patterned ground with ice wedge growth. Therefore, studies on recent cryogenesis and on recent ice wedge growth were carried out last summer especially on the high flood plain and the 1st Lena river terrace on Samoylov Island (Figure 3-15).

The main aim of studying recent cryogenesis processes is to establish a stable isotope thermometer for ice wedges. The reconstruction of paleotemperatures with ground ice, especially with ice wedges is possible (Vasil'chuk 1992, Nikolaev & Mikhalev 1995). So far, this is reduced by the missing correlation of the ice veins - of which ice wedges are composed - to the year of their formation as well as by the large distances of field locations to the next weather station. The attribution of recent ice veins to the discrete year of their formation can be carried out with tracer experiments. A tracer (such as coloured spores) applied to a polygon with recent cryogenesis enables us to identify all types of ground ice, which were formed in the considered year. The combination with a nearby climate station would allow to correlate the temperature with the isotope geochemistry of ice wedges. It was also aimed to characterise and to identify the conditions prevailing, when frost cracking and recent ice wedge growth take place. For this purpose, an ice wedge polygon had to be selected in the field for monitoring according to several site-specific characteristics. These were:

1.) the occurrence of recent ice wedge growth,
2.) a clearly visible frost crack,
3.) a well-developed relief between polygon wall and polygon centre, which additionally had to be typical for the site,
4.) a rather young stage of ice wedge polygon formation without signs of degradation such as standing water in the trough above the ice wedge,
5.) for drainage reasons, a low inclination and exposition of the polygon,
6.) a low insolation from above by the soil, the vegetation and the snow cover for best possible cracking conditions (e. g. low temperatures entering the permafrost).

Additionally, it was aimed to select a polygon close to both, the weather and the soil stations on Samoylov in order to use the existing climate and soil data to characterise the site and to better understand the boundary conditions for recent ice wedge growth (see Chapter 3.2).

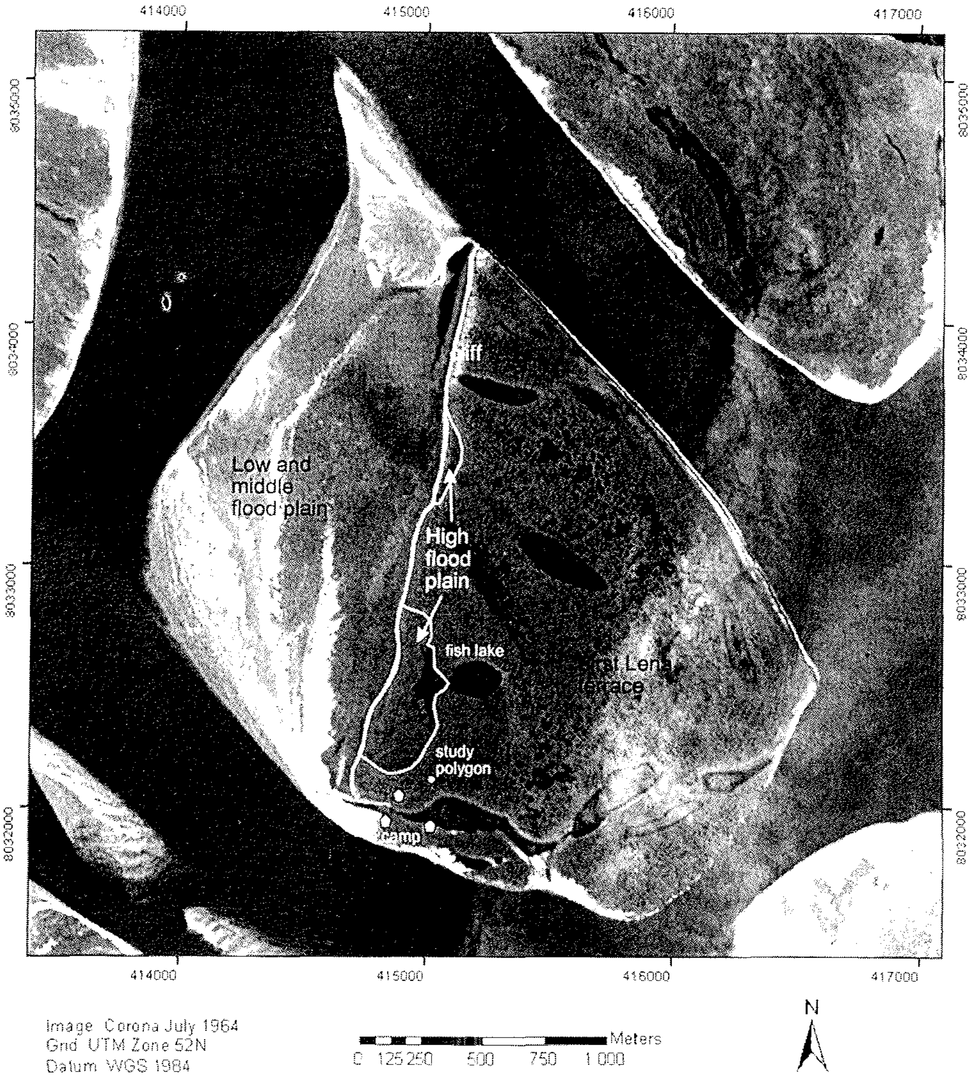

Figure 3-15. Study site on Samoylov Island. Corona satellite image, 1964.

3.3.2 Survey of different polygon types on Samoylov Island

In order to select an ice wedge polygon for studies on recent cryogenesis, the first days were used to recognise the different polygon types occurring on Samoylov Island, which were differentiated by their stage of development and the availability of recent ice veins. For this purpose, the island was subdivided into different specific areas, each of which was briefly visited and mapped for the following characteristics of the polygons.

These characteristics are: polygon size, polygon net type (French 1996), exposition, vegetation cover, soil type, hydrological conditions (drainage and distribution of standing water), thickness of the active layer, relief (height difference between polygon wall and polygon centre) as well as the frost cracking activity (occurrence of recent ice wedge growth). This first survey resulted in seven modern polygon types presently occurring on Samoylov Island.

1. polygon type: juvenile

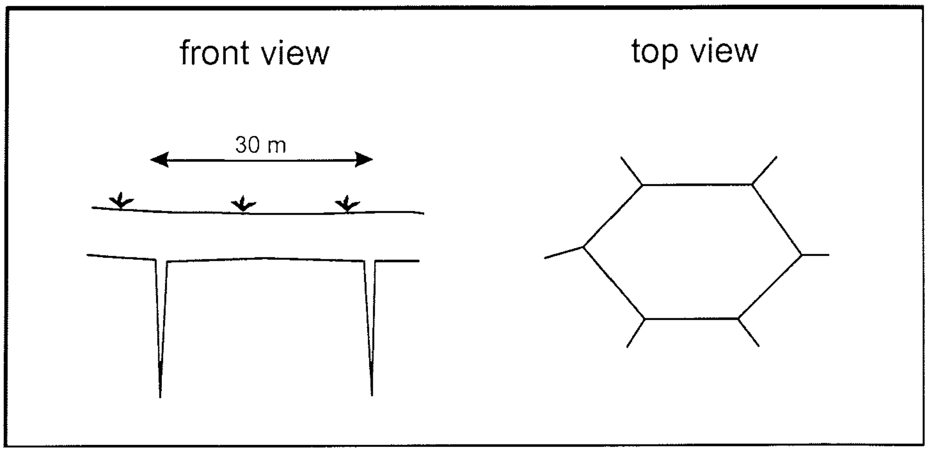

Figure 3-16. Front and top view of the juvenile polygon type.

A juvenile polygon (Figure 3-16) type is found in relatively dry, well-drained sites, such as the uppermost flood plain located between the lower and middle floodplain and the first Lena river terrace (Figure 3-15). It is characterised by a low relief with very small height differences between polygon wall and centre and relatively big (30 m in diameter) hexagonal ice wedge polygons. The active layer is about 0.4 m to 0.5 m thick with a thin vegetation cover without large differences between plant in the polygon wall and the centre. Frost cracks are clearly visible and recent ice veins are regularly found.

2. polygon type: mature

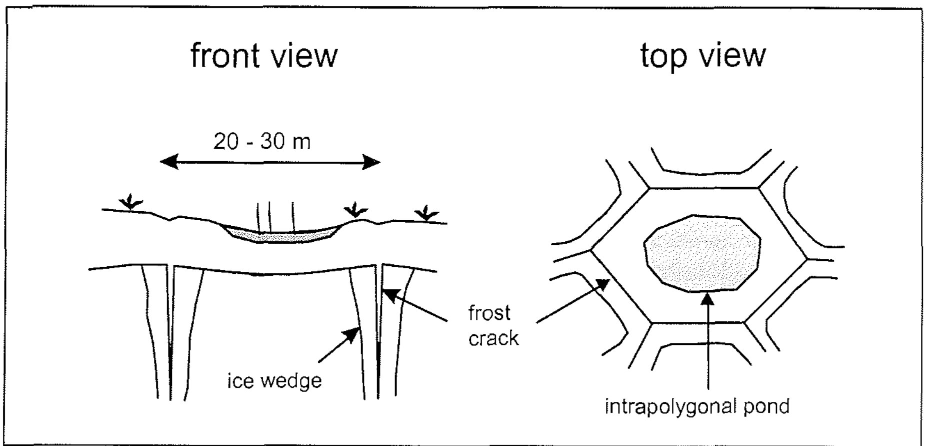

Figure 3-17. Front and top view of the mature polygon type.

The mature polygon type (Figure 3-17) is found all over the first Lena terrace. It is characterised by a relatively high relief with height differences of about 0.5 m between the polygon wall and the centre. An intrapolygonal pond is typical for the polygon centres, but this depends on drainage conditions. A trough above the ice wedge is clearly visible and active frost cracks with recent ice veins are frequent. The moss cover of the polygon wall is often cut into two pieces by the frost cracking process. The polygons are relatively big (20-30 m in diameter) and consist of pentagonal or hexagonal ice wedge nets. In general, the active layer is between 0.2 m to 0.6 m thick, mainly varying around 0.35 m. The vegetation cover differs clearly between polygon wall (mosses dominant) and polygon centre (sedges dominant). Typical mature polygons are located close to the weather station on Samoylov Island.

During the field campaign, different types of ice wedge polygons were found showing signs of degradation (such as water standing in the trough above the ice wedge). Most of them are linked with a change in hydrological conditions of the juvenile or mature polygons. For the selection of a polygon for the experiments on recent cryogenesis, it was differentiated between three main stages: 1.) initial degradation, 2.) degraded and 3.) final degradation (wet and dry). However, numerous substages between these degradation polygons were observed and the transitions between them are smooth.

3. polygon type: initial degradation

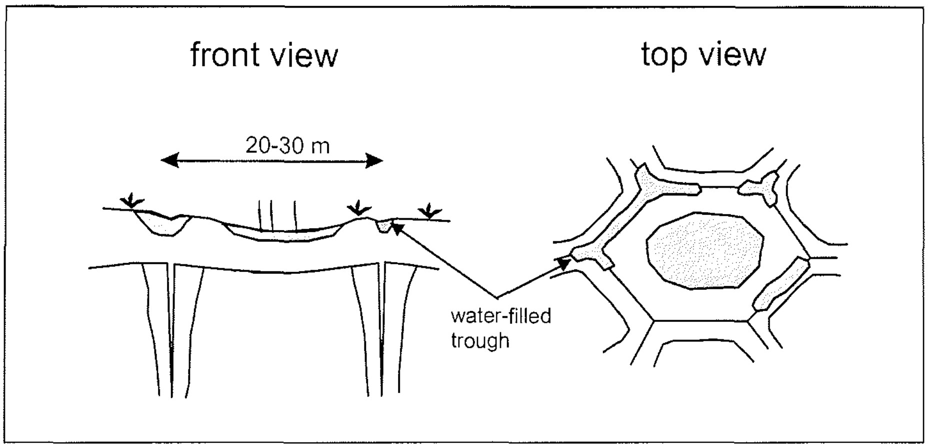

Figure 3-18. Front and top view of the polygon type of initial degradation.

This polygon type develops from the mature type, with the formation of small ponds in the polygon wall, which often form triangular ponds in the triple junctions of frost cracks or elongated ponds along the frost crack. It can actually be considered as intermediate polygon type between the mature and the degraded stages (Figure 3-18). Therefore, the size and the number of edges of the polygon are related to the mature type polygon, which starts degrading. The intrapolygonal pond as well as the clear differentiation of the vegetation between polygon wall and centre are still present. The polygon is characterised by a high relief with height differences of more than half a meter between polygon wall and centre. This polygon type is still active with common frost cracking and recent ice wedges, which are commonly found in the drier parts of the polygon.

4. polygon type: degraded

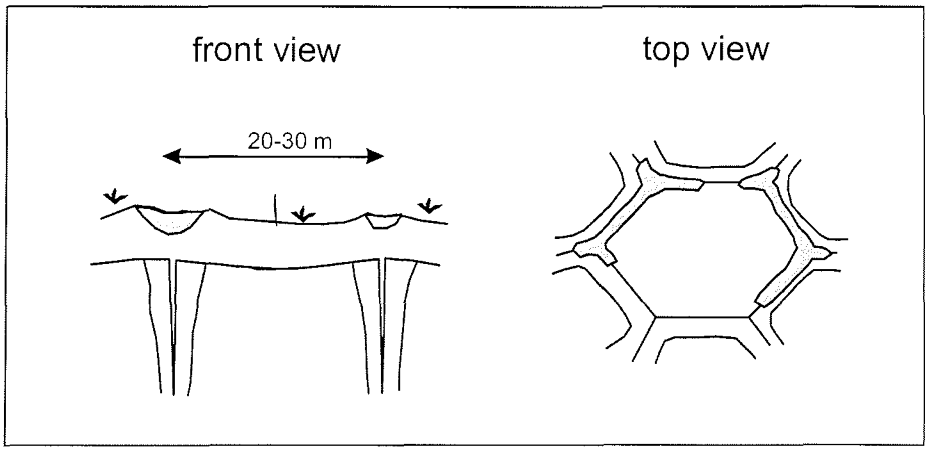

Figure 3-19. Front and top view of the degraded polygon type.

If the degradation of the polygon continues, the intrapolygonal pond falls dry and the vegetation used to standing water disappears (Figure 3-19). In contrast, the ponds in the polygon walls may deepen and sometimes get connected to a pentagonal or hexagonal pond above the frost crack. The relief is still high because of relatively high rims in the polygon walls, but when the pools fall dry, the polygon centres diminish in depth. Frost cracking certainly occurs in these polygons, but the recent ice wedges are hard to sample, because of the water standing in most parts of the trough above the ice wedge. This polygon type is commonly found all over the island, e. g. near the "Fish Lake" and near the northern point of the island.

5. polygon type: final degradation, dry, high centre polygon

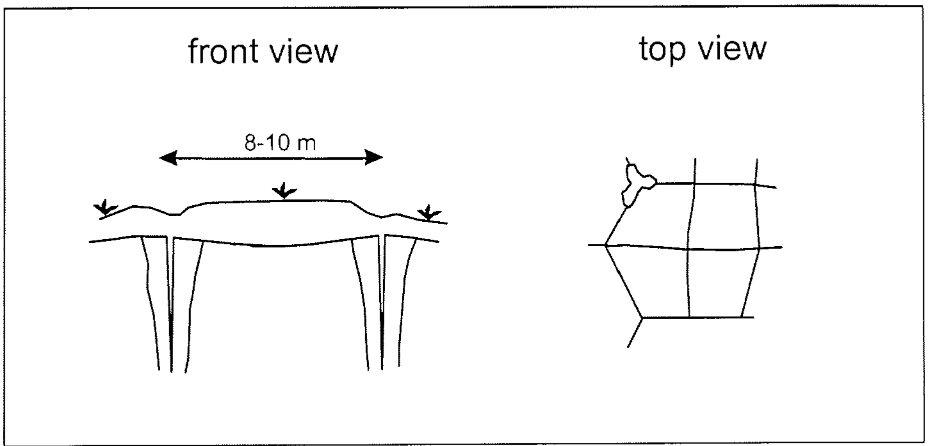

Figure 3-20. Front and top view of the final dry degradation or "high-centre" polygon type.

If degradation occurs in a well-drained and relatively dry environment, the polygon seldom has open water ponds. In general, the trough above the ice wedge is deep and still relatively wet, but the polygon centre is completely dry (Figure 3-20). Secondary polygons subdivide the degraded pentagonal or hexagonal polygons mostly into four smaller polygons which in most cases are tetragonal, sometimes pentagonal in shape. With a size of 8 - 10 m in diameter, the high-centre polygons are much smaller than the preceding low-centre polygons. Recent frost cracking is observed, and especially in the secondary cracks (of the high-centre polygons), recent ice veins are found. This polygon type is found near the northern point of Samoylov Island.

6. polygon type: final degradation, wet

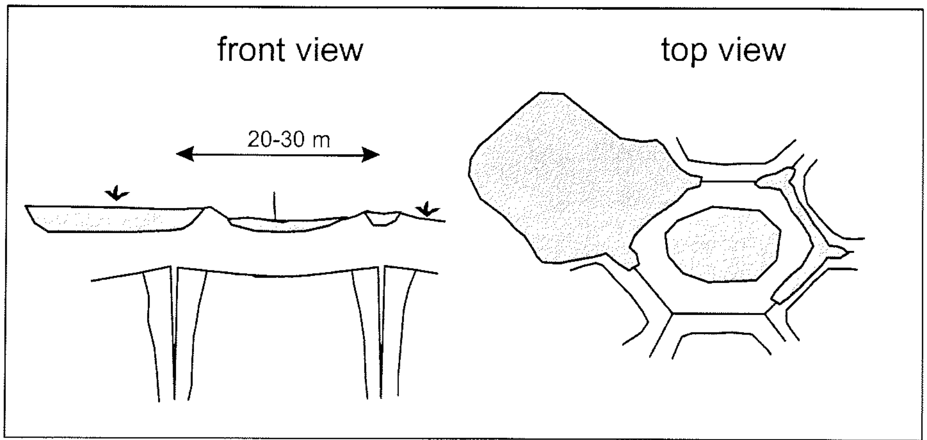

Figure 3-21. Front and top view of the final wet degradation polygon type.

If the degradation propagates in a poorly-drained and wet environment, the polygon is often characterised by standing water and sometimes it is even completely flooded (Figure 3-21). The trough above the ice wedge is deep and wet and the polygon centre has open water ponds, which may extend and then interconnect with ponds in the polygon wall or with intrapolygonal ponds of other polygons. This polygon type is characteristic for depressions on Samoylov, where the flux of surface waters and precipitation often leads to the formation of lakes with variable size and polygonal structure. This polygon type typically occurs e. g. 200 m NW of the eddy covariance tower (here in an old river branch of the paleo-Lena). Recent ice veins were not found in these polygons, because of the water standing in the trough above the ice wedge. Nevertheless, for these lakes, which in general are not deeper than 1.2 m, frost cracking cannot be excluded.

7. polygon type: slope polygon

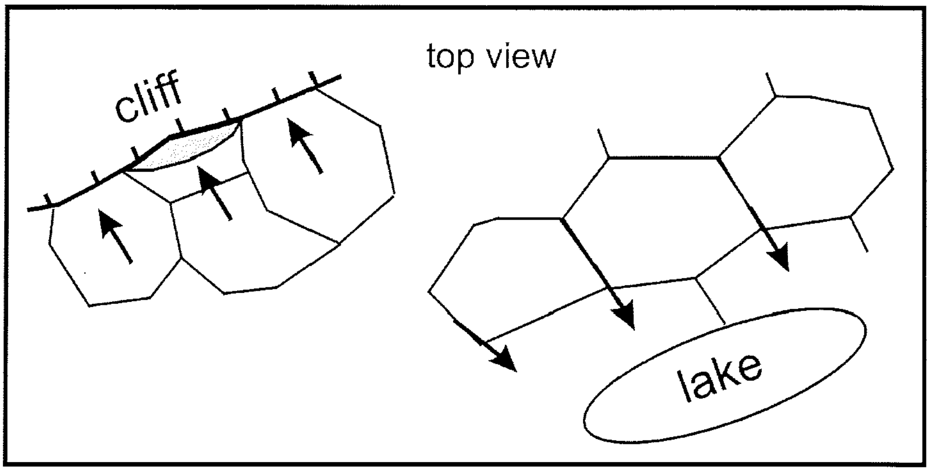

Figure 3-22. Top view of two types of slope polygons (near lakes and cliffs).

Slope polygons (Figure 3-22) develop in all places, where the meso-relief is lowered, i. e. near cliffs and around lakes. The drainage is directed towards the lake or the cliff leading to relatively dry polygons near the slopes. They may develop from all other polygon types and, hence, differ in size, shape and morphology. A low relief similar to that of the juvenile polygon is a common but not necessary observation, even though the trough above the ice wedge is sometimes deepened being used as channel for running water. The main feature is the dryness compared to the surrounding polygons. The slope polygon type is found all along the cliff as well as around every lake. Recent ice wedges have not been found in two dig holes and, therefore, this polygon type has been considered as not appropriate for recent cryogenesis studies.

This classification is certainly a simplification, e. g. not taking into account the soil type as well as the type of sediments, which were found to vary not so much on Samoylov Island. It is mainly based on the drainage conditions and linked phenomena (such as the exposition). The main result of a few days' of field work was the finding, that the presented subdivision of polygons is helpful to track and to characterise polygons, which are suitable for recent ice wedge studies (juvenile, mature type) and which polygons are not useful (degraded types, slope polygons). The subdivision of polygon types may serve as the base for a more detailed mapping of polygon types on Samoylov Island.

3.3.3 Mapping and survey of the selected polygon

According to the subdivision of polygon types on Samoylov Island, juvenile and mature ice wedge polygons seem to be the most promising for studies on recent cryogenesis. Both types commonly show recent frost cracking and no water standing in frost crack, hence, hampering the sampling of the recent ice vein in summer. The mature type is characterised by a well-developed relief between polygon wall and polygon centre and clearly visible frost cracks with troughs above the ice wedge. Therefore, a mature type ice wedge polygon was selected for the studies on recent cryogenesis located near the old weather and soil stations. The same polygon is also used for the new soil and the weather stations, which gives the excellent possibility to combine weather and soil data with the studies on recent cryogenesis.

The selected site is characterised by low inclination towards the north, and is located on the first Lena terrace approximately 250 m NE of the ice cellar of the station. The polygon is hexagonal and 20.6 m in diameter. It is characterised by a relatively high relief with the polygon centre about 0.5 m lower than the polygon walls, which in general are relatively flat. The polygon centre is moist but without open water conditions. The vegetation cover differentiates the polygon walls, which is dominated by mosses from the polygon centre (sedges). This leads to an abrupt transition from the polygon wall to the centre. The moss cover of the polygon wall is often cut by frost cracking activity. The frost cracks are clearly visible and the troughs above the ice wedges may be up to 10 cm wide and 20 cm deep. On two polygon walls, secondary frost cracks were observed. The active layer is usually between 0.2 m to 0.6 m thick, mainly varying around 0.35 m. With a height of approximately 12 m, it is situated relatively high above sea level and, logistically important, relatively close to the camp. A thin snow cover can be expected for the site, since at this height the snow may be easily drifted by wind. Therefore, the heat insolation of the snow cover, which prevents frost cracking (MacKay 1993), can be assumed to be small. This hypothesis will be tested with a snow depth sensor installed near the "study polygon".

For the survey of the polygon carried out in co-operation with Waldemar Schneider, a laser tachymeter (type Trimble 3300) was used. The height of the reflector was 1.4 m; 5 cm were added to every measurement because of the subsidence of the reflector into the vegetation cover. First, a measuring field of 24 x 34 m covering the study polygon and parts of the neighbouring polygons was surveyed with a grid size of 2 x 2 m. This resulted in 204 measuring points. For all of them, the relative x-, y-, z-coordinates of the polygon surface as well as the active layer depth were retrieved relative to a zero angle (Stolb trigonometric point) and a fix point (an elevated point in a neighbouring polygon). In the same way, the polygon walls of the study polygon were mapped with additional 157 points with a special emphasis on the position of frost cracks, highest elevations of the polygon wall as well as the border between polygon wall and centre. Moreover, the position of 22 steel poles was determined. These poles were inserted into the permafrost as markers for the experiments on recent frost cracking. This results in a total number of 383 measuring points for the study polygon. In Figure 3-23, the results of the survey of the polygon are displayed.

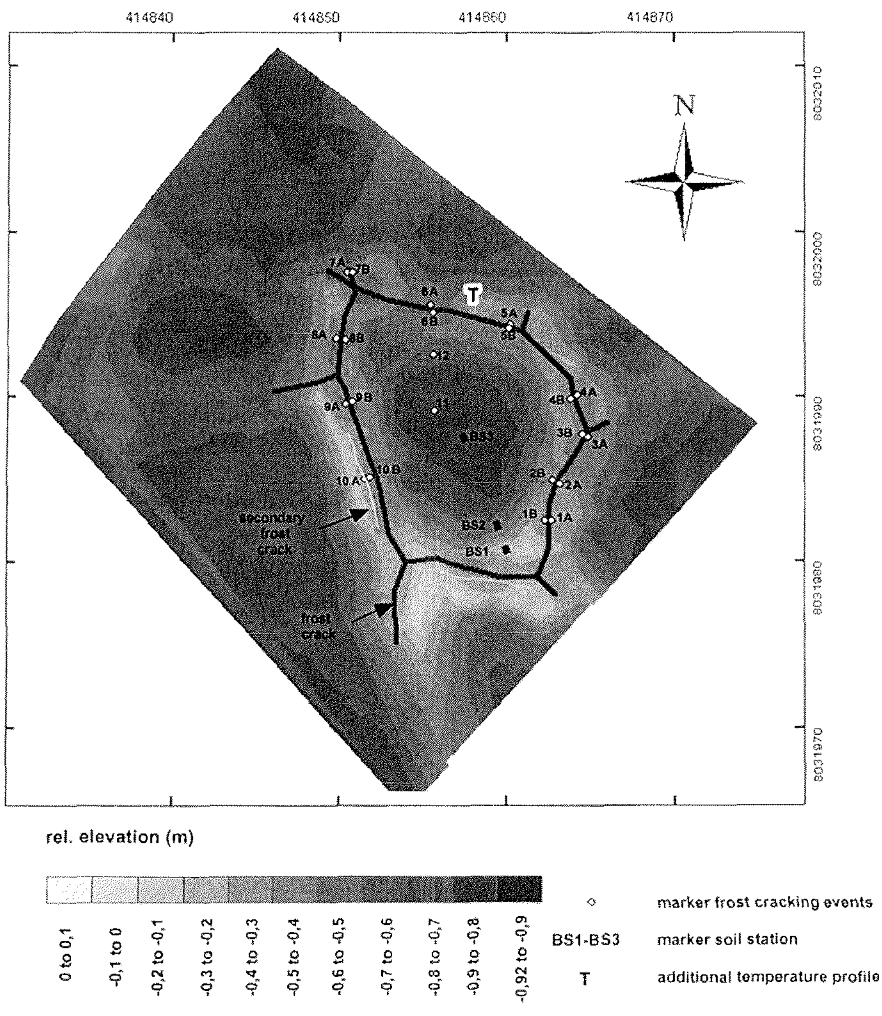

Figure 3-23. Results of the survey of the study polygon with the exact position of the steel poles for frost cracking experiments.

3.3.4 Frost cracking experiments

Studies on recent ice wedge growth were carried out for one selected polygon on the 1st Lena river terrace of Samoylov Island in order to first identify, if in any place recent frost cracking had taken place, and if so, at what time and to what extent. The climatic conditions occurring during frost cracking indicate the boundary conditions (concerning air and soil temperatures, temperature gradients in the sediment, soil moisture, air humidity, wind direction and speed, precipitation and snow cover) necessary for recent ice wedge growth. It must be stressed again that the combination of soil and weather stations with the experiments on recent cryogenesis is optimal for this kind of studies.

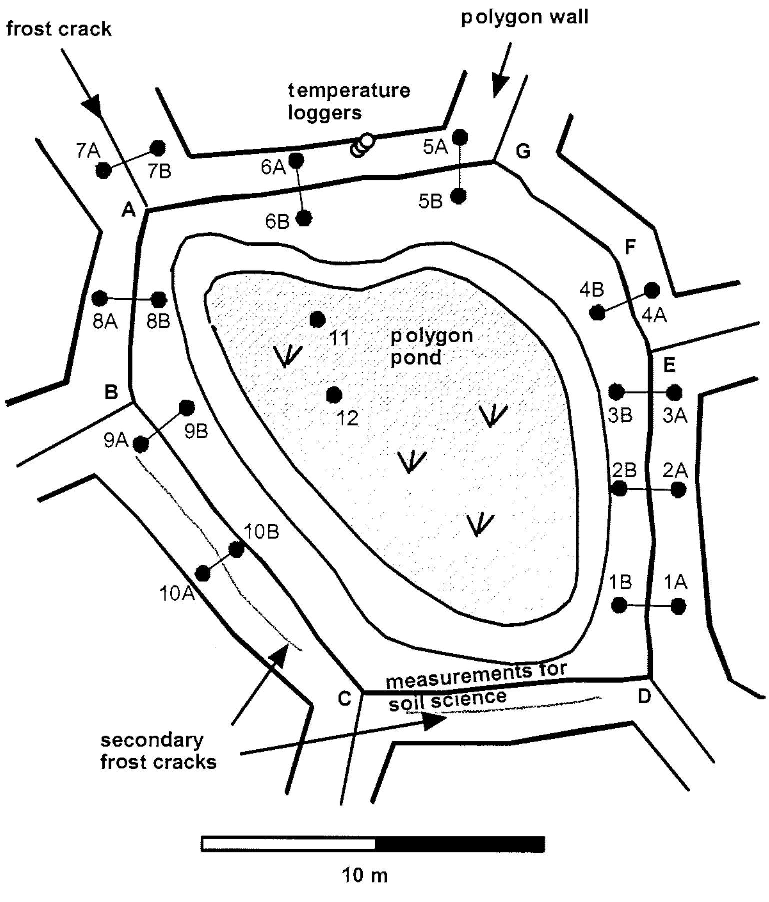

Figure 3-24. "Study polygon" with experimental set-up for the detection of recent frost cracking processes. Black dots represent steel poles, white dots temperature data loggers in the active layer and the uppermost part of permafrost.

For the identification of frost cracking processes, 10 different experiments were carried out. The above mentioned 22 steel poles were used for these recent cracking experiments - only two poles for survey purposes. The general set-up of every single experiment consists of two steel poles (e. g. 1A and 1B) inserted to the permafrost on both sides of a frost crack (see Figures 3-25, 3-26).

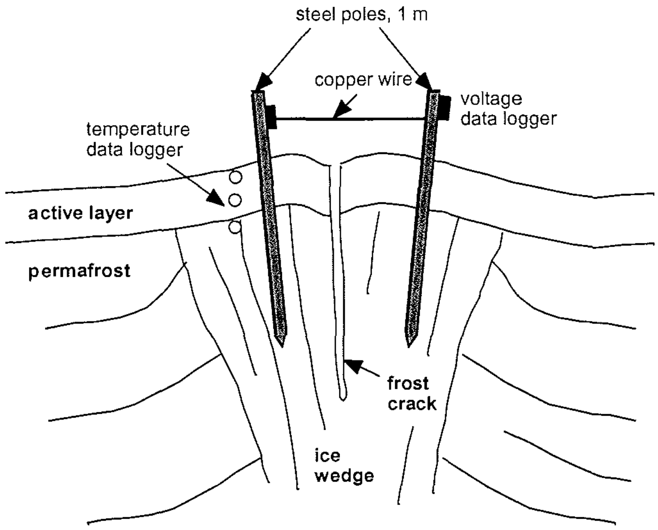

Figure 3-25. Frost cracking experiments on Samoylov Island. A breaking cable connected to a data logger is stretched between two steel poles for the identification of frost cracking and its timing. Temperature loggers are used to derive temperature gradient in the soil.

The two steel poles were 1 m long, and inserted as deep as possible to the permafrost, in general between 30 cm and 45 cm. This depends evidently on the depth of the active layer, which also varies between 30 cm and 45 cm (measured on August 6 and 7, 2002). The length of all 22 steel poles, the height of the poles above surface and the active layer depth as well as the distance to two fix points (poles 11 and 5b) was measured (Table 3-13). Additionally, the respective depth every stick penetrates the permafrost was calculated.

Between two steel poles, a breaking cable was installed. Three different kinds of copper wires were used (Cu wire, 0.5 mm; Cu two-wire braid (HO3VH-H, 2x0.75), Cu single-wire braid (HO3VH-H, 1x0.75). Copper wire was selected, because this metal has a high coefficient of linear extension of about $16.1 . 10^{-6}$/K. It was assumed that the copper wire may bear intraday temperature variations as well as the cooling in winter without cracking, but breaks when a sudden rupture of about 0.5 cm, e. g. frost cracking, takes place. Tabasco was used to make the cables unattractive for animals.

Table 3-13. Characteristics of 22 steel poles: length, height above surface, distance to fix points (poles 11 and 5b) and depth in permafrost as well as the active layer depth.

Steel pole Nr.	steel pole length (cm)	steel pole above surface (cm)	steel pole in permafrost (cm)	active layer depth (cm)	steel pole distance to M11 (cm)	steel pole distance to 5b (cm)
1a	95	22	39	34	957,4	-
1b	100	22	45	33	930,5	1171,8
2a	100	20	39	41	866,7	-
2b	100	23	42	35	818,8	944,0
3a	92	23	29	40	921,4	-
3b	100	24	37	39	887,2	763,2
4a	100	22	43	35	846,5	-
4b	100	25	39	36	806,7	552,3
5a	93	26	26	41	681,6	-
5b	100	26	42	32	660,2	0,0
6a	92	27	32	33	635,4	-
6b	100	25	38	37	589,3	465,0
7a	100	27	33	40	977,0	-
7b	100	24	40	36	965,0	991,1
8a	92	20	37	35	727,5	-
8b	100	26	34	40	679,3	977,2
9a	98	21	38	39	531,8	-
9b	100	19	42	39	492,0	1030,4
10a	99,5	24	32,5	43	581,1	-
10b	100	25	34	41	555,6	1217,3
11	100	55	16	29	0,0	660,2
12	100	43	22	35	339,3	472,8

Six (out of ten) experiments were equipped with voltage data loggers (type ESIS Minidan Volt) connected to the breaking cables. The loggers started measuring at an amperage of 10 μA and a voltage of 270 mV every 20 minutes from the moment of installation until the moment of frost cracking. If the cable does not break (because no frost cracking took place or for any other reason), the loggers will continue to measure until October 8, 2003. By that, the information if frost cracking takes place should be derived as well as the precise moment of frost cracking.

In Figure 3-26, one of these experimental set-ups is displayed. The breaking cable is connected to the data logger and fixed to the pole. On the other side, the cable is attached to a brass clamping fixture (Figure 3-27). The tension of the wires was increased by counting the revs (or turnarounds) of the nut (type M5) on the thread rods. First, breaking experiments were carried for every cable type. For this purpose, the cables were stretched until rupture and it was found that the number revs are mainly a function of the cable length. Therefore, maximum revs were calculated for every cable type and different initial tensions were then applied to the wires (Table 3-14 and 3-15).

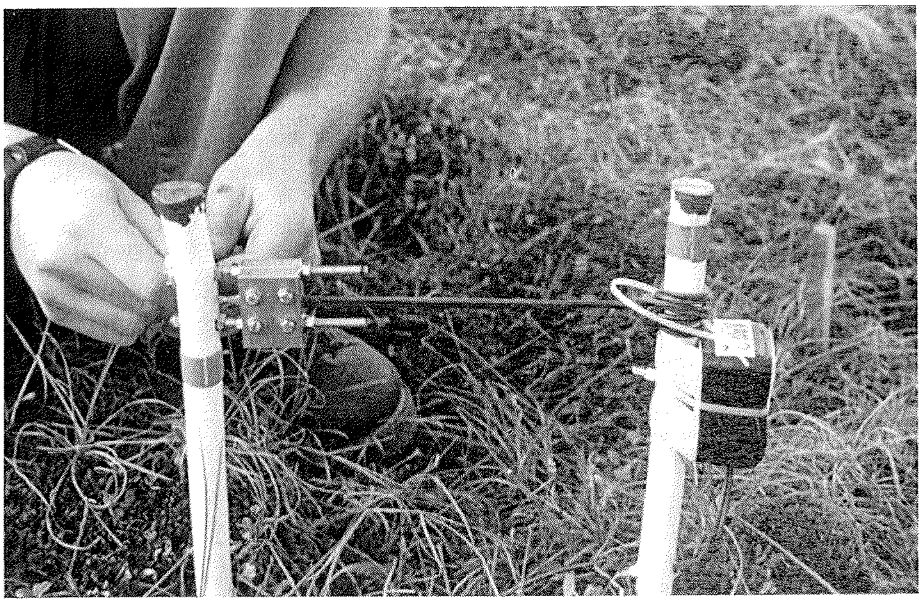

Figure 3-26. Frost cracking experiment 5A-5B with Voltmeter 5. A copper two-wire braid with a length of 181 mm was used. After 32 revs of the nut M5 on the threads, the wire was 184 mm long.

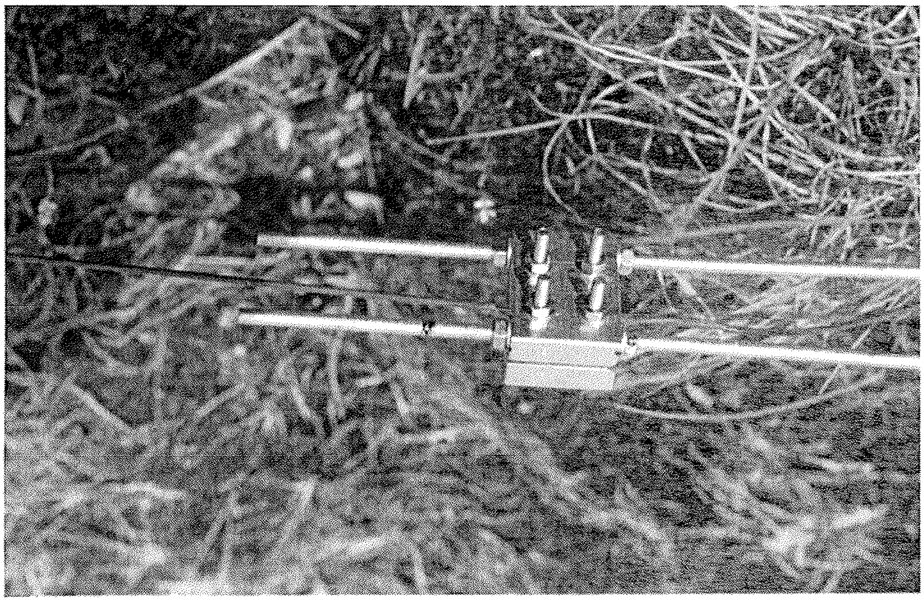

Figure 3-27. A closer view how a copper single-wire braid was fixed to a brass clamping fixture. The tension was regulated by nuts M5 on two thread rods.

Table 3-14. Ten stretching experiments with applied cables and voltmeters, the lengths of the breaking cables between the poles A and B before spanning the cable (1) and after the cables were stretched (2) with a control on September, 4th. The tension of the wires was increased by counting the revs (or turnarounds) of the nut (type M5) on the thread rod. In some cases, the tension was raised on September, 4th. For every cable type, maximum revs were calculated according to its length by means of the breaking experiments.

Marker	Volt-meter	Cable type	Cable length (9.8)		Diffe-rence	Control (4.9)	Turn-arounds	Turn-arounds	Max.
			1	2		2	(9.8)	(4.9)	
1A-1B	None	Cu two-wire braid (HO3VH-H, 2x0.75)	316	321	-5	336 (new)	35	38	75
2A-2B	2	Cu wire, 0.5 mm	263	278	-15	274	24	26	35
3A-3B	None	Cu wire, 0.5 mm	298	301	-3	304 (new)	10	16	40
4A-4B	1	Cu wire, 0.5 mm	359	376	-17	376	30	30	50
5A-5B	5	Cu two-wire braid (HO3VH-H, 2x0.75)	181	184	-3	186	32	32	45
6A-6B	3	Cu single-wire braid (HO3VH-H, 1x0.75)	379	384	-5	386	28	28	38
7A-7B	None	Cu single-wire braid (HO3VH-H, 1x0.75)	296	298	-2	298	10	14	30
8A-8B	4	Cu single-wire braid (HO3VH-H, 1x0.75)	447	453	-6	453	25	25	45
9A-9B	6	Cu two-wire braid (HO3VH-H, 2x0.75)	343	348	-5	350	35	35	85
10A-10B	None	Cu two-wire braid (HO3VH-H, 2x0.75)	216	220	-4	221	38	38	54

In order to understand how the low temperatures in winter penetrate the active layer and the permafrost, temperature loggers were introduced to the permafrost (Figure 3-23 to 3-25) to derive the temperature gradients necessary for frost cracking activity. The loggers were inserted every 15 cm in depths of 0.05 m, 0.2 m, 0.35 m and 0.5 m. In this place the active layer is 0.4 m thick.

Table 3-15. Ten stretching experiments with the respective distances (in mm) between the poles A and B measured from the a.) top to the top, b.) tape mark to the tape mark and c.) bottom to the bottom, before spanning the cable (1) and after the cables were stretched (2).

Marker	Distance Top-Top		Difference	Distance Tape-Tape		Difference	Distance Bottom-Bottom		Difference
	1	2		1	2		1	2	
1A-1B	**383**	**358**	**25**	**393**	**372**	**21**	**400**	**386**	**14**
2A-2B	**479**	**465**	**14**	**473**	**457**	**16**	**465**	**454**	**11**
3A-3B	**360**	**351**	**9**	**364**	**361**	**3**	**348**	**343**	**5**
4A-4B	**421**	**406**	**15**	**427**	**415**	**12**	**418**	**407**	**11**
5A-5B	**255**	**231**	**24**	**257**	**240**	**17**	**244**	**236**	**8**
6A-6B	**455**	**435**	**20**	**447**	**429**	**18**	**423**	**411**	**12**
7A-7B	**362**	**351**	**11**	**362**	**349**	**13**	**356**	**348**	**8**
8A-8B	**521**	**503**	**18**	**517**	**509**	**8**	**504**	**498**	**6**
9A-9B	**404**	**380**	**24**	**412**	**392**	**20**	**424**	**404**	**20**
10A-10B	**284**	**259**	**25**	**287**	**264**	**23**	**308**	**289**	**19**

A second attempt to measure frost cracking processes was undertaken by means of a Sonic Ranging sensor (type SR50). This experiment was installed near experiment 3A-3B (Figure 3-28). The ultrasonic sensor measures the distance from a sensor to a target by transmission of ultrasonic sound pulses and measuring the echoes coming back from the target. The time from transmission to the return of the echo is the basis for the distance measurement (minimum distance 0.5 m). This method is most commonly applied to the measurement of snow depths and water levels. Temperature compensation is necessary for the distance reading, because the speed of sound in air varies with temperature. The accuracy of the absolute distance measurement is ±1cm or 0.4% of the distance to the target (in our case about 0.6 m). However, the resolution is measured with a much higher precision of 0.1 mm. Consequently, a change in the distance between sensor and target (such as a frost cracking event) will be detected with high precision.

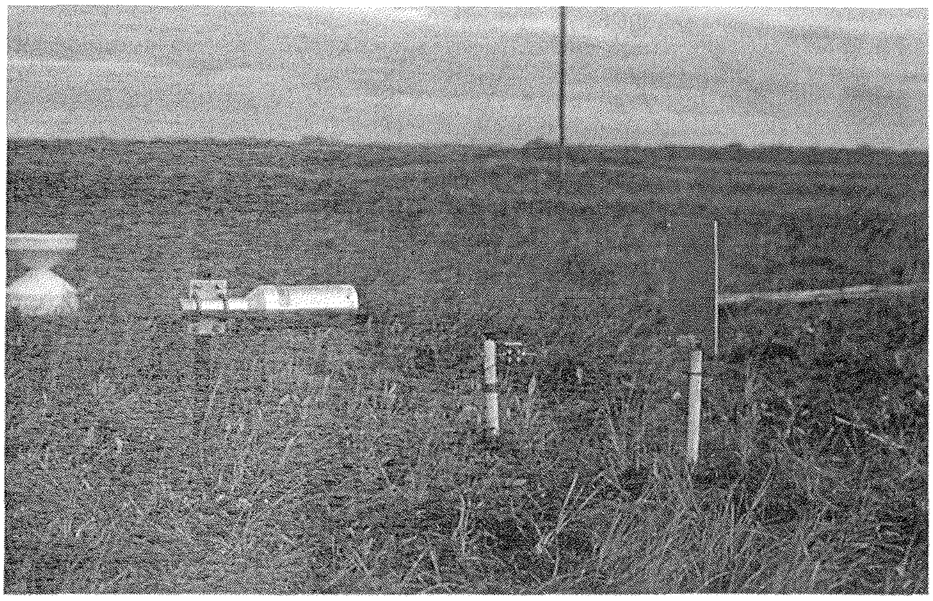

Figure 3-28. The experimental set-up of the detection of frost cracking processes by means of a Sonic Ranging sensor (type SR50).

The knowledge of the existence and timing of recent frost cracking activity is important for the second part of the studies, i. e. to trace recent ice veins (by means of colored spores) in order to attribute an ice vein to the discrete year of its formation. This information derived from ice veins of several years is necessary for a precise calibration of a stable hydrogen and oxygen isotope thermometer for ice wedges. The identification of frost cracking activity provides the information if at one site digging for ice veins has the chance to be successful. For this purpose, recent ice veins of several years will be sampled (after some years), measured for stable isotopes and related to the climatic situation in the year of its formation. In general, it is difficult to know the age of an ice vein. Tritium analyses have shown to be a useful tool (Dereviagin et al. 2002) to decide, whether frost cracking can be considered as active or inactive. However, the discrete year of formation of an ice vein is not derived. The sampling of recent ice veins in early summer at the bottom of the - still frozen - active layer is misleading, since these veins may have been influenced by the surrounding sediment and segregated ice, which is formed in a different way and, thus being chemically and isotopically completely different. Consequently, a tracer experiment is an elegant way to trace the age of an ice vein in order to assign it to the respective climatic situation.

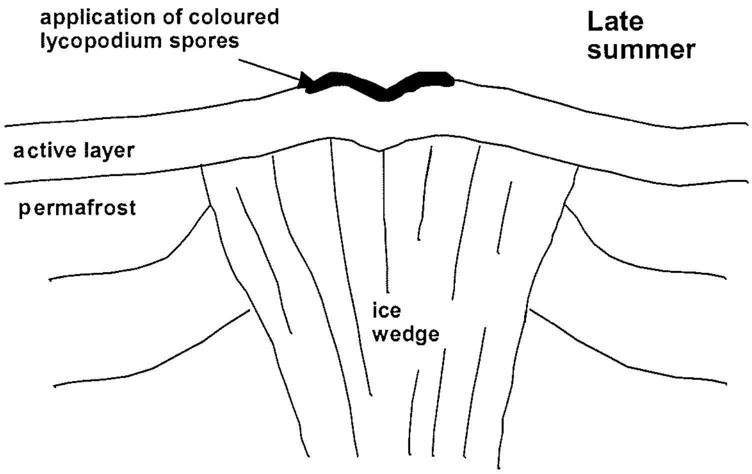

Figure 3-29. Application of *lycopodium* spores to the polygon.

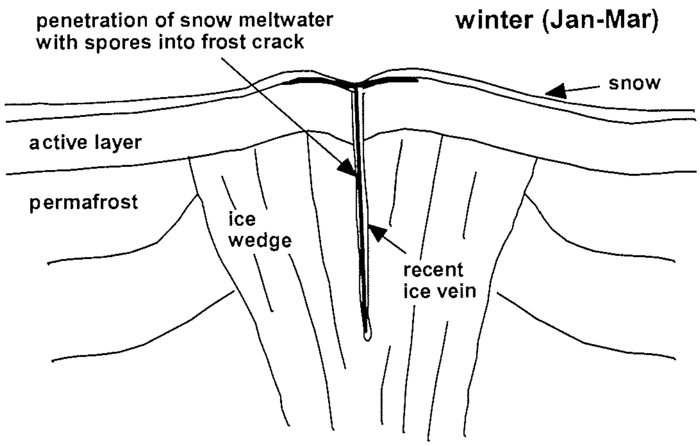

Figure 3-30. Penetration of *lycopodium* spores into the frost crack.

In late summer, 1 kg of red colored *lycopodium* spores was applied to the polygon walls, especially to the troughs in order to avoid drifting of the spores by wind (Figure 3-29). After application, the spores were expected to be covered by the first snow as soon as possible.

In winter, frost cracking takes place and some of the spores may fall into the frost crack. In spring, when the snow cover starts melting, more spores are washed into the crack. Since the water freezes immediately, the spores will be conserved as a thin layer in the newly formed ice vein. This is due to the movement of particles along the freezing front, e. g. towards the centre of the frost crack (Figure 3-30).

After three to five years, the frost cracking activity of every crack can be evaluated. This will give the chance to find a promising digging location for recent ice veins .

3.4 Seasonal progression of thaw depth dependent on mircrorelief

Lars Kutzbach, Ekatarina N. Abramova and Waldemar Schneider

3.4.1 Background

The topography of the Leńa Delta is fairly flat, but well-structured by a prominent microrelief, caused by the development of ice-wedge polygons. Most common are low-centred polygons. The depressed centres of these polygons are surrounded by elevated rims, which are situated above the ice-wedges. The prominent microrelief causes a high spatial heterogeneity of soil properties on the small scale of decimeters to meters. In order to up-scale results of process studies to the landscape scale, it is necessary to describe and quantify the spatial hetorogeneity of soils. A major factor for all physical and biological processes in permafrost soils is the active layer depth (=thaw depth).

3.4.2 Projects

A thaw depth monitoring programm was conducted on Samoylov Island in the period June 10 – August 30. An investigation site of 28 m x 18 m was established close to the new soil survey station (Chapter 3.2, Figure 3.12). A grid of 150 measurement points in intervals of 2 m x 2 m were marked and mapped with a laser tachymeter (type Trimble 3300). At every measurement point, thaw depth was measured every 3 to 7 days by driving a steel rod into the unfrozen soil until the hard frozen sediments were encountered.

3.4.3 First results

Contour maps of the microrelief at the thaw-depth monitoring site and the spatial variability of the mean thaw velocity during the study period are shown in Figures 3-31 and Figure 3-32.

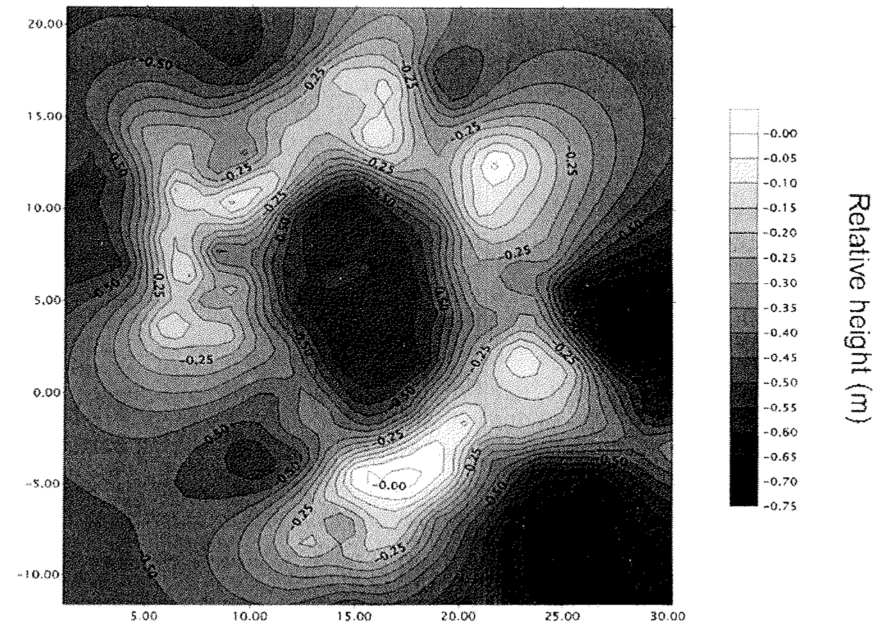

Figure 3-31. Contour map of the microrelief at the thaw-depth monitoring site, Samoylov Island. Units of the coordinate system are meters.

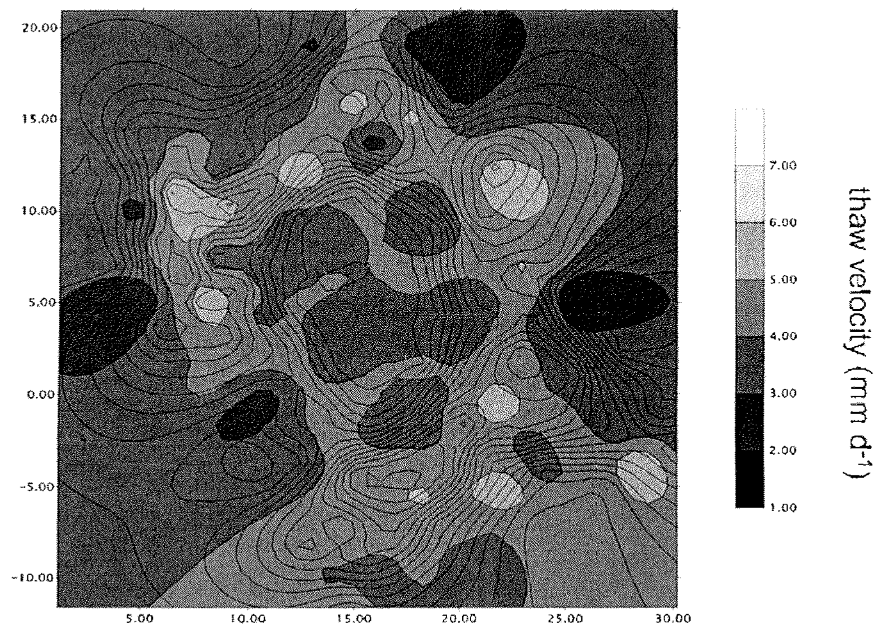

Figure 3-32. Mean thaw velocity during the study period June 10 – August 30 at the thaw depth monitoring site, Samoylov Island. The contour lines of the microrelief (Figure 3-31) are indicated for orientation.

3.5 Patterned ground lakes and their function as sources of atmospheric methane

Oliver Spott, Svenja Kobabe, Lars Kutzbach, Dirk Wagner and Eva-Maria Pfeiffer

3.5.1 Introduction

Lakes are important sources of atmospheric methane (CHANTON et al. 1989; THEBRATH 1991; MICHMERHUIZEN & STRIEGL 1996; SEMILETOV et. al. 1996; PHELPS et al. 1998; DUCHEMIN et al. 1999; MAKHOV et. al. 1999; HUTTUNEN et al. 2001). Permafrost landscapes of the Lena-Delta are often covered by polygonal tundra and patterned ground lakes, respectively. Up to now little is known about the contribution of those small but widespread lakes regarding their function as sources of atmospheric methane. Thus, surveying patterned ground lakes is a necessary part of investigations for estimating both global and local methane fluxes.

3.5.2 Objectives and Methods

In this study, patterned ground lakes were investigated in order to measure their methane fluxes toward the atmosphere. Following questions were set up.

1. How much methane is emitted from the investigated lakes?
2. Which meaning has the path of emission (plant mediation, diffusion, ebullition)?
3. Which habitat parameters (sedimentary, hydrological and atmospheric parameters) are crucial for the emission behavior?

Measurements of methane emissions were carried out by two different types of floating chambers (three of each type) from beginning of July 2002 to beginning of September 2002. Chamber type I was used for measuring methane emissions by plant mediation. The measuring field was stationary and placed within the edge of the lakes where vegetation penetrates the water surface. Plants enclosed by the chamber were *Carex aquatilis* in case of lake IS, *Carex a.*, *Carex chordorhiza* and *Potentilla palustris* concerning PS1 and *Arctophila fulva* within PS2 (Figure 3-33) The enclosure time for plant mediated emission measurements was 30 minutes. Chamber Type II was stationary installed within a non-vegetated lake area (except water mosses at the lake bottom) for measuring both diffusion and ebullition. This type consists of a chamber (diffusion measurements) likewise type I and an additional assembled pyramid below (ebullition measurements) (Figure 3-33). The enclosure time for emission measurements was approx. 48 h. Gas samples from Type I and Type II (concerning only diffusion) were taken by gastight glass receptacles (Gasmaus) (cf. PFEIFFER et al. 1999). Ebullition samples were taken by syringes through a rubber stopper and were immediately conserved in gastight glass tubes filled with saturated NaCl-solution. Emission measurements by the different chamber types were carried out in a time frame of 12.00 to 16.00 o´clock in an alternating

2-day-rhythm. All methane gas analysis were conducted by a gas chromatograph (CP 9003).

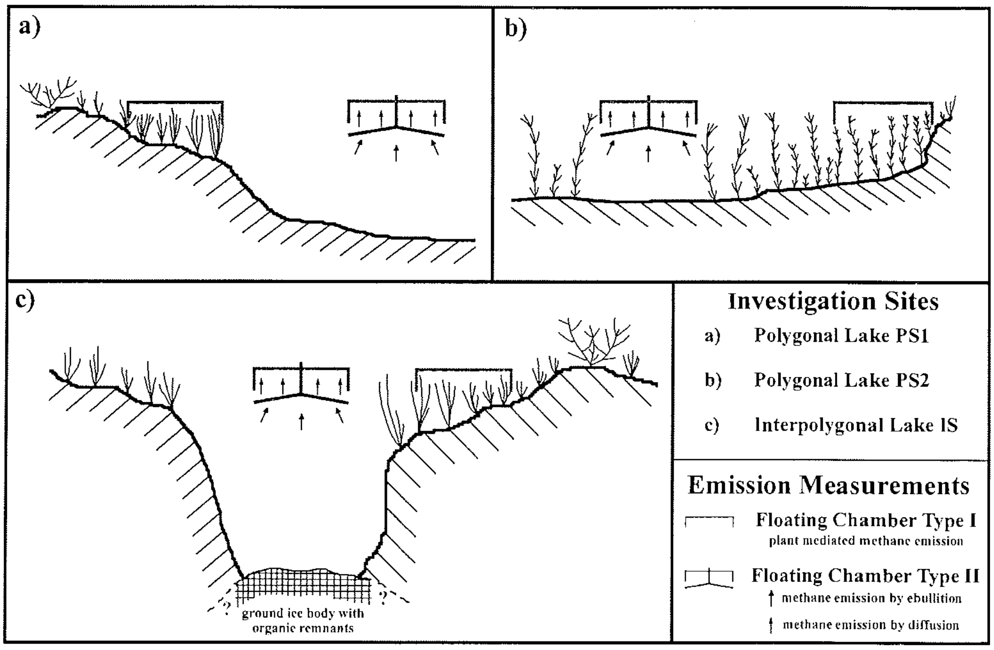

Figure 3-33. Application of floating chambers for methane emission measurements.

Accompanying the methane gas sampling, measurements of permafrost depth, water level, sediment temperature, water temperature, dissolved oxygen (OXI 325 / WTW company) and climatic parameters (temperature, moisture, pressure, wind direction and velocity) where conducted on a daily basis.

Dissolved methane in lake water was analyzed in intervals of 10 to 14 days (Table 3-16). Water samples were collected in gastight glass receptacles (3 parallel samples). Previously an adequate amount of NaCl-salt was weighted into the receptacles to force dissolved methane into headspace. Gas concentrations were analyzed after 1 to 2 days of storage at a room temperature of approx. 18 °C.

For the investigation of lake sediments, 4 drilling cores were captured from PS1 and PS2, respectively (Appendix 3-2). One core in each case were cut up for measuring methane content. Fresh sediment samples (15 to 25 g) were weighted into a 50 ml glass jar (3 parallel samples). 20 ml saturated NaCl-solution was added subsequently to force methane gas into headspace. The glass jar was closed with a septum and a screw cap and gas concentrations were analyzed after one day of storage under cold conditions (0 to 2 °C). The 6 remaining drilling cores were used for analyzing water content, raw density, grain size, pH-value, TOC and DOC as well as for experiments concerning methane production and methane oxidation (Appendix 3-2). For surveying methane gas enclosed in the ground ice body of lake IS (Figure 3-33), one drilling core of ice was obtained and gas concentrations were analyzed (likewise dissolved methane analysis).

For a general description of investigated sites pH-values of the lakes were analyzed. Vegetation was mapped within an area of 2 to 3 m² spreading from the surrounding lake area to the shallow edge of the lakes. Samples of mosses and lichens were taken for later characterization (Appendix 3-1). Morphology and position of the lakes were surveyed by a tachymeter device.

3.5.3 Investigation Sites

Samoylov Island, as a representative example for Polygonal Tundra, is covered by a large number of small patterned ground lakes. Based on the polygonal network of ice-wedges, superficial depressions enable the formation of patterned ground lakes, that can be distinguished in polygonal and interpolygonal lakes. The first type is formed within a lowered center of an ice-wedge-polygon. Interpolygonal lakes are formed between the polygons within lowered frost-cracks.

During the Expedition "Lena-Delta – New Siberian Islands 2002" two polygonal (PS1 and PS2) and one interpolygonal lake (IS) were investigated. All three lakes are situated close to each other in the middle of Samoylov Island in an area of degenerated ice-wedge-polygons. PS1 is nearly round shaped, approximately 15 m in diameter and 0.9 to 1.0 m in depth. PS2 is of an elliptical shape with an a-axis of approx. 18 m and a b-axis of approx. 9 m. The depth reaches 0.6 to 0.7 m. The lake IS is of an elongated network structure with a maximum extension of approx. 40 m. The depth exceeds 1.2 m in some parts .

The investigated lakes are characterized by some remarkable differences. The lake area of PS2 is densely covered by *Arctophila fulva* grass, whereas this is completely absent within PS1 and IS. Lake IS showed large ground ice bodies (ice wedge?). The upper lake sediments of PS1 and PS2, however, were unfrozen during the field work.

3.5.4 Preliminary results and discussion

Methane emission rates within the vegetated edge of investigated lakes show mean values of 58.6 ± 12.5 mg m^{-2} d^{-1} for PS1, 41.7 ± 13.6 mg m^{-2} d^{-1} for PS2 and 34.2 ± 8.0 mg m^{-2} d^{-1} for IS. The maximum rate of 88.7 ± 0.8 % mg CH_4 m^{-2} d^{-1} was measured on 14th of August for PS1. The minimum rate of 13.7 ± 5.0 % mg CH_4 m^{-2} d^{-1} was measured on 31st of July for PS2 (Figure 3-34).

Relatively high rates are caused by mainly plant mediated methane emissions. The amount of emitted methane depends on composition and density of vegetation cover. Plant mediated methane emissions could be proven for *Arctophila fulva* (Figure 3-34). and *Carex aquatilis* (not depicted) as dominant species within the vegetated edges of the lakes. Additionally, sediment temperature shows a distinct influence of emission strength. In case of PS1 the temperature (5 cm depth) correlates significantly (r = 0.80) with the methane emission rate. PS2 and IS show less dependency on sediment temperature, but a weak seasonal trend of the emission strength.

The distinct variability of emission rates from vegetated edges of the lakes is assumed to be mainly caused by the continuous change in air temperature and its feedback in microbial activity as well as plant mediation. The higher emission rates of PS1 may be caused by the density and composition of vegetation (see investigation sites) at the measuring field which acts positive on nutrient cycles and methane formation.

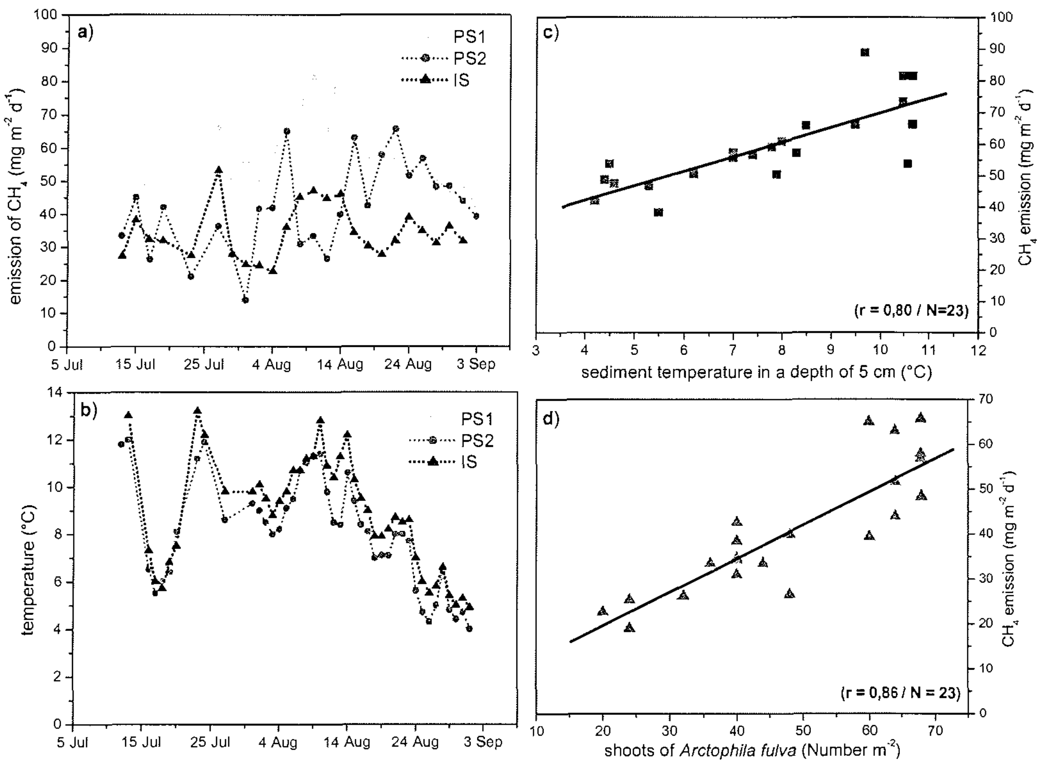

Figure 3-34. Preliminary results of methane flux measurements from vegetated edges of the lakes. (a – methane emission rates; b – sediment temperature in depth of 5 cm; c – temperature dependence of methane emission (PS1); d – plant mediated methane emission by *Arctophila fulva* (PS2))

Methane emission rates from water surface by diffusion show mean values of 1.9 ± 1.1 mg m-2 d-1 for PS1, 3.0 ± 1.6 mg m-2 d-1 for PS2 and 2.2 ± 2.0 mg m-2 d-1 for IS. The maximum and minimum rate were measured for lake IS on 16th of July with 9.9 ± 5.0 % mg m-2 d-1 and on 21st of August with 0.51 ± 1.3 % mg m-2 d-1, respectively. Lake IS shows highest diffusion rates during July whereas PS1 and PS2 increase their diffusion rates at the end of August (Figure 3-35). In case of lake IS the ground ice body is the methane source. Thus, highest emission rates occur in spring time when methane enriched ice from the freezing period of the previous year is melting. Similar effects were already discussed by Phelps (1998) and Michmerhuizen & Striegl (1996). Diffused methane concerning PS1 and PS2 was currently produced by methanogens within the lake sediment. Thus, highest emission rates occur at the summer and early autumn when microbial activity reaches its maximum.

The diffusion behavior towards the atmosphere shows repeating impulses with emission rates up to 7 times of the mean value (Figure 3-35). Following processes are considered to be causal. Regarding air temperature, higher rates occur after rapid temperature decreases (not depicted). Subsequently the vertical water temperature becomes more homogenous and bottom water enriched with dissolved methane (Table 3-16) can be moved easier to the air-water interface by mass transport. Additionally, diffusion at the air-water interface is intensified during a low gradient between water and air temperature.

Methane emission rates from water surface by ebullition show most distinct differences between the lakes. With mean values of 11.7 ± 8.1 mg m^{-2} d^{-1} only lake PS2 can be considered as important for methane emissions by ebullition. The maximum and minimum rate were measured on 23rd of August with 30.24 ± 0.3 % mg m^{-2} d^{-1} and on 18th of July with 1.27 ± 5.0 % mg m^{-2} d^{-1}, respectively. Emission rates of lake PS1 and IS were continuously lower than 1 mg m^{-2} d^{-1}. In contrast to PS2 diffusion from water surface is the dominant path of emission (Figure 3-35).

Differences of ebullition are caused by the volume and methane content of released bubbles. Mean volume of captured bubbles show 3.8 ± 2.4 ml m^{-2} d^{-1} for PS1, 40.0 ± 20.4 ml m^{-2} d^{-1} for PS2 and 3.1 ± 2.7 ml m^{-2} d^{-1} for lake IS. The methane content, however, seems to be of greater influence. Bubbles released from PS2 show a distinct increase up to 50 % methane towards the end of the season, which remains rather constant. Captured bubbles from PS1 show lower methane contents. Only in mid of July and mid of August some higher values up to 19 % were reached. Different conditions for methane formation and/or oxidation within the sediment are considered to be responsible for measured differences. Bubbles from lake IS show lowest methane contents. The bubble release is considered to work similar to the diffusion where melting ice regulates the emission (Figure 3-35).

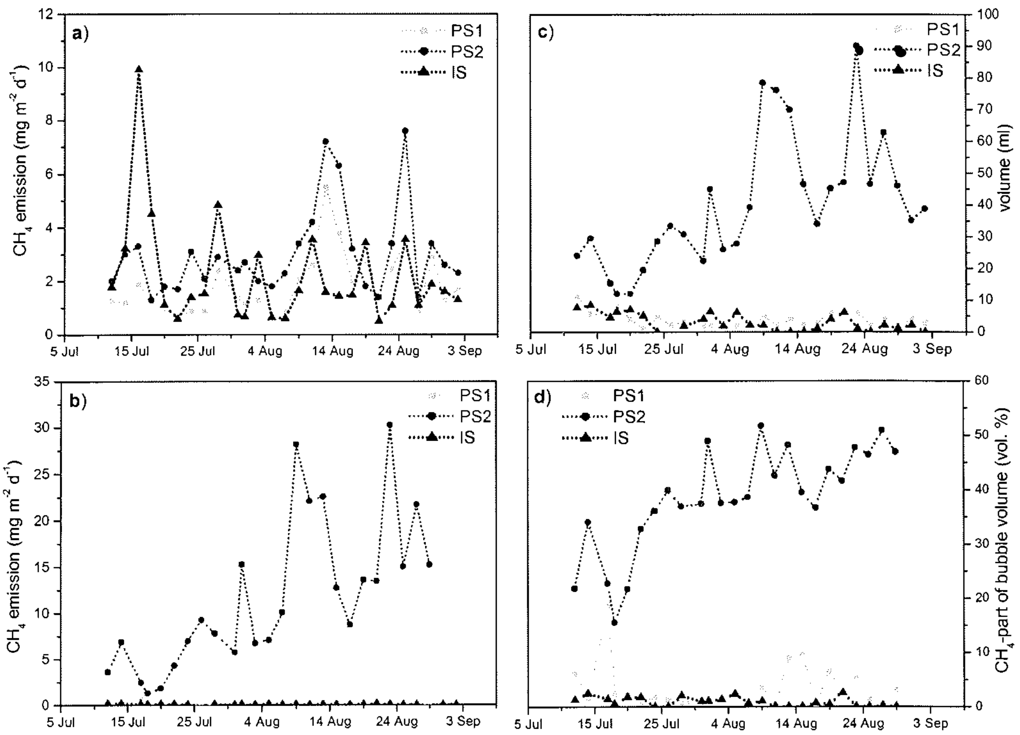

Figure 3-35. Preliminary results of diffusion and ebullition flux measurements from water surface. (a – methane emissions by diffusion; b – methane emissions by ebullition; c – volume of released gas bubbles; d – methane concentration of released gas bubbles).

Table 3-16. Dissolved methane in lake water.

Date of sampling	*surface water (µmol/L)*			*bottom water (µmol/L)*		
	PS1	PS2	IS	PS1	PS2	IS
14. Jul. 2002	0.40	0.98	1.17	0.48	41.09	33.05
24. Jul. 2002	0.34	1.56	1.08	0.38	3.09	32.68
3. Aug. 2002	0.97	1.26	3.97	1.10	0.87	1.48
19. Aug. 2002	1.49	1.50	1.12	1.34	1.99	3.01
31. Aug. 2002	1.45	2.51	2.02	1.83	2.38	2.81

In general, methane emissions from vegetated edges of patterned ground lakes occur similar to methane emissions from wet polygons as described by PFEIFFER et al. (1999; 2000) and WAGNER et al. (2001). Emission by plant mediation acts as the most efficient path for methane gas release into the atmosphere. Thus, vegetated edges of lakes are most important methane sources within investigated lakes. Regarding the efficiency, diffusion as well as ebullition only serve as ancillary paths of methane release towards the atmosphere. Only in few cases methane emission rates reach values of plant mediated emissions. However, considering the spatial distribution of lake areas unbiased by plant mediation the importance of diffusion and ebullition should be assumed to be higher.

3.6 The flora of Samoylov Island – documentation

Lars Kutzbach, Günther Stoof and Anna Kurchatova

3.6.1 Background

The flora composition in the Lena Delta is comparatively rich (373 vascular plant species, 106 moss species and 74 lichen species). There is a combination of arctic, hyparctic and boreal flora elements. Most of the Lena Delta (and so our study site on Samoylov Island) is situated in the northern belt of the geobotanical subregion of the subarctic tundra. Only the most northern areas of the delta belong to the true-arctic tundra subregion (Aleksandrova 1980).

A variety of multidisciplinary ecological and paleoecological studies are conducted on Samoylov Island and the neighbouring islands in the framework of joint projects of the Alfred Wegener Institute and several Russian partner institutions. For many of these studies, for instance investigations on soil genesis or the carbon budget of tundra landscapes, a profound knowledge of the vegetation composition is of great value. Phytosociological studies of present ecosystems are crucial for the paleoecological interpretation of plant remnants in permafrost or lake sediment cores.

3.6.2 Projects

In summer 2002, we conducted two botanical projects:

(1.) We started to establish a digital image database of plants of the study area with a focus on flowering vascular plants. 94 vascular plants, 8 mosses and 8 lichens were photographed and identified. Vascular plants were determined according to Polunin (1959). Mosses and lichens were determined using a reference herbarium prepared by M. Zhurbenko and I. V. Czernyadeva (Komarov Botanical Institute, St. Petersburg). A list of all plants that were included until now in the photo database is provided in Table 3-17 (n = 110). Two exemplary photographs are shown in Figure 3-36 and Figure 3-37.

This documentation of the flora of the central Lena Delta will be published as internet page. It shall help future students, scientists, and other visitors of the region to recognise the plants of this peculiar landscape.

Table 3-17. List of species included in photo database.

vascular plants 1	vascular plants 2	mosses
Alnus crispa	Pedicularis sudetica	Aulacomnium palustre
Alopecurus alpinus	Pedicularis villosa	Aulacomnium turgidum
Antennaria spec.	Poa alpigena	Cinclidium spec.
Arctagrostis arundinacea	Poa arctica	Dicranum elongatum
Arctagrostis latifolia	Polemonium acutifolium	Dicranum spec
Arctophila fulva	Polygonum bistorta	Limprichtia revolvens
Arctostaphylos alpina	Polygonum Laxmanii	Sphagnum spec.
Arenaria arctica	Polygonum viviparum	Timmia austriaca
Arenaria lateriflora	Potentilla palustris	
Armeria maritima	Pyrola rotundifolia	
Artemisia borealis	Pyrola secunda	
Astragalus alpinus	Ranunculus lapponicus	
Astragalus frigidus	Rhodiola rosea	**lichens**
Betula nana	Rumex arcticus	Cetraria laevigata
Caltha palustris	Rumex graminifolius	Cladonia spec
Campanula rotundiflora	Salix glauca	Dactylina arctica
Cardamine tenuifolia	Salix nummularia	Flavocetraria cucullata
Carex aquatilis	Salix polaris	Peltigera spec.
Carex chordorrhiza	Salix pulchra	Stereocaulon alpinum
Carex ensifolia ssp. arctisibirica	Salix reptans	Stereocaulon rivolorum
Carex maritima	Salix reticulata	Thamnoila vermicularis
Carex rariflora	Sanguisorba officinalis	
Cassiope tetragona	Saussurea alpina	
Castilleja pallida	Saussurea nuda	
Chrysosplenium alterniflorum	Saxifraga bronchialis	
Delphinium cheilanthum	Saxifraga caespitosa	
Deschampsia caespitosa	Saxifraga cernua	
Draba nivalis	Saxifraga hirculus	
Draba oblongata	Saxifraga hieracifolia	
Dryas octopetala	Saxifraga punctata	
Epilobium spec.	Tanacetum bipinnatum	
Equisetum arvensis	Tofielda coccinea	
Equisetum variegatum	Tofielda pusilla	
Eriophorum angustifolium	Trifolium repens	
Eriophorum medium	Trisetum sibiricum	
Eriophorum scheuchzeri	Vaccinium uliginosum	
Eriophorum vaginatum	Vaccinium vitis-idaea	
Habernaria viridis	Valeriana capitata	
Hedysarum hedysaroides		
Hieracium alpinum		
Hippuris vulgaris		
Juncus arcticus		
Koeleria asiatica		
Lagotis glauca		
Ledum paluste		
Luzula confusa		
Luzula nivalis		
Luzula tundricola		
Myosotis alpestris		
Myosotis spec.		
Oxytropis arctica		
Papaver radicatum		
Parnassia palustris		
Parrya nudicaulis		
Pedicularis dasyantha		
Pedicularis oederi		

Table 3-18. Moss communities at different habitats. – Sample ID, habitat, species.

ID	habitat	species		
		dominant	**admixed**	**single**
	Samoylov			
I-1	middle floodplain	Tomentypnum nitens		
I-2	- / -	Aulacomnium palustre		
I-3	- / -	Tomentypnum nitens		
I-4	- / -	Tomentypnum nitens		
I-5	- / -	Aulacomnium palustre	Tomentypnum nitens	
II-1-3	high floodplain (microlow)	Limprichtia revolvens	Calliergon giganteum, Meesia uliginosa	Aulacomnium turgidum, Orthothecium chryseum
II-4	(between m/low and m/high)	Ceratodon purpureus	Calliergon giganteum, Limprichtia revolvens	
II-5	(between m/low and m/high)	Tomentypnum nitens	Campylium stellatum, Limprichtia revolvens	
II-6	(microhigh)	Aulacomnium palustre	Tomentypnum nitens, Distichium capillaceum	Campylium stellatum
II-7	(microhigh)	Aulacomnium turgidum	Campylium stellatum	
III-1	first terrace (low-centre polygon)	Meesia longiseta		
III-2	- / -	Calliergon giganteum		
III-3	- / -	Meesia triquetra		
IV-1	first terrace (slope of l/c polygon)	Sphagnum orientale		
IV-5	- / -	Tomentypnum nitens		
IV-6	- / -	Hylocomium splendens var. obtusifolium	Tomentypnum nitens, Aulacomnium palustre, Sphagnum orientale	Aulacomnium turgidum
V-1	first terrace (top of l/c polygon)	Hylocomium splendens var. obtusifolium	Aulacomnium turgidum	
V-2	- / -	Dicranum elongatum		
V-3	- / -	Dicranum congestum		Hylocomium splendens
V-4	- / -	Timmia austriaca var. arctica	Climacium dendroides, Aulacomnium turgidum	
V-5	- / -	Aulacomnium turgidum	Timmia austriaca var. arctica	Abietinella abietina
V-6	- / -	Tetraplodon mnioides	Hylocomium splendens var. obtusifolium	
VI-1-2	first terrace (frost crack)	Limprichtia revolvens	Calliergon giganteum, Campylium stellatum	
VI-4	- / -	Limprichtia revolvens	Tomentypnum nitens	
VI-7	- / -	Campylium stellatum	Limprichtia revolvens	
VII-2	first terrace (low-centre polygon)	Cinclidium arcticum	Calliergon giganteum, Limprichtia revolvens	Aulacomnium turgidum
VII-3	- / -	Meesia uliginosa	Limprichtia revolvens	
VII-4	- / -	Limprichtia revolvens	Calliergon giganteum	
VIII-1	first terrace (wide crack)	Limprichtia cossonii		Calliergon giganteum
VIII-2	- / -	Calliergon giganteum		
VIII-3	- / -	Calliergon giganteum	Limprichtia revolvens	

Table 3-18. continuation.

ID	habitat	species		
		dominant	**admixed**	**single**
IX-1	first terrace (high-centre polygon)	Rhytidium rugosum	Hylocomium splendens var. obtusifolium	
X-1	swamp	Tomentypnum nitens	Aulacomnium turgidum	
X-2	polygon	Dircanum congestum		
X-3	polygonal swamp	Limprichtia revolvens	Campylium stellatum,	
1	polygonal lake 1/slope	Timmia austriaca var. arctica	Tomentypnum nitens, **Hylocomium splendens var. obtusifolium,** Rhytidium rugosum	Polytrichum juniperinum, Aulacomnium turgidum
3	polygonal lake 1/surrounding area		Aulacomnium turgidum, Aulacomnium palustre, Climacium dendroides	Sphagnum contortum
4	polygonal lake 1/litoral zone	Hamatocaulis lapponicus		
6+7	polygonal lake 2/ slope	Aulacomnium turgidum	Hylocomium splendens var. obtusifolium, Tomentypnum nitens, Timmia austriaca var. arctica	
8	polygonal lake 2/ slope	Dicranum acutifolium	**Hylocomium splendens var. obtusifolium,** Tomentypnum nitens	
9+10	polygonal lake 2/surrounding area	Tomentypnum nitens, Aulacomnium turgidum	Hylocomium splendens var. obtusifolium	Sphagnum contortum, Sanionia uncinata
11	polygonal lake 2/surrounding area	Dicranum angustum	**Sanionia uncinata,** Aulacomnium palustre Rhizomnium pseudopunctatum	
12	polygonal lake 2/surround. area	Sphagnum contortum	Aulacomnium palustre, Limprichtia cossonii	
1	Kurungnakh	Polytrichum strictum		
2	- / -	Aulacomnium turgidum	Dircanum congestum	
3	- / -	Hylocomium splendens var. obtusifolium		

(2.) A phytosociological study was conducted on mosses and their adaption to different water regimes dependent on the relief situation. 46 samples of moss cushions were collected from typical landscape units of the islands Samoylov and Kurungnakh. Species were determined by Dr. E. I. Ivanovna (Institute for biological problems of cryolithozone SB RAS, Yakutsk). A list of samples, habitat descriptions, and species composition is provided in Table 3-18. A list of all moss species found in the study is given in Table 3-19 (n=31).

Moss remnants are often very well preserved in permafrost sediments. Thus, the analysis of moss remnants in permafrost drilling cores combined with phytosociological studies on recent moss communities may allow conclusions on ecological conditions in ancient times.

Table 3-19. List of all determined moss species.

moss species (n = 31)
Abietinella abietina (Hedw.) Fleisch
Aulacomnium palustre (Hedw.) Schwaegr.
Aulacomnium turgidum (Wahlenb.) Schwaegr.
Calliergon giganteum (Schimp.) Kindb.
Campylium stellatum (Hedw.)
Ceratodon purpureus (Hedw.) Brid.
Cinclidium arcticum Bruch et Schimp.
Climacium dendroides (Hedw.) Web. et Morh
Dicranum acutifolium (Lindb. et H.Arnell) C.Jens ex Weinm.
Dicranum angustum Lindb.
Dicranum congestum Brid.
Dicranum elongatum Schleich. ex Schwaergr.
Distichium capillaceum (Hedw.) Bruch et Schimp.
Hamatocaulis lapponicus (Norrl.) Hedenaes
Hylocomium splendens var. obtusifolium (Geh.) Par.
Limprichtia cossonii (Schimp.) Anderson et al.
Limprichtia revolvens (Sw.) Loeske
Meesia longiseta Hedw.
Meesia uliginosa Hedw.
Meesia triquetra (Richter) Aongstr.
Orthothecium chryseon (Schwaegr. ex Schultes) Schimp.
Polytrichum strictum Brid.
Polytrichum juniperinum Hedw.
Rhytidium rugosum (Hedw.) Kindb.
Sanionia uncinata (Hedw.) Loeske
Sphagnum contortum Schultz
Sphagnum orientale L.Savicz
Tetraplodon mnioides (Hedw.) Bruch et Schimp. in B.S.G.
Timmia austriaca var. arctica (Lindb) Arnell
Tomentypnum nitens (Hedw.)

Determination by Dr. Biol. Ivanova, Elena I.,
Institute for biological problems of cryolithozone SB RAS, Yakutsk

Figure 3-36. *Pedicularis sudetica*, Samoylov – first terrace, July 02.

Figure 3-37. *Eriophorum scheuchzeri*, Samoylov - middle floodplain, August 19.

3.7 Recent freshwater ostracods in the Lena Delta

Sebastian Wetterich

3.7.1 General introduction

Ostracods are small crustacea (in general up to 1 mm in length) occurring most frequently in the plankton and benthos of oceans, but also in rivers, lakes and swamps. They are characterised by a calcite exoskeleton of two valves. Their exoskeleton is often well conserved in sediments and therefore used in paleoenvironmental reconstructions of temperature, calcium content, salinity and water velocity (Meisch, 2000).

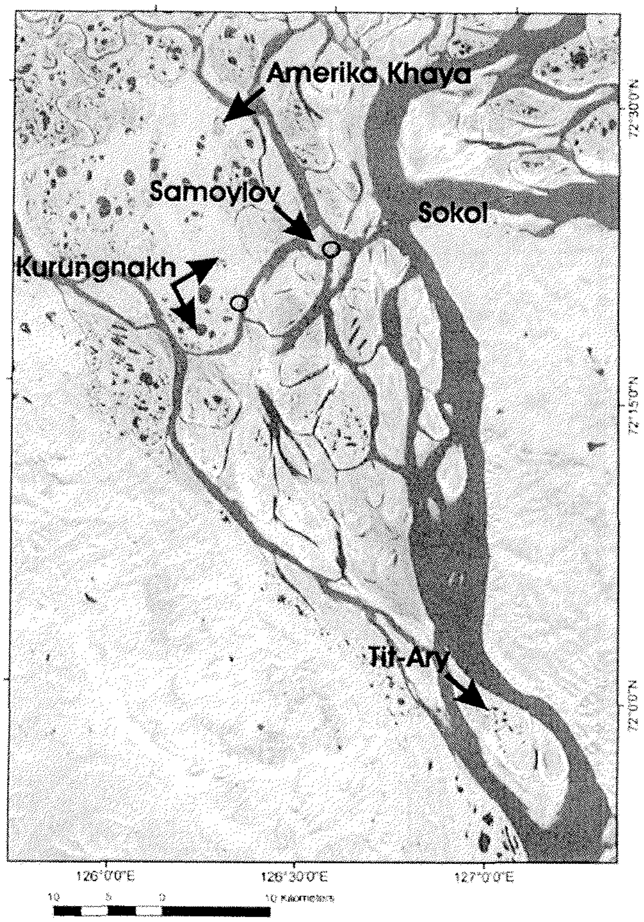

Figure 3-38. Map of the investigation sites (satellite image provided by Statens Kartverk, UNEP/GRID-Arendal and Landsat 2000).

During the Lena Delta Expedition 2002 ostracods were investigated in polygon lakes and alases for description of their species diversity in the delta under recent ecological conditions and for comparison with ostracods of this area dated to the Holocene and the Pleistocene. In total, living ostracods were investigated in 40 lakes in the southern part of the Lena Delta (Figure 3-38) on 4 islands, Samoylov, Kurungnakh (Buor Khaya), Tit-Ary and Amerika Khaya.

3.7.2 Methods

Hydrochemical parameters such as pH, carbonate hardness and total hardness of water [°dH], concentration of oxygen (O_2 [mg/l]), ammonium (NH_4^+ [mg/l]), nitrate (NO_3^- [mg/l]), nitrite (NO_2^- [mg/l]) and phosphate (PO_4^{3-} [mg/l]) were analysed during the fieldwork on means of an analysing set (compact laboratory) by Aquamerck® (Appendix 3-4). The Aquamerck® analysing set works with a scale based on optical gradation, which may be linked with matter concentrations and gives only preliminary results of the investigated parameters. For further investigations in laboratory water samples from each investigated lake were taken (Appendix 3-5). Samples for cation analysis (30 ml) were conserved with 25 μl HNO_3 and samples for anion analysis (15 ml) and residue samples (60 ml) were conserved by freezing. Before conservation samples for cation and anion analysis were filtered on means of a cellulose-acetate filtration set (0.45 μm). Additionally, samples for $\delta^{18}O$-isotope analysis (30ml) were prepared without any conservation and filtration. The conductivity and the surface temperature of the open water bodies were measured with a Conductivity Pocket Meter WTW Cond 330i (Appendix 3-4).

For further analyses samples of the lake sediment about 0.5 kg were taken in each lake. It will be measured the carbon content, ignition loss and granularity. The sediment samples will also be quantitatively analysed for ostracods valves.

Recent ostracods were caught by an exhaustor system (Viehberg, 2000) and conserved in 70 % alcohol. The determination of species will be carried out by characteristics of the soft body in combination with characteristics of the valves.

In addition were described some environmental parameters such as vegetation in and around the lakes, type of sediment and type of lake (Appendix 3-6). For a description of sediments we used the following classification by NÜCHTERLEIN (1969):

- lithogenic (sandy) ground (mineral hard ground)
- loamy ground (mineral soft ground)
- muddy ground (mineral-organic soft ground)
- mouldy ground (organic soft ground, peat)
- plant ground (subaquatic plants).

The most common species of the vegetation in and around the lakes are presented in Appendix 3-6.

The ostracods data in combination with the environmental, ecological and hydrochemical parameters will, for the first time, give a description of the life conditions for ostracods in the Lena Delta.

3.7.3 Types of lakes

In the southern part of the Lena Delta freshwater habitats foı ostracods in the periglacial landscape were investigated. The investigated lakes are situated in several geomorphological units (terraces) of the Lena Delta. The most important processes for the evolution of freshwater lakes are the formation and destruction (ice wedge formation and thermokarst) of polygons (Vtyurin, 1956). So the lakes were characterised as erosion-thermokarst lakes (old branches) and thermokarst lakes (polygons and alases). The following types of lakes were differentiated (Appendix 3-6):

- little polygon lakes with distinct polygonal structure (LPL)
- bigger polygon lakes, formed by several little polygon lakes (BPL)
- polygon trench lakes (PTL)
- alas lakes (AL)
- old branches (OB)

3.7.4 Study areas

Investigation site Samoylov

The main study area was Samoylov Island (Figure 3-38). Altogether 35 lakes on the first Lena river terrace and low, middle and high floodplains (Pfeiffer et al., 1999) were investigated. This island is characterised by several types of polygon lakes in different stages of development and old branches of the Lena river. Not all of the these old branches were regularly floated by the Lena up to now.

Investigation site Kurungnakh

In summary, on Kurungnakh island were investigated 4 lakes: two alas lakes, one little polygon lake and one polygon trench lake on southern part of this island (Figure 3-38). These lakes are situated on the third Lena river terrace.

Investigation site Amerika Khaya

On Amerika Khaya island (Figure 3-38) samples were taken in an alas lake on the third Lena river terrace.

Investigation site Tit-Ary

On the island Tit-Ary (Figure 3-38) in distance of about 50 km to the south of the main study area were sampled four lakes on the lowest floodplain, in old branches and in a lake (SAM-06) between the first and the second terrace, probably formed as a result of neotectonic processes (friendly information of M. Grigoriev).

3.7.5 Preliminary results

Because of the very low concentration of nutrients, the lakes were characterised as ultraoligotrophic. The investigated fauna of ostracods is poor, that means only a few number of species is able to exist under the polar conditions. But the here existing species occur with great abundances. The conductivity of the waters depend on their position in geomorphology (terraces). In lakes regularly floated by the Lena river on floodplains or in old branches higher conductivity were measured than in lakes of the higher terraces. The latter get their water only from precipitation. All investigated lakes were characterised by low value for water hardness and depending on temperature relatively high oxygen concentrations.

3.8 Recent insects of the Central Lena Delta

Svetlana Kuzmina

3.8.1 General Introduction

Because the ecology and distribution of some tundra insects are not sufficiently known, a collection of recent insects from the tundra is very interesting for science. Collections of modern insects are of special importance for paleoentomological research, as they are used to identify fossil remains. In 2000, S. Kuzmina collected modern insects (mainly beetles) during the geological research in the western Lena Delta (Nagym) and in the Central Delta (Kurungnakh and Samoylov Islands). In 2002, the collection of recent insects was a special part of the research program. We installed 20 soil traps on Samoylov Island, established in various biotopes: on the stream bank, in wet and dry tundra and on sand patches among scarce vegetation. The traps were checked every three days. However, most insect specimens were collected by hands in different parts of the island. In total, 762 beetle specimens were collected on Samoylov Island (Appendix 3-7, Figure 3-39).

During a short (three days) excursion to the Tit-Ary Island south of the Lena Delta (Figure 3-39) we managed to collect 107 specimens of modern beetles (Appendix 3-7). The insect fauna of the Tit-Ary area is different from that on Samoylov Island, because Tit-Ary still lies within the forest-tundra zone. One of our aims was to visit Belaya Skala (White Rock) on the right bank of the Lena near Tit-Ary. This location is one of the very rare areas in the Arctic, where the recent occurrence of a pill beetle *Morychus viridis* was recorded. This species was very widespread and abundant in the Pleistocene, and is used as one of important indicators of the past environment. Its modern distribution is considered as a relic one. This extant species was described only recently (Kuzmina, Korotyaev, 1987), but the first modern specimens were found in the lower Lena area (near Bulun) as early as in 1908 by E. Pfizenmayer). About 15 years ago A. Tsybulsky collected *Morychus viridis* further north, at Belaya Skala. We intended to visit the site to study the species habitat in more detail, and probably catch more beetles. Unfortunately, our visit to Belaya Skala was only for a few hours, and we failed to find beetles.

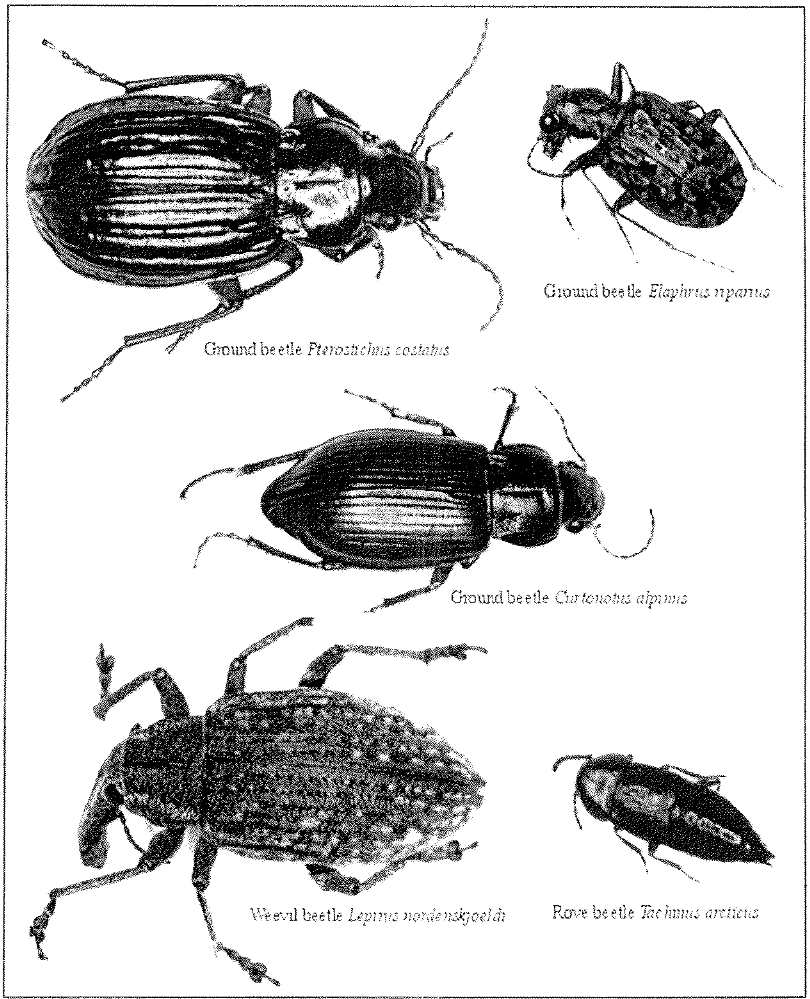

Figure 3-39. Some recent beetles from Samoylov Island.

Some modern beetles were additionally collected by the hydrologists I. Fedorova and M. Tretyakov near the polar station "Sokol", on the right bank of Bykovsky Channel (Figure 3-39). Furthermore, some recent insects were collected near Tiksi. Thus, the collection includes modern beetles from four sites: Samoylov, Tit-Ary, Sokol, and Tiksi (Appendix 3-7).

3.9 Permafrost drilling on Kurungnakh Island

Dirk Wagner, Anna Kurchatova, Waldemar Schneider, Günther Stoof and Mikhail N. Grigoriev

In order to improve our understanding of the carbon dynamic and budget for the Lena Delta region, the methane and carbon content as well as the processes, diversity and physiology of the microbial community have to be addressed not only in the active layer but also in the underlying perennially frozen permafrost deposits. Therefore a permafrost drilling on Kurungnakh Island (N 72°20, E 126°17, Figure 3-38) was carried out in August 2002.

Kurungnakh Island belongs to the oldest terrace of the Lena Delta which was formed in the middle to late Pleistocene and is fragmentarily exposed (30-55 m a.s.l.) in the southern part of the delta. The terrace consists of ice complexes containing fine-grained silty sediments with a high content of segregated ice. The ice complex more over includes enormous layers of organic-rich material and less decomposed peaty material (Chapter 3.10).

The drilling was accomplished with two transportable drilling equipments. The first drilling (KUR-02R) was carried out from the top of the cliff near the exposure (43.4 m a.s.l.), while the second drilling (KUR-02G) was done in an area of thermo erosion, which was about 12 m below the surface (31.2 m a.s.l.) on top of a baydzherakh. With these two drillings it was succeeded to drill through the whole ice complex into the Lena sands. Altogether a 25 m long permafrost core was received by this campaign. A detailed description of the cores is represented in Appendix 3-8. The cores were transported in frozen conditions to Germany for microbiological, molecular ecological and geochemical analysis.

3.10 Paleoecological and sedimentological studies of Permafrost deposits in the Central Lena Delta (Kurungnakh and Samoylov Islands)

Svetlana Kuzmina, Sebastian Wetterich and Hanno Meyer

3.10.1 Introduction

The geological research in the Lena Delta on Kurungnakh (site No. 1: 72° 20' 41" N, 126° 18' 33" E; site No. 2: 72°, 20' 35" N, 126° 18' 20" E) and Samoylov Islands (Figure 3-38) in 2002 was carried out by tree scientists. The main tasks of this small team were:

- cryolithological description of the sections
- sampling of sediments for multi-proxy analysis (e.g. pollen, ostracods, geochemistry, sedimentology) and age determination
- screening sediment for fossil insects
- collection of mammal bones
- determination of the ice content the in the frozen sediments
- taking of ice wedge samples for stable isotope and hydrochemistry analyses by means of an ice screw

The Buor Khaya section on the Kurungnakh Island was the main object of field studies. Besides that we studied two Holocene sections on Samoylov Island. The methods of geological and paleontological investigations were similar as described in the previous expedition reports (Siegert et al., 1999; Sher et al., 2000, 2002). In addition, some other places within the Lena delta were used for recent ecological studies (e.g. Tit-Ary, Sokol).

The Buor Khaya section on the Kurungnakh Island was previously examined by the participants of the Russian-German expeditions "Lena Delta 98, 99, 2000, 2001". (Schwamborn, 1999; Pavlova & Dorozhkina, 2000; Kuznetsova & Kuzmina, 2001; Schirrmeister et al., 2001; Pfeiffer et al., 2002). But for the first time it was possible to study these profiles in more detail. There are a number of age-determinations by radiocarbon and Optic Stimulated Luminescence (OSL) dating and results of sedimentological studies (Schwamborn et al., 2002, Krbetschek et al., 2002). But the sediments have never been screened for fossil insects. During previous research on the Samoylov Island the surface sediments were cored and described (Pfeiffer et al., 2002).

3.10.2 Geological description of the Buor Khaya section (Kurungnakh Island) and two Holocene sections (Samoylov Island)

Chronology

Like in some other Lena Delta sites (Lungersgausen, 1961; Kunitsky, 1989; Grigoryev, 1993), the Quaternary deposits of the Buor-Khaya section are represented by two main units. The lower unit consists sandy deposits corresponding to the stratigraphic locally named Bulukur-Suite. The upper unit is the ice-rich Kobakh-Suite. In this report we use the more common names "Ice Complex" or "Yedoma" for these ice-rich deposits. The sandy unit was dated from 65 to 88 ka BP by the IR-OSL method and from 57 to 37 ka BP by AMS (Schwamborn, 2002). The contradictions of age determinations by different methods are still under discussion (Grosse et al., 2002). The upper ice-rich unit was dated from 50 to 33 ka BP and 17 ka BP in the uppermost part of the Ice Complex. The top of the Buor Khaya section was dated to 7.7 ka BP (Schirrmeister et al., submitted).

Kurungnakh Island

The sands of the Bulukur-Suite are well exposed along the whole section. In some places, especially in the lower part, the sands contain abundant roots and stems of large grasses, probably of *Arctophila fulva*. The exposed "*Arctophila*"-rich sand usually forms very steep or even vertical walls. We observed a similar situation in the Nagym section in the North of the Olenyok Channel (Schirrmeister et al., 2001). The middle part of the sandy unit usually contains silt layers with plant detritus. The upper part of the Bulukur-Suite is built mostly by clean (washed out) sand with little organic material (Table 3-20). Only in some places we found thin layers of fine plant detritus. Thus, the sandy unit consists of the different facies, changing in vertical and horizontal directions. The Bulukur-Sands were studied at site No.2 (Figure 3-401).

Table 3-20. Description of the lower unit (Bulukur-Suite) at the Kurungnakh section.

Altitude [m, a.r.l]	Description
17.2-17.5	grey fine-grained sand (probably a buried soil layer)
10.5-17.2	yellow medium- and coarse-grained sand without visible stratification
7-10.5	intercalation of yellow clean fine-grained sand and grey silty sand with plant detritus; individual layers are up to 0,1-0,15 m thick
5-7	yellow medium-grained sand without visible stratification
0-5	slope debris: sand from the upper part of Bulukur-Suite, peat blocks and liquid mud from ice-rich Ice Complex

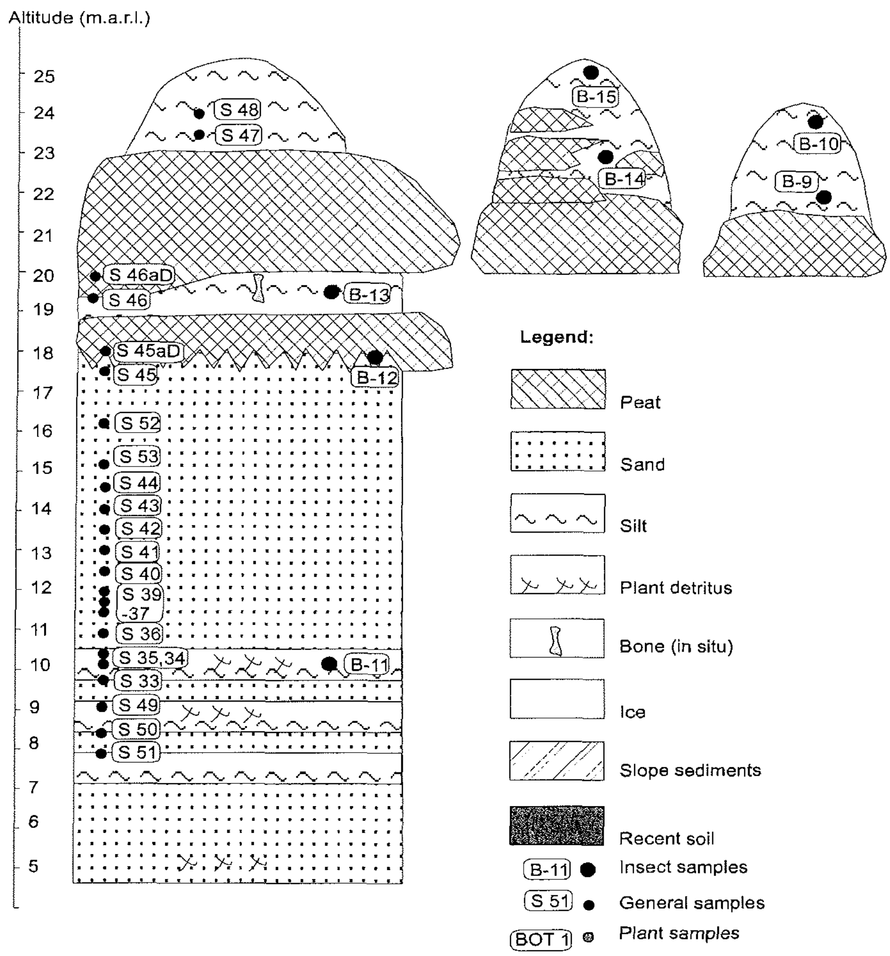

Figure 3-40. Kurungnakh section, site No. 2, Bulukur-Suite and the low part of Yedoma.

The Bulukur-Sands are covered by Ice Complex deposits - ice-rich silt with thick peat horizons, sand lenses and large ice wedges. The boundary between the Bulukur-Suite and Ice Complex is sharp and visible along the whole section (Figure 3-41). The Ice Complex ice wedges sharply narrow near the boundary with the Bulukur-Suite, and their long and narrow tails penetrate 2-3 m into the sand. In 2000, special ice wedges were found and sampled within the Bulukur-Sands (Schirrmeister et al., 2001, p. 95, fig. 5-9, Schirrmeister et al. submitted), but in 2002 we could not observe ice wedges belonging to the Bulukur-Suite. In the Buor Khaya section, the Ice Complex unit is often exposed like an ice wall along the river-bank. This wall, being up to 1 km long, is probably a longitudinal section of the polygonal ice-wedge system. The ice wall is covered by overhanging blocks of peat with frozen silt. These blocks fall down if the underlying ice thaws, and roll down to the Lena bank (Figure 3-41).

Consequently, we could take samples from a block if the place of its original position was evident.

Figure 3-41. Kurungnakh section: Bulukur-Suite and the low part of Yedoma.

The Ice Complex sediments are mostly ice-rich silt with thick peat layers (Table 3-21). The thickest peat layers are observed in the lower part of the Ice Complex. At least three of such layers are clearly observed along the section. In the upper part of the section the peat layers are more rare and less thick. Sandy layers or lenses are often observed near the boundary ice wedge - sediment.

Table 3-21. Description of the Ice Complex sediments at the site No. 1 from the top.

Depth [m]	Description
0-0.2	soil layer
0.2-2.5	grey silt with brown peat hummocks (0.1x 0.15 m) - point 1
2.5-3.2	Ice
3.2-5.7	grey silt with plant detritus – baydzherakhs B and C
5.7-6.5	yellow medium-grained sand near ice wedge – Baydzherakh C
6.0-6.7	grey silt with plant detritus – baydzherakh E
6.7-7.2	reddish-brown peat – baydzherakh E
7.2-9.2	grey silt with plant detritus – baydzherakh E
9.2-11.5	grey sandy silt with grass roots and woody twigs – baydzherakhs F, G, H
11.5-12.2	brown peat – baydzherakh H
12.2-13.2	grey silt – baydzherakh H, G, P
13.2-15.7	brown peat, third (from the bottom) marker horizon in the vertical wall
15.7-19.0	grey silt with plant detritus
19.0-21.5	grey silt with abundant peat lenses and spots
21.5-23.2	brown peat, the second marker horizon in the vertical wall
23.5-24.8	grey silt with plant detritus
24.8-26.5	brown peat, the first marker horizon in the vertical wall

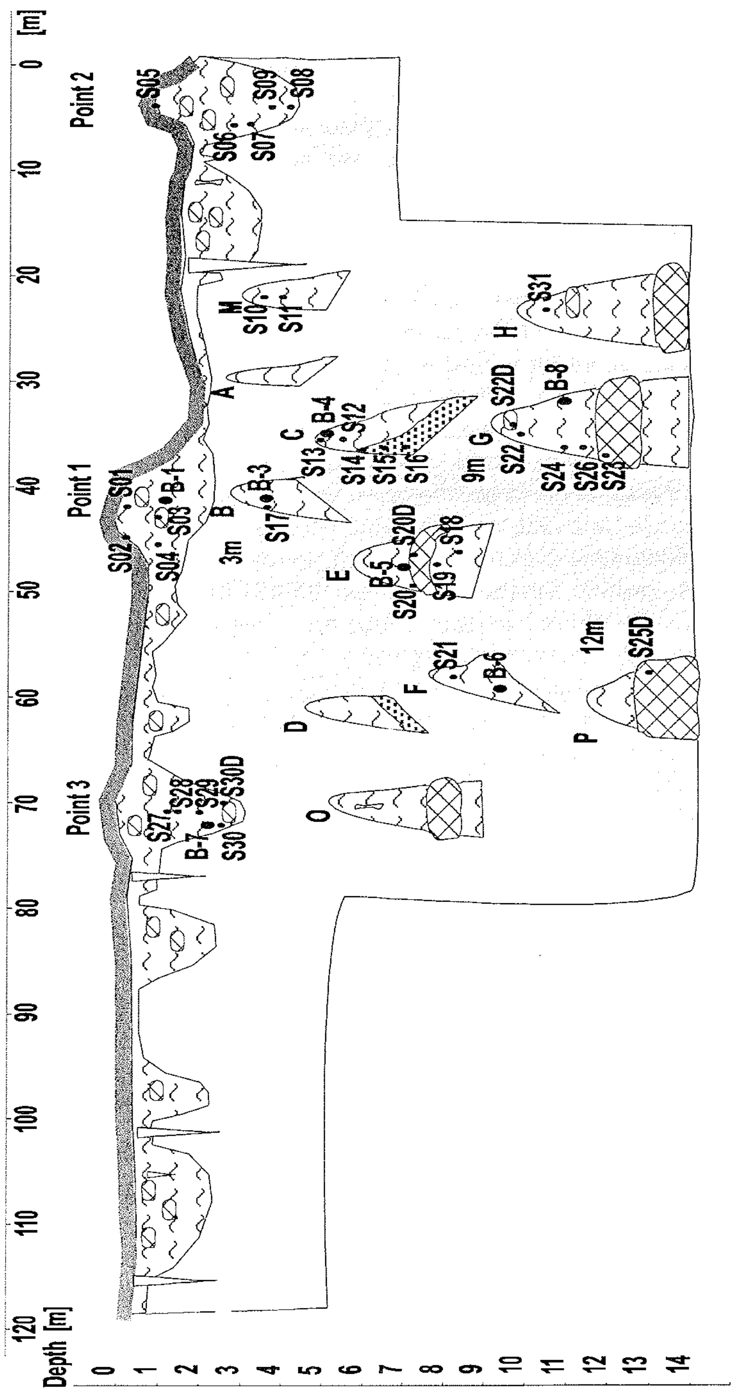

Figure 3-42. Kurungnakh section, site No. 1, Yedoma-Suite.

In the top part of the section, under the active layer, we found a horizon of silt with peat hummocks presumably of the Holocene age. The thickness of this horizon amounts from 0.1 - 0.2 m to 2 m. Small Holocene ice wedges are present here, which often penetrate into the much larger Pleistocene ice wedges (Figure 3-42). A similar situation was observed at the top of the Ice Complex sections on the Bykovsky Peninsula and on Bol'shoy Lyakhovsky Island.

Samoylov Island

In addition, two sections were studied on the Samoylov Island. Section 1 is situated on the bank, 90 m SSE of the camp (the river upstream) on the first terrace above the floodplain, which is built up mostly by peat (Table 3-22) and contains a series of Holocene ice wedges. A site was chosen, where the ice wedges were well- exposed and could be studied best (Figure 3-43). At this site on the South coast of Samoylov Island, a Holocene ice wedge of the first terrace (SAM-IW-1) in the Lena Delta was sampled and described in detail. The ice wedge is 1.4 m wide and 2.2 m high, and because of its preferential thawing, situated approximately 5 m behind the cliff above the Lena river. It is cut perpendicular to its growth direction and characterised by yellowish-white and milky ice with well-developed vertical structures. Single elementary ice veins are 2-3 mm wide, but not easy to differentiate, and contain a lot of small gas bubbles (< 1 mm). At the left side, the ice wedge is limited by clear and transparent ice. At 20 cm from this side, the upper part of a small ice vein continues into the overlying sediment layer. The ice wedge shows a number of cracks, which extend from the upper left to the lower right side of the wedge. These seem to be linked to other processes than frost cracking e.g. tectonic influence, but the reason is still unknown, yet. A number of 17 samples was taken from a 1.4 m long horizontal sampling transsect in a height of 7.0 m a.s.l.. These samples were poured into 30 ml PE bottles, which were closed tightly and sealed with special tape to avoid evaporation of the samples. The samples will be measured for stable oxygen and hydrogen isotope composition at AWI Potsdam.

Table 3-22. Description of the section No. 1 from the Samoylov Island.

Altitude [m, a.r.l]	Description
8.0-7.8	soil layer
7.8-7.3	Horizon I-yellow and greyish-yellow medium grained sand with peat lenses (above the ice wedge) and fine layers (aside of the top of the ice wedge), peat consists of moss and grass stems, the grass is probably Arctophila fulva
7.3-5.7	Horizon II-peat, near the ice wedge turns into peaty silt, brownish-grey silt with woody roots and twigs and relatively large pieces of wood, brown peat, mostly consists of green moss with sedges and "Arctophila" grass, the top of the peat layer has a reddish-brown band of green moss peat.
5.7-5.4	Horizon III-greyish-yellow medium grained sand with grass roots
0-5.4	slope debris

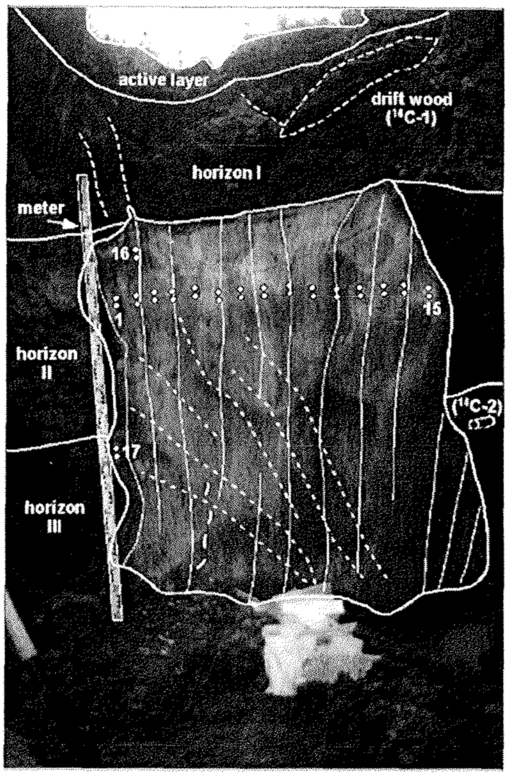

Figure 3-43. Holocene ice wedge in section No. 1on Samoylov Island.

The section No. 2 is the first terrace above the floodplain on Samoylov Island and is composed of silty sand (Table 3-23). The site is situated at the Lena bank, 500 m SSE of the camp. The lower part of the exposure has a wave-cut niche, covered by debris. The upper part is an almost vertical wall, because of abundant plant remains: woody twigs, roots, wood fragments, grass stems, preventing erosion (Figure 3-44).

Table 3-23. Description of the section No. 2 from the Samoylov Island.

Altitude [m, a.r.l]	Description
8.0-7.8	soil layer
7.8-7.2	horizon I-grey fine-grained sand with plant detritus and thin (3-5 cm) layers of yellow clean medium-grained sand
7.2-6.5	horizon II-grey fine-grained sand with lenses of plant detritus, wood fragments, grass roots and stems
6.5-5.5	horizon III-grey silt with woody twigs and roots, plant detritus
0-5.5	slope debris

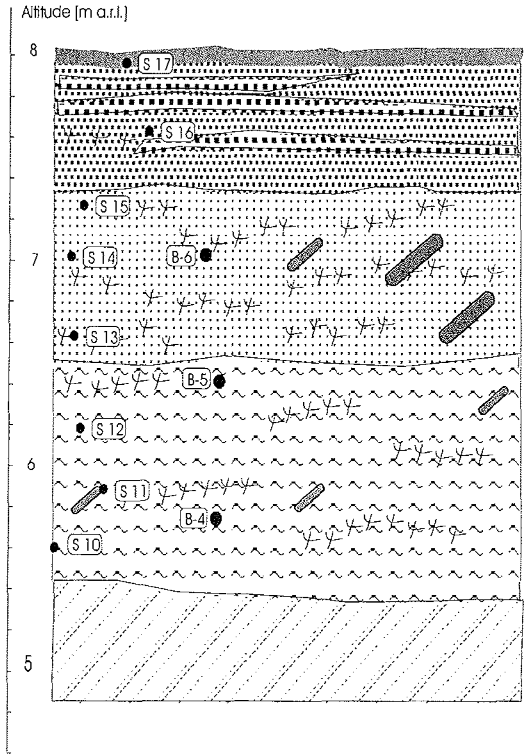

Figure 3-44. section No. 2 on Samoylov Island.

3.10.3 Sampling of permafrost sediment and ice

The samples from the permafrost were taken by knife or axe. In the upper part of the section (Ice Complex unit) we could take samples along a stratigraphic vertical sequence of thermokarst mounds (baydzherakhs) with overlapping tops and bottoms (Figure 3-42). Samples for pollen analyses, ice content determination, sedimentological analysis and ostracod studies were taken separately. Additionally, peat layers were sampled for conventional radiocarbon dating (Appendix 3-9). The ice content was determined gravimetrically on a dry-weight basis, as the ratio of the mass of ice in a sample to the mass of the dry sample, expressed as a percentage (van Everdingen, 1998).

For stable isotope and hydrochemical analysis samples were taken from one Holocene ice wedge penetrating into an older Pleistocene ice wedge in the upper part of the Ice Complex unit (Appendix 3-11, Figure 3-45). We used ice screws to drill a transverse across the ice wedge, in a distance between the drill-holes of about 0.07 m (on three levels) for the this ice wedge. Altogether we get 13 samples for stable isotope analysis and 2 samples for hydrochemical analysis from the first ice wedge. Ice samples were also taken from an ice wedge in the lower part of the section (Appendix 3-11, Figure 3-46), where ice wedges from the Ice Complex penetrate into the underlying sands of the Bulukur – Suite. Next to the ice wedge we found horizontal layered ground ice. Along a transverse across the ice wedge and the ground ice in a distance between the drill-holes of about 0.1 m (on one level) were taken 12 samples for stable isotope analysis and 2·samples for hydrochemical analysis. After melting the ice samples were poured into 15-ml-HDPE bottles. The samples for anion hydrochemical analyses were conserved by freezing and for cation hydrochemistry analyse were conserved with 25 μl HNO_3.

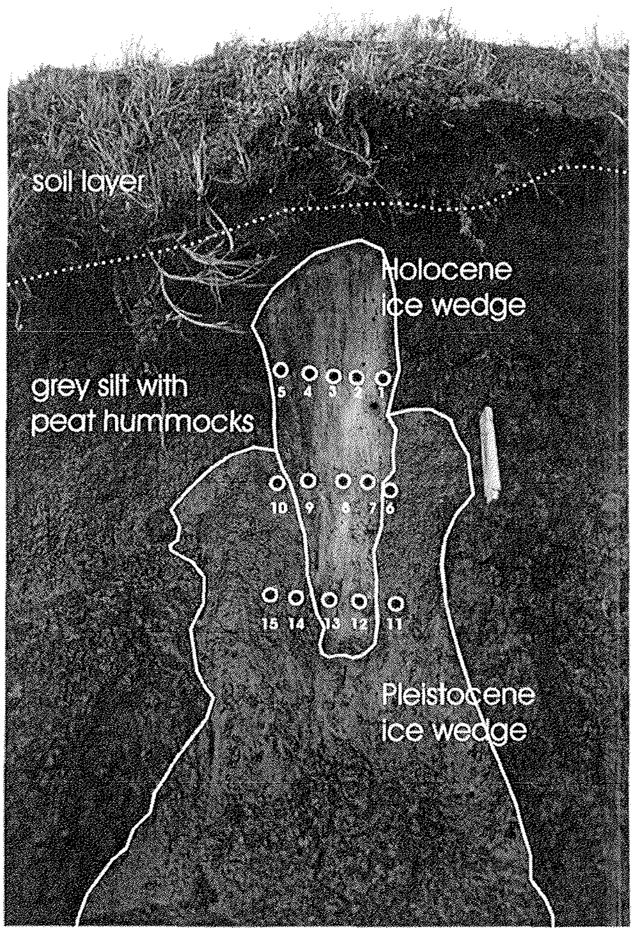

Figure 3-45. Holocene ice wedge in the upper part of the Ice Complex unit on Kurungnakh Island.

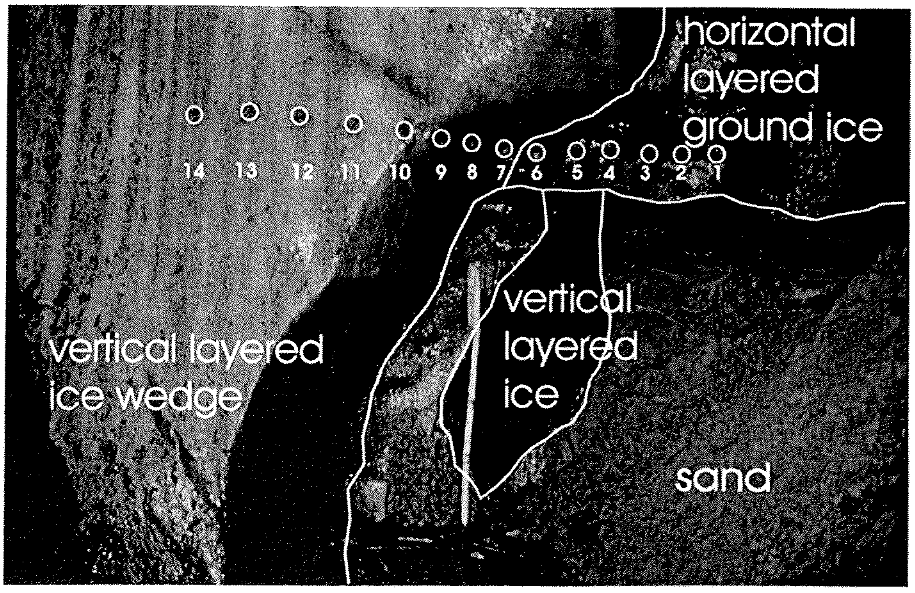

Figure 3-46. Ice wedge in the Bulukur-Suite on Kurungnakh Island.

3.10.4 Screening sediment for insect fossils

In contrast to the previous year, almost all fossil insect samples were taken from thawed sediment in 2002 (Sher et al., 2002). Only one sample (BKh-2002-B7) was chopped by axe from frozen deposits. In this case it was sufficient to take about 30 kg of sediment, instead of 50 kg normally, because insect remains were rather abundant in the screened detritus. Usually, a preliminary screening showed a low content of insect fossils. In these cases, up to 200 kg of sediment were screened.

In the Buor Khaya section, one sample (BKh-02-B1) was screened from the upper, presumably Holocene layer. Nine samples (BKh-02-B2 – B8, B12, B13) were taken from the Ice Complex baydzherakhs (Figure 3-40), four samples (BKh-02-B9, B10, B14, B15) - from two fallen blocks of frozen Ice Complex sediments; one sample (BKh-02-B11) from the Bulukur-Suite (Figure 3-42). From Samoylov Island three samples (Sam-B1 – B3) were taken from the section No.1 (Figure 3-43) and three samples (Sam-B4 – B6) from the section No. 2 (Figure 3-44). In total, we took and screened 15 samples from Buor Khaya site and 6 samples from Samoylov Island (Appendix 3-12).

3.10.5 Collection of mammal bones

Mammal bones were collected during the whole field studies. Following the tradition of 1998-2000 field seasons, we tried to collect all bones found, except evidently indeterminable pieces. In Moscow, Dr. A. Sher helped to identify the bones. However, the total number of collected bones (31) is incomparably less, to those previously found on Bykovsky Peninsula and Bol'shoy Lyakhovsky Island. Only one possibly fossil bone (fragment of reindeer tibia) was found on Samoylov Island. It was picked up on the beach below the section No. 2. During an excursion to Amerika-Khaya Island (Fig. map) a part of deer vertebral column was found, consisting of four connected vertebras. It was buried in peat in the upper part of the first terrace above the floodplain. The terrace is about 6 m high, the vertebral column was found at a depth of 2 m. The main bone collection was found on the Kurungnakh Island. The majority of bones belong to horses. Many bones were found in situ or in liquid mud of the bluff. A few bones (femur, tibia and metatarsale BKh-2002-O9, O17, O20) come from one horse individual. They fell down from the frozen wall related to a location between two peat horizons in progress of permafrost thawing. This place is located about 200 m upstream from section No. 2. A pelvis bone was observed thawing out the permafrost, but it was no chance to collect it. In the same layer near section No. 2 we noticed a big bone, probably femur of horse or bison, that could also not reached. Later, the bone immediately disappeared in liquid mud after melting out and falling down, and our attempts to find it again. In the same layer within several days two branches of one horse mandibula (Bkh-2002-O5, O13) were collected. Thus, the lower horizon of the Ice Complex unit of the Buor Khaya section contains rather abundant bone material. An interesting finding of a muskox metatarsal (BKh-O3), sticking out of frozen silt near an ice wedge was made in the upper part of the Buor Khaya section.

3.11 Hydrological investigations in the Lena River Delta

Dmitry Bolshiyanov, Irina Fedorova and Mikhail Tretiakov

3.11.1 Introduction

The regime of the Lena River as one of the largest rivers of the Arctic has been investigated for more than 70 years (Ivanov and Piskun, 1999). The river delta is most interesting for the study as there is constant reforming of this area related to deposition of a large sediment load.

Exiting to the mouth area, the main river flow divides into numerous arms and transverse channels (Figure 3-47) forming an enormously extensive delta, the third in the world. The total delta area comprises more than 25 thousand km^2 if the Stolb Island is assumed to be the delta apex. If the delta apex is referred to the beginning of bifurcation of its first (Bulkurskaya) channel slightly downstream Tit-Ary Island, the delta area will significantly expand and comprise more than 32 thousand km^2.

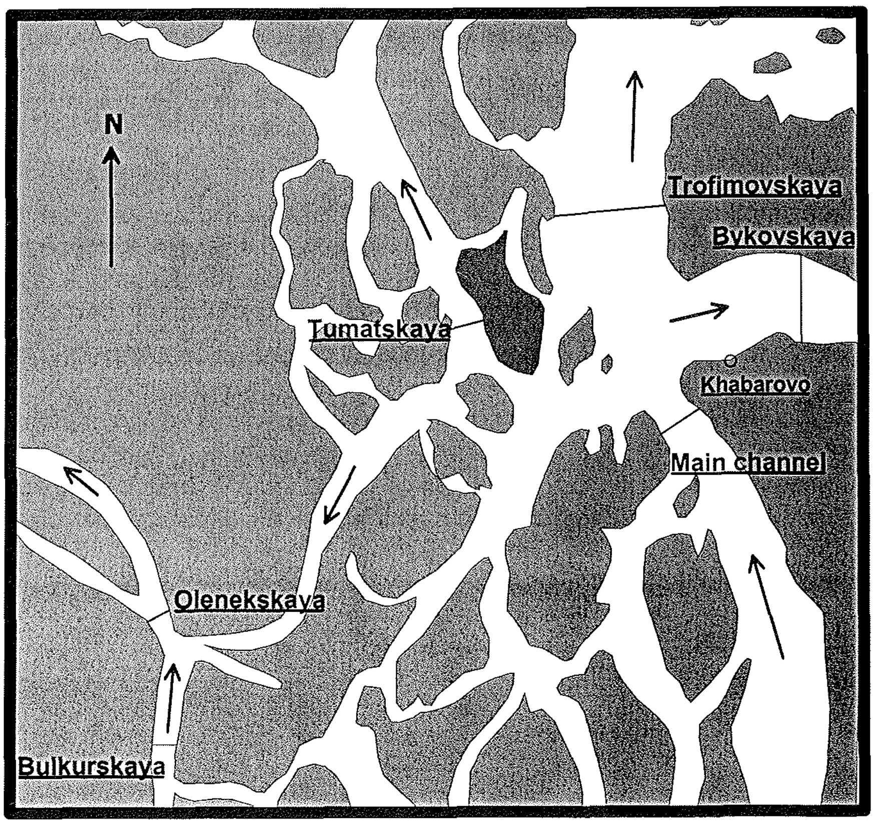

Figure 3-47. Lena River bifurcation by the main delta arms in the vicinity of Stolb Island.

To reveal the typical delta formation features (redeposition of sediments, water discharge changes in the main Lena River channels) for the last decades, a number of hydrometric studies were undertaken in summer of 2002 during the Russian-German Expedition predominantly at the bifurcation point near Stolb Island and at the Sardakh-Trofimovsky bifurcation point. In addition, materials of observations at Khabarov gauging station not published in yearbooks were collected for the period 1982-2002.

3.11.2 Materials and methods

Two main parts of the study can be identified: direct hydrometric measurements and collection of archived data of the Khabarov gauging station. Field observations were conducted twice at the Sardakh-Trofimovsky bifurcation point at the beginning of August and twice at the apex of the Lena delta (Bykovskaya, Trofimovskaya and Main channels in 4.7 km from Stolb Island) – in the middle and end of August.

A complex of hydrometric studies included depth measurements and measurements of the river current speeds and its turbidity (Manual for Hydrological Stations and Posts, 1978).

At the Sardakh-Trofimovsky bifurcation point (STBP), the discharges were measured at four gauge lines made in 2001 (lines 1-4, Bolshiyanov and Tretiakov, 2002) at the time of the "Lena 2001" Expedition and at the additional gauge lines made in 2002 (lines 5-9, Figure 3-48).

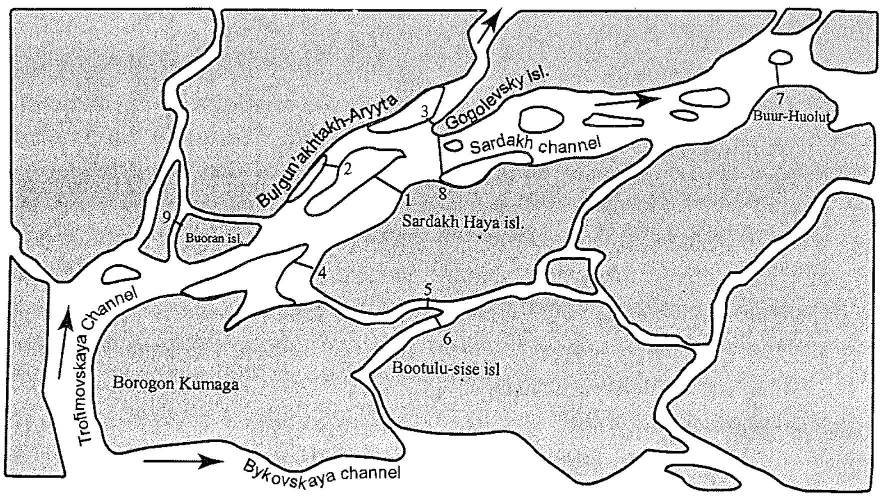

Figure 3-48. Location of the expedition gauge lines in the area of the Sardakh-Trofimovsky bifurcation point in 2002.

At the apex of the Lena River delta, there are 5 gauge lines of standard hydrological observations: the Main Channel of the Lena River in 4.7 km upstream Stolb Island; gauge lines in the Bykovskaya, Trofimovskaya. Tumatskaya and Olenekskaya Channels (Figure 3-47). For the analysis of the river regime at the delta apex and for revealing the main typical features, data on water discharges and turbidity measured in all channels at the main gauge lines (Annual Data on the Regime and Water Quality, 1991-2002) and archived data of multiyear runoff and sediment load fluctuations in the main Lena River channels/Khabarov gauging station were used.

The following scope of work was performed during the expedition:

- Plots of cross-sections of the channels were constructed where in addition to depths, the current speed diagrams are presented allowing us in turn to speak about the distribution of the current speeds in the hydraulic bed section;
- Turbidity in the gauge lines and discharge of the sediment load were calculated;
- Water discharges in the flows of two investigated bifurcation points (first – Sardakh-Trofimovsky and second – near Stolb Island);
- For greater illustration of the runoff redistribution by the channels, the discharges of water and sediment load are plotted in the diagrams.

An analysis of multiyear changes of the water runoff and sediment load discharge in the main channels of the Lena River - Bykovskaya, Trofimovskaya. Tumatskaya and Olenekskaya Channels was performed:

- The percentage ratios of the distribution of water runoff and sediment load discharge by the main channels were obtained;
- The maximum Lena River runoff is estimated;
- The measured and calculated water and sediment load discharges are compared;
- The plots of the water content variations of the main channels over the entire observation period were constructed;
- The difference integral curves of mean annual water discharges of the main channels were plotted.

The cross-profiles of the sections of hydrometric lines in the main Lena channels were constructed on the basis of depth measurements over the period 1980-2000.

3.11.3 Results and discussion

In the course of field work and processing of multiyear observation data, the following facts were revealed:

- The Lena River runoff has a pronounced seasonal character. The greatest runoff portion falls on the first 10 days of June. During this period up to 80 % of the annual water runoff and sediment load discharge passes, that is why the hydrometric measurements during this period are necessary presenting a serious problem due to natural conditions in this period in the Lena delta.
- In the Lena River delta, the water runoff is redistributed as follows: a large portion passes through the Trofimovskaya Channel, 20-25 % falls on the Bykovskaya channel and the fraction of Tumatskaya and Olenekskaya Channels comprises about 10 % (Table 3-24). Thus, the main reformation (deepening) of the river delta bed occurs exactly in the Trofimovskaya Channel.

Table 3-24. Distribution of water discharges for the gauge lines of the main Lena delta channels on August 13 and 26 as compared with a multiyear distribution.

Channel / Date	Main Channel	Bykovskaya	Trofimovskaya	Bykovskaya and Tumatskaya
August 13, 2002	18854	4007	12824	2023
	100%	21,3%	68%	10.7%
August 26, 2002	19247	4778	13394	1075
	100%	24,8%	69,6%	5,6%
Based on multiyear data for the summer low water	100%	25%	65%	10%

During the last twenty years, the runoff fraction through the Trofimovskaya Channel increases. For this, the difference integral curves of the mean annual water runoff in the Main Channel of the Lena River and the main branches of its delta were constructed. As can be seen from Figure 3-49, the water content fluctuations were observed in the Main Channel for the last half a century at the background of the general runoff decrease, however, there is no significant runoff change. Whereas in the Trofimovskaya Channel a clear tendency for the increased water discharge is obvious (Figure 3-50), the same is observed to a lesser extent in the Tumatskaya Channel. For a serious substantiation of these conclusions the currently available data are insufficient and further studies in this direction are required.

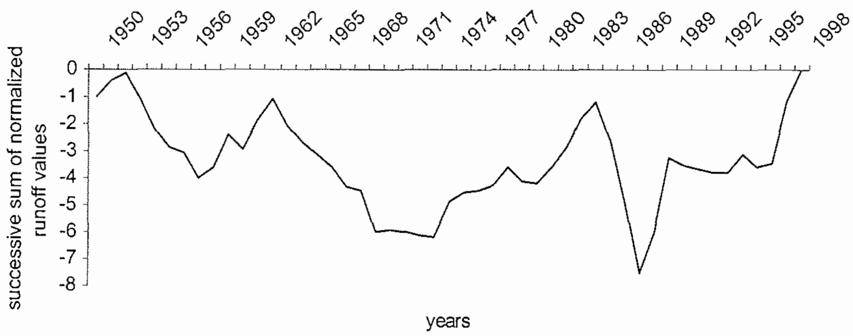

Figure 3-49. Difference intergral curve of the mean annual discharge of the Main Channel.

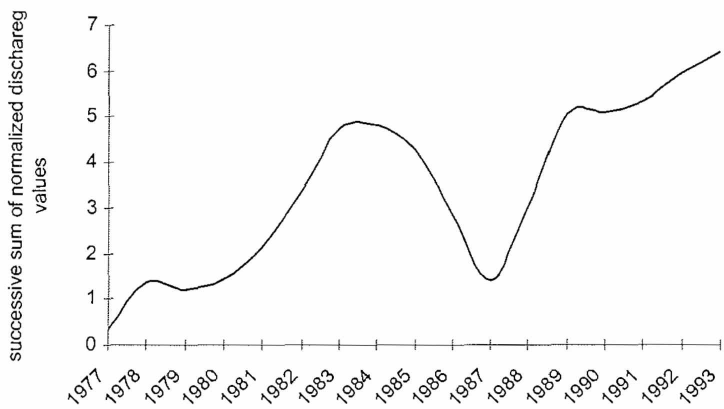

Figure 3-50. Difference integral curve of mean annual discharge of Trofimovskaya Channel.

The distribution of the maximum runoff by the main branches of the Lena River delta presented in Table 3-25 is slightly different: the runoff by the Trofimovskaya Channel decreases to 40-50 % with a simultaneous increase of the fraction of the Olenekskaya and to a greater extent the Tumatskaya Channels.

Table 3-25. Distribution of the maximum water discharge for a multiyear period by the Lena delta branches.

	Period	Main Channel	Bykovskaya	Trofimovskaya	Olenekskaya	Tumatskaya
Greatest discharge (m3/s)	1950-2001	189000 01/06/84	52500 12/06/78			28800 10/06/83
	1977-2001			76300 08/06/74 12/06/83	34300 09/06/85	
		100 %	≅27 %	≅40 %	≅18 %	≅15 %

It is necessary to note that during the measurements and calculations of the maximum runoff (both liquid and solid), large errors are possible. The absence of the observation data on turbidity and sediment load discharge during the flood period does not allow a precise evaluation of the solid discharge volume and its distribution by the main delta channels. For example, the measurements in the Olenekskaya and Tumatskaya Channels are extremely few for their reliable interpretation while measurements of the locality and speeds of current during the flood period are more often absent.

As can be seen from the plots of depth measurements in the Lena River branches, the depth decreases in the major gauge line of the Main Channel of the River and in the Bykovskaya Channel along with its expansion (Figure 3-51). Bed silting is also typical of the Olenekskaya and Tumatskaya Channels. There were no significant bottom changes in the Trofimovskaya Channel for the last 20 years confirming once again the increased water runoff to this delta branch. However, at the Sardakh-Trofimovsky bifurcation point, erosion of Sardakh Island shore occurs (Figure 3-52, Atlas of Sardakh Channel, 1949; Seleznev, 1986), which is accompanied with significant current speeds (Figure 3-53) and a large discharge of sediment load in the Trofimovskaya Channel (between 50 to 80 % of the total solid discharge volume in the delta).

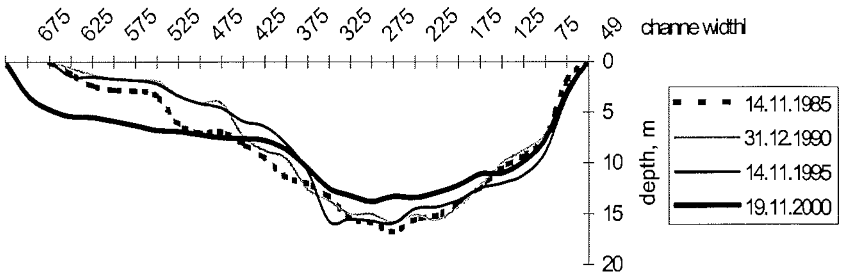

Figure 3-51. Depth change of Bykovskaya Channel for the last 15 years.

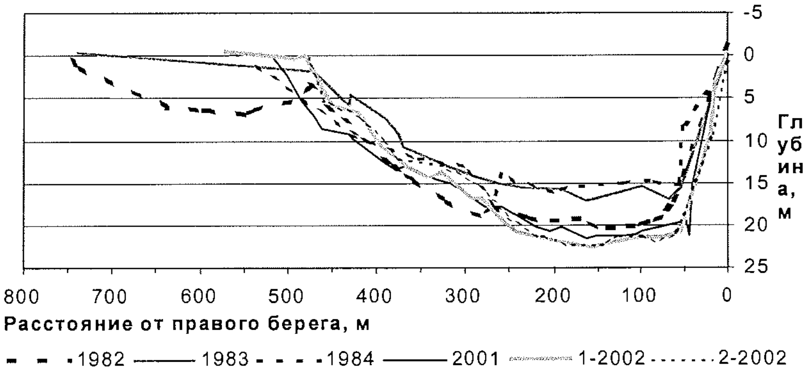

Figure 3-52. Depths in the gauge line No. 3 over the period 1982-2002.

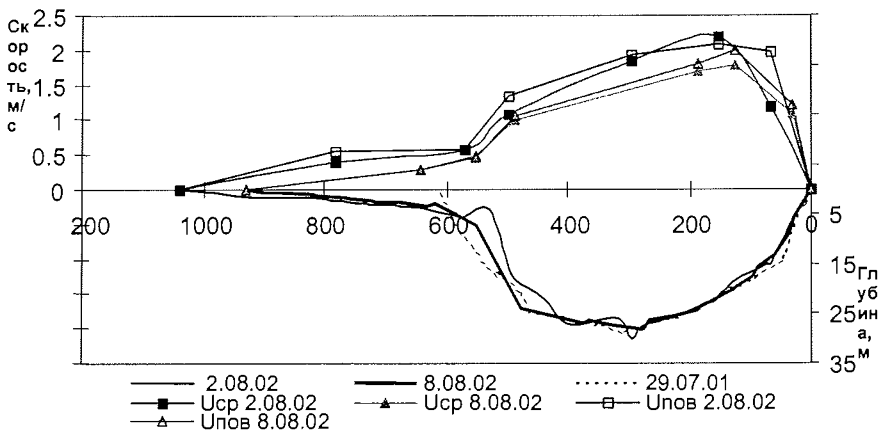

Figure 3-53. Depths and current speeds in the gauge line near Sardakh Island.

- At the Sardakh-Trofimovsky bifurcation point, there is an intense increase of Trofim-Kumaga sand shoal with a simultaneous erosion of the right bank near Sardakh Island (Figure 3-54). At the present time, 95% of the runoff of the Trofimovskaya Channel passes close to this island, which bifurcates then into two parts (Figure 3-55). An evaluation of the bed stability in this region and the construction of the hydrodynamic model can be the next stage of the studies in the Trofimovskaya Channel.

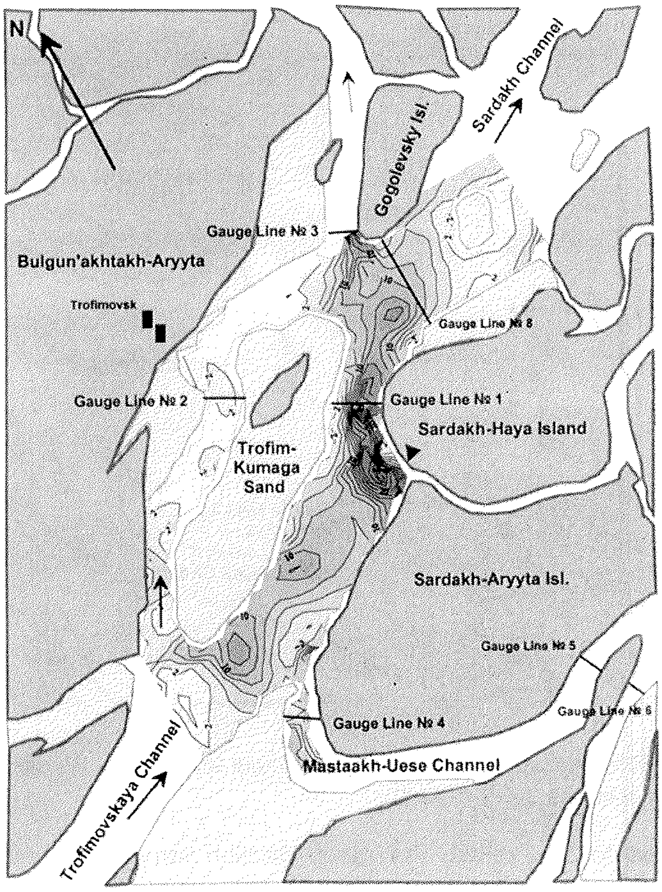

Figure 3-54. Bathymetric map-diagram of depths plotted from data of measurements on August 5-7, 2002.

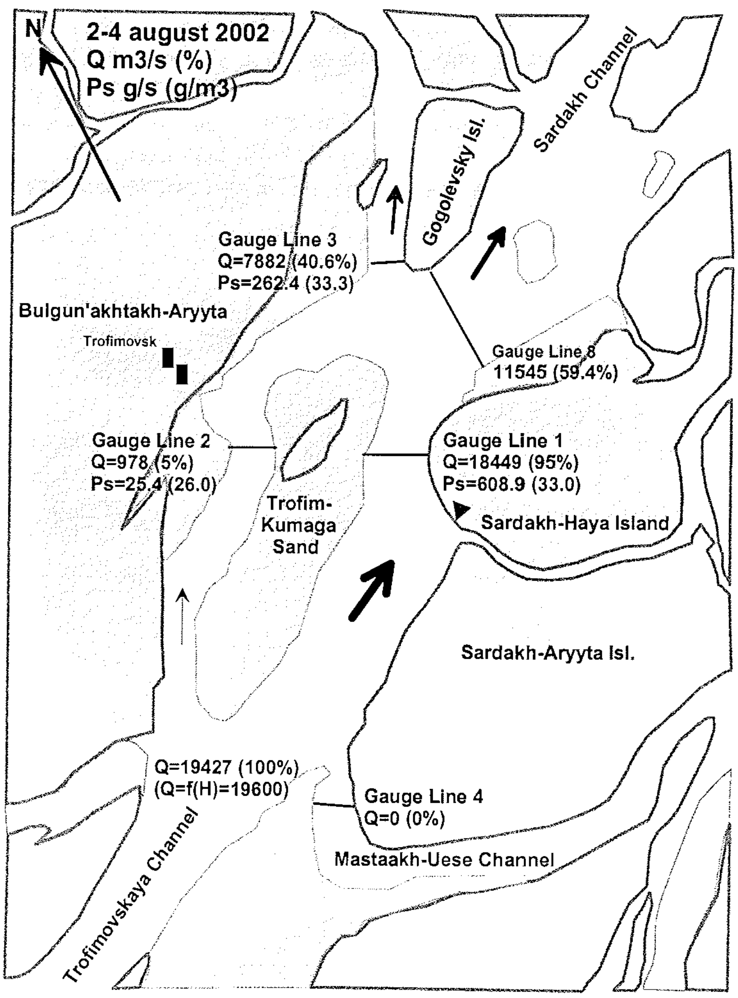

Figure 3-55. Discharges of water and sediment load at the Sardakh-Trofimovsky bifurcation point, August 2-4, 2002.

- Compared to the 1980s, the runoff fraction through the Trofimovskaya Channel has decreased to 40% increasing up to 60% correspondingly for the Sardakh Channel. Water turbidity in this channel downstream the bifurcation point increases. All this indicates that the Sardakh Channel at present is a developing water stream and further changes should be expected here.

3.11.4 Conclusion

The obtained results indicate a constant and sufficiently intense delta formation at two investigated bifurcation points: near Stolb Island and near Sardakh Island. There are obvious tendencies for the change in the direction of bed deformations of the channels in these regions, which provides grounds for further full-scale studies. It is also of interest to investigate the ion and heat sink in the Lena River delta since as compared to large rivers belonging to the Arctic Ocean Basin, the Lena River has a greater concentration of ions. As a qualitative indicator of the heat sink, one can use a constancy of water temperature, which is often twice as high as the air temperature for a long summer period.

The Lena River delta is a unique object of studies especially from the viewpoint of the hydrological and hydrodynamic features of the processes that govern the delta formation factors.

3.12 Shore erosion in the apex of the Lena Delta

Mikhail. N. Grigoriev

3.12.1 Introduction

Accumulation and erosion in the coastal zone and deltas are of major importance for the sediment budget of the Laptev Sea. The sediment balance within the Lena Delta is still an open question. The portion of sediment that is deposited in the Lena Delta and the sediment flux from eroded delta islands is not known. However, the modern sediment output from the Lena Delta exceeds the amount of deposits accumulating in that area.

One of the goals of the coastal team was to conduct reconnoitering studies of shore dynamics in the apex of the Lena Delta. The first part of the studies carried out in July 2002 was to evaluate the dynamics of erosive island shores and to study the resulting sediment flux. In total 34 key sites, which are characterized by active shore erosion, were investigated in order to estimate the range of shore retreat rates and the amount of sediment entering the branches of the Lena Delta due to shore erosion (see Fig. 3-56). Most studied sites belong to the islands composing the first terrace above the floodplain, which is the dominating geomorphological level in the studied area.

3.12.2 Methods

The methods to estimate shore dynamics are simple in principle. Measurements of the distance between the shoreline and some natural land forms (marks), which can be identified on an aerial photograph or a small scale map, have been carried out by a special tape measure. As natural marks mostly small lakes with stable shores were used. Most often we simply measured the distance to the cliff edge ignoring the width of the beach. The comparison of the modern field data with remote sensing information taken in the past decades allows to calculate the average annual retreat rates of selected shores. Aerial photographs (scale 1:40 000-1:70 000, taken 1951, 1962, 1972), topographic maps (scale 1:25 000-1:100 000) and satellite images were used. For the quantification of the sediment flux resulting from shore erosion, average ice content and specific density of the deposits composing the shores in the apex of the Lena Delta were taken into account. In total ca. 60 km of shore cliffs were studied in respect of erosion rate.

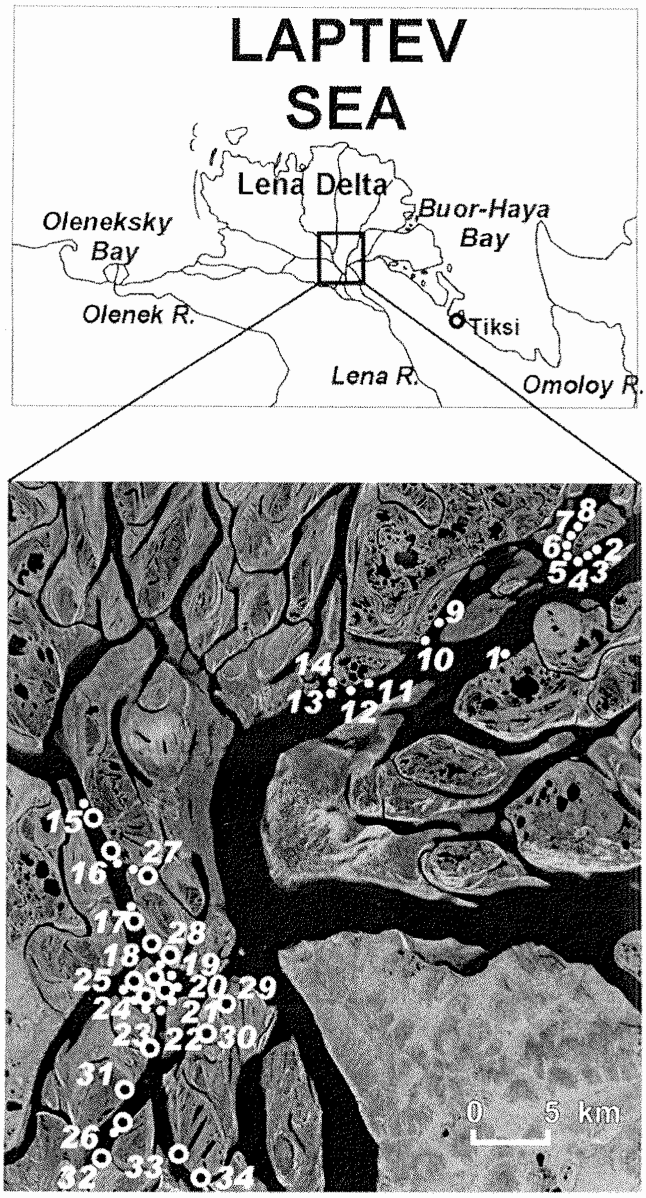

Figure 3-56. Key sites for measurement of shore retreat rates in the Lena Delta Apex (2001-2002). White circles – key sites 2001, Black-and-white circles –key sites 2002.

3.12.3 Results

The main results are shown in Table 3-26. All stations were located along the shores of the first terrace and the floodplain in the delta apex. The average cliff height is about 6 m (3-11 m) and the average retreat rate of actively eroded coast is about 3.9 m/yr. The shores exposed to the current of the main channels are destroyed much faster - for example stations 4-6 (Gogolevsky Island) and station 20-21 (Samoylovsky Island). The maximum retreat rates were observed at Gogolevsky Island (station 5, south-western cape) which divides the two largest delta channels: Trofimovsky and Sardakhsky (Fig. 3-56).

The comparison of the shoreline position on an aerial photograph of Samoylovsky Island taken in September 1980 with the shoreline taken from a satellite image (Landsat, July 2000) shows that there has been a considerable modification of the margins of the island during the last 20 years. It has to noted that changes of the western and northern shorelines positions are difficult to evaluate because the contours of these low and flooded shores strongly depend on the river-water-level, which is highly variable.

In 2001 the average retreat rate of all studied actively eroded coasts was 4.7 m/yr. In 2002 new data on additional eroded sites were obtained, which indicate lower retreat rates. The average retreat rate of all (2001 and 2002) studied coasts is 3.9 m/yr and the sediment flux calculations were revised accordingly.

At the moment it is not possible to accurately quantify the volume of sediments resulting from eroded shores for the whole delta. But the preliminary results indicates that this sediment flux cannot be ignored. Based on average retreat rates of 3.9 m/yr (R), average cliff height of 6 m (H), average ice content of 20% (Ice coefficient = 0.8) and an average specific density of 1.6 g/cm^3 (SD), the sediment flux from the studied 60 km shores (L) in the Lena Delta can be quantified in the following way:

3.9 (R) • 60000 (L) • 6 (H) • 0.8 (Ice coefficient) • 1,6 (SD) = 1797120 t/yr

3.12.4 Discussion and conclusion

There are a number of unsolved questions concerning the sediment balance of the Lena Delta: (1) it is not known how much sediment is deposited within the delta, e.g. on the surface of floodplains, along the delta margins and within near-delta shallows; (2) it is very difficult to estimate the sediment input from eroded sand banks; (3) there is no information on the volume of the bed-load discharge; (4) almost nothing is know about the sediment dynamics during the spring-flood. Nevertheless, the fact that only local sections (60 km length) of the eroded island shores within the delta can supply about 1.8 m million tons of sediments per year, shows the great importance to erosion processes in the sediment balance of the delta.

We have only studied actively eroded cliffs in the area where the delta channels are characterized by fastest currents and highest water levels. Evidently, it is impossible to transfer the obtained sediment flux parameters to the entire Lena Delta. However, in any case the preliminary results of this study suggest that the sediment flux from eroded shores of the Lena Delta plays an important role in the sediment budget of the Laptev Sea. In 2001-2002 our measurements concentrated on erosive shores only and the next step will be to include accumulative shore sections as well.

Table 3-26. Average retreat rates of actively eroded shores at the key sites in the apex of the Lena Delta (2001-2002).

Key sites	Average retreat rate, m/yr	
	July -August 2001	July 2002
1. Sardakh-Aryta Island	4.8	-
2. Gogolevsky Island	2.1	-
3. Gogolevsky Island	1.9	-
4. Gogolevsky Island	12.2	-
5. Gogolevsky Island	14.2	-
6. Gogolevsky Island	13.4	-
7. Gogolevsky Island	4.5	-
8. Gogolevsky Island	2.3	-
9. Trofimovsky Island	8.4	-
10. Trofimovsky Island	6.7	-
11. Baron Island	9.2	-
12. Baron Island	3.6	-
13. Small Baron Island	5.4	-
14. Small Baron Island	3.7	-
15. Matvey-Aryta Island	4.7	4.5
16. Matvey-Aryta Island	6.1	6.0
17. Yrbylakh-Aryta Island	2.7	2.4
18. Samoylovsky Island	1.4	1.4
19. Samoylovsky Island	1.6	1.5
20. Samoylovsky Island	2.9	3.0
21. Samoylovsky Island	3.4	3.3
22. Samoylovsky Island	1.9	2.0
23. Samoylovsky Island	1.9	1.8
24. Samoylovsky Island	1.5	1.4
25. Samoylovsky Island	2.1	2.0
26. Sordokh-Aryta Island	1.6	1.7
27. Matvey-Aryta Usland	3.3	3.4
28. Yrbylakh-Aryta laland	-	1.8
29. Debenek-Aryta Island	-	1.2
30. Sistekh-Aryta Island	-	3.0
31. Sasyl-Ary Island	-	2.4
32. Sordokh-Ary Island	-	2.7
33. Sistekh-Aryta Island	-	4.2
34. Sistekh-Aryta Island	-	5.1
Average retreat rates of actively eroded shores	**3.9**	

3.13 Species composition, ecology, population structure and seasonal dynamic of zooplankton from tundra water basins in the Lena Delta

Ekatarina N. Abramova

3.13.1 Objectives

Information concerning pelagic fauna of the lakes and rivers at extreme latitudes in the Russian Arctic is still limited, and the Lena Delta is no exception. Investigations of zooplankton in the Lena Delta started at the beginning of the XX century, during Russian Polar expedition 1901-1903. However, the knowledge about the structure and functioning of zooplankton community in this big region is insufficient numbering only several papers (Rylov, 1928; Bening, 1942; Urban, 1949; Pirozhnikov & Shulga, 1957; Pirozhnikov, 1958; Botvinnik & Vershinin, 1958; Ammosov, 1961; Kerer, 1968; Serkina, 1969, Sokolova, 1984, Abramova, 1996; Stepanova & Abramova, 1997; Abramova & Sokolova, 1999; Gukov, 2001; Akhmetshina & Abramova, 2002) that offer certain information about species composition and abundance of zooplankton from some parts of the Lena Delta. Generalization of the special investigations is still lacking. This primarily concerns seasonal variations in the structure of zooplankton assemblages.

In the present study, we examined the zooplankton assemblages in channels, terrace lakes, big and small thermokarst lakes from the different regions in the Lena Delta. The data on species composition, distribution, population structure, and seasonal dynamic of zooplankton abundance in relation to water temperature were analyzed.

3.13.2 Materials and Methods

In July – September 2002, 75 quantitative and qualitative zooplankton samples were collected as a part of biological investigations in the Delta-2002 expedition. The samples were obtained in water basins of different type on the Samoilovskii, Tit-Ary, Amerika-Khaya, and Buor-Khaya islands in the Lena Delta (Table 3-27). Regular investigations were carried out on the Samoilovskii Island only.

Table 3-27. Location and number of zooplankton samples.

	Samoilovskii	Tit-Ary	Amerika-Khaya	Buor-Khaya
Olenekskaya channel	9			
Terrace lake	13	5		
Big thermokarst lake	4	3		
Deep polygon without plants	10			
Shallow polygon with plants	9	2		2
Crack between two polygons	9			
Alass			4	5

Sampling was performed by filtering of 100 liters of water through a 100 µm meshsize net with periodicity of 5-10 days and fixation with 70% alcohol. The whole sample or its part was studied in the Bogorov's camera under microscope, and the abundance of organisms was calculated. We determined species, sex and moulting stages. The data were recalculated to 1 m^3 of water. Water temperature was measured simultaneously with plankton sampling.

3.13.3 Preliminary results

Species composition

In the water pools of the Lena Delta, 106 taxa of zooplankton belonging to 2 types (Rotatoria and Arthropoda) were determined: Rotatoria – 61 taxa, Arthropoda, subclass Crustacea – 45 species, among them: Copepoda – 30 species (Cyclopoida – 14, Calanoida – 14, Harpacticoida – 2), Cladocera – 13, Phyllopoda – 2 (Appendix 3-14). There are well-manifested differences in species composition in water basins of different types. The highest species diversity was recognized in the terrace lake on the Samoilivskii Island (54 taxa), and the lowest species diversity was determined in the alass on the Amerika-Khaya Island (11 taxa). Zooplankton species composition was clearly dominated by Rotatoria. The latter reached maximum diversity in the channel, terrace lakes, and alases, where they constituted up to more than 60% of the total species richness (Fig. 3-57). Copepoda (about 45% of the total species number) and two species of Phyllopoda were the main component of zooplankton in the polygon lakes. Cladocera was widely distributed in all types of water pools, especially *Chidorus sphaericus*, but species diversity of this group was comparatively low.

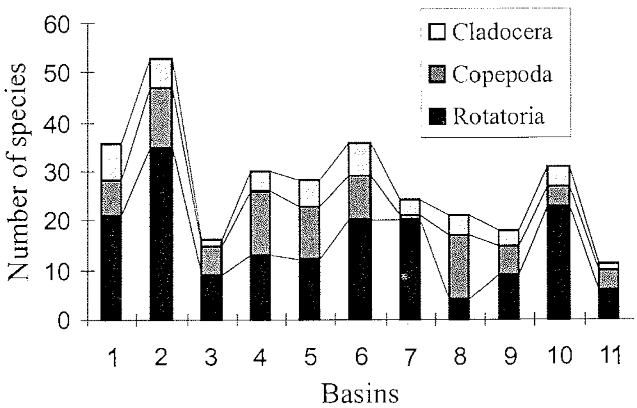

Figure 3-57. Distribution of species numbers in the different water basins in the Lena Delta: Samoilovskii Island: 1 – Olenekskaya channel, 2 - terrace lake, 3 – big thermokarst lake, 4 - polygons , 5 - crack between polygons; Tit-Ary Island: 6 - flood-plain lake, 7 – big thermokarst lake, 8 - polygons; Buor-Khaya Island: 9 - polygons, 10 – alas; America-Khaya Island: 11 - alas.

Variations in the species composition and abundance dynamics

Seasonal variations in the species composition and zooplankton abundance were well manifested in the water basins on the Samoilovskii Island. Rotatoria demonstrated high density in zooplankton communities of the Olenekskaya channel and terrace lake during the whole period of our investigation. Maximum zooplankton abundance in the Olenekskaya channel (16860 ind.m^{-3}) had been observed at the beginning of July at 14°C of water temperature and was related to reproduction of common species of Rotatoria: *Asplanchna priodonta; Keratella cochlearis* and *K. quadrata,* which composed about 60% of the total abundance. Later, a decrease in the total zooplankton abundance and a change in the dominant species were observed (Fig. 3-58).

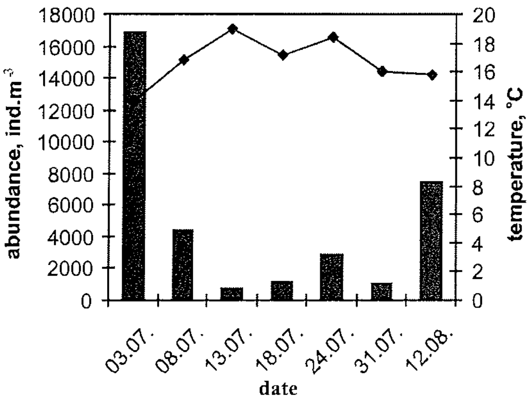

Figure 3-58. Seasonal variations in temperature and total zooplankton abundance in the Olenekskaya channel. (Abundance —◆— T° C)

Several species of Euchlanis genus became dominant instead of the above-mentioned. In August the increase in abundance was marked again. *Trichocerca cylindrica* had reproduction period and demonstrated the high density during this period. The average summer zooplankton abundance in the Olenekskaya channel was 4907 ind.m^{-3}.

Strong variations in the total zooplankton abundance were observed in the terrace lake on the Samoilovskii Island (Fig. 3-59). The lower density (less than 700 ind.m^{-3}) was recorded at the beginning of July at 9°C of water temperature. *Synchaeta sp.* was the dominant species. The first peak of the total zooplankton abundance was observed at the end of July (24560 ind.m^{-3}), when four Euchlanis species were numerous. The highest abundance (about 50000 ind.m^{-3}) was marked in middle August, when water temperature was 14°C. This maximum corresponded to the reproduction of several Rotatoria species belonging to Keratella, Polyarthra and Euchlanis genera. The average zooplankton abundance in the terrace lake throughout summer was 12018 ind.m^{-3}.

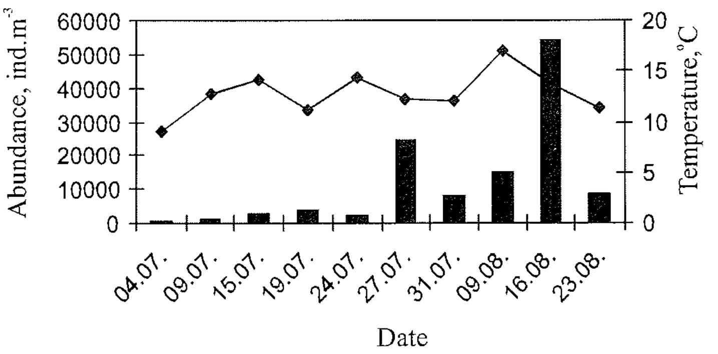

Figure 3-59. Seasonal variations in temperature and total zooplankton abundance in the terrace lake on the Samoilovskii Island. (Abundance —◆— T° C)

Copepoda predominated in zooplankton communities of the small polygon lakes of two different types, deep polygon without plants and shallow polygon with plants, and, also, the crack between polygons. Cladocera and Rotatoria occurred in comparatively small amounts. In these types of the water pools seasonal fluctuations in the total zooplankton abundance were insignificant (Fig. 3-60).

Calanoids *Heterocope borealis* and *Mixodiaptomus theeli* were the most numerous copepods during the whole period of investigation. Only in the crack cyclopoids were dominant in mid-August. Variations in zooplankton density were connected with the life cycles of the common Copepoda species. The maximums of the total abundance coincided with appearance of juvenile stages of these species. Three peaks of the total zooplankton abundance were recorded in the deep polygon with maximum (7000 ind. m^{-3}) in the second decade of July at 11.2°C water temperature (Fig. 3-60A). The average summer density was 5018 ind. m^{-3}.

Two peaks of the total zooplankton abundance were observed in the shallow polygon and the crack. In the first case, maximum of the total abundance (14580 ind. m^{-3}) was marked at the beginning of July at 15.2°C water temperature (Fig. 3-60B). The average summer density was comparatively high - 9557 ind. m^{-3}. Opposite, in the crack, maximum zooplankton density (7280 ind. m^{-3}) was recorded in the second decade of August, when water temperature was 13.4°C. The average abundance during the whole period of investigation equaled to 4578 ind.m^{-3}.

It is well known, that zooplankton organisms are susceptible to variations of a wide number of environmental factors including water temperature, light, food, chemistry, etc. According to our results, there was no evident correlation between temperature conditions and dynamics of zooplankton abundance during the period of investigation. Considerable variations in zooplankton density and species composition occurred seasonally due to changes in the life cycles of different populations.

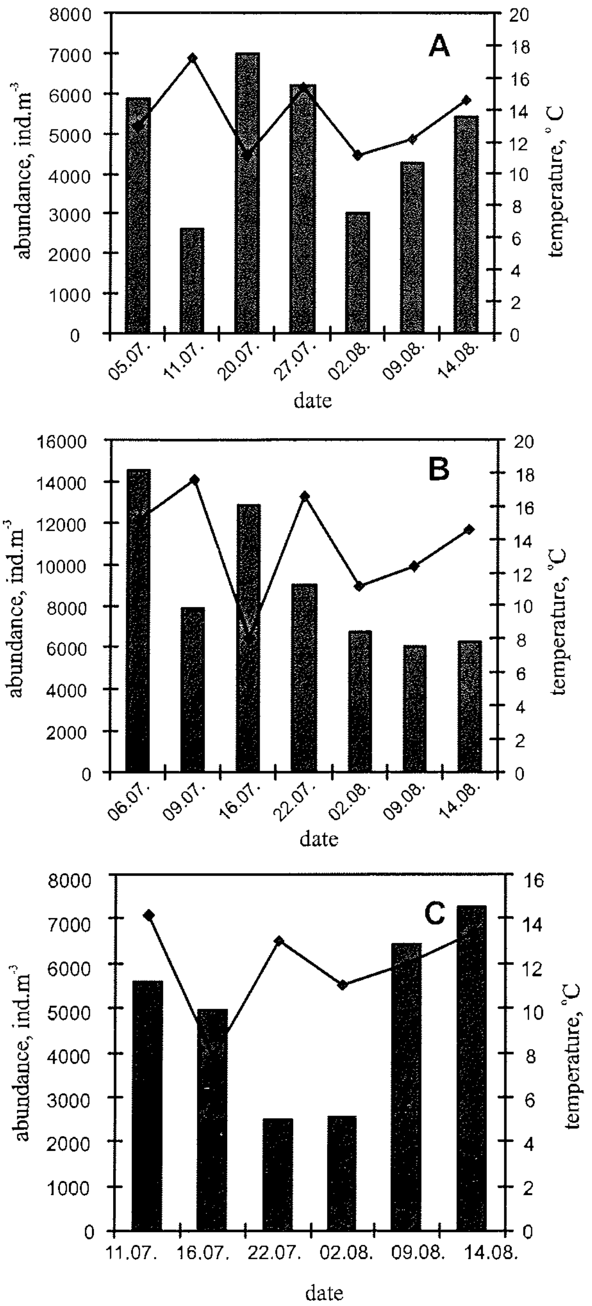

Figure 3-60. Seasonal variations in temperature and total zooplankton abundance in the deep polygon lake (A), shallow polygon lake (B) and in the crack between polygons (C) on the Samoilovskii Island (Abundance —◆— T° C)

3.14 Appendix

Appendix 3-1. List of soil and plant samples (total amount = 76), collected at central Lena Delta during the expedition Lena Delta 2002.

no.	sample ID	date	location	description	depth (cm)	planned analyses
1	LD02-6941	22.07.2002	Samoylov 72° 23` 11.9 N 126° 28`54.0 E	soil sample, profile 2002-1	0-5	geo chemical,microbiological, molecularbiological
2	LD02-6942	22.07.2002	Samoylov 72° 23` 11.9 N 126° 28`54.0 E	soil sample, profile 2002-1	5-9	geo chemical,microbiological, molecularbiological
3	LD02-6943	22.07.2002	Samoylov 72° 23` 11.9 N 126° 28`54.0 E	soil sample, profile 2002-1	9-18	geo chemical,microbiological, molecularbiological
4	LD02-6944	22.07.2002	Samoylov 72° 23` 11.9 N 126° 28`54.0 E	soil sample, profile 2002-1	20-35	geo chemical,microbiological, molecularbiological
5	LD02-6945	22.07.2002	Samoylov 72° 23` 11.9 N 126° 28`54.0 E	soil sample, profile 2002-1	35-40	geo chemical,microbiological, molecularbiological
6	LD02-6946	22.07.2002	Samoylov 72° 23` 11.9 N 126° 28`54.0 E	soil sample, profile 2002-1	40-52	geo chemical,microbiological, molecularbiological
7	LD02-6947	22.07.2002	Samoylov 72° 23` 11.9 N 126° 28`54.0 E	soil sample, profile 2002-1	>52	geo chemical,microbiological, molecularbiological
8	LD02-6948	24.07.2002	Kurungnakh 72° 20' 00.6 N 126° 17`09.2	soil sample, active layer on top of permafrost drill hole	+7-0	geo chemical,microbiological, molecularbiological
9	LD02-6949	24.07.2002	Kurungnakh 72° 20' 00.6 N 126° 17`09.2	soil sample, active layer on top of permafrost drill hole	0-10	geo chemical,microbiological, molecularbiological
10	LD02-6950	24.07.2002	Kurungnakh 72° 20' 00.6 N 126° 17`09.2	soil sample, active layer on top of permafrost drill hole	10-20	geo chemical,microbiological, molecularbiological
11	LD02-6951	24.07.2002	Kurungnakh 72° 20' 00.6 N 126° 17`09.2	soil sample, active layer on top of permafrost drill hole	20-35	geo chemical,microbiological, molecularbiological
12	LD02-6952	24.07.2002	Kurungnakh 72° 20' 00.6 N 126° 17`09.2	soil sample, active layer on top of permafrost drill hole	35-60	geo chemical,microbiological, molecularbiological
13	LD02-6953	24.07.2002	Kurungnakh 72° 20' 00.6 N 126° 17`09.2	soil sample, active layer on top of permafrost drill hole	60-80	geo chemical,microbiological, molecularbiological
14	LD02-6954	24.07.2002	Kurungnakh 72° 20' 00.6 N 126° 17`09.2	soil sample, active layer on top of permafrost drill hole	80-110	geo chemical,microbiological, molecularbiological
15	LD02-6968	07.08.2002	Samoylov 72° 22.2' N 129° 28.5' E	soil sample, polygoncentre	0-5	microbiological
16	LD02-6969	07.08.2002	Samoylov 72° 22.2' N 129° 28.5' E	soil sample, polygoncentre	5-10	microbiological
17	LD02-6970	07.08.2002	Samoylov 72° 22.2' N 129° 28.5' E	soil sample, polygoncentre	10-15	microbiological
18	LD02-6971	07.08.2002	Samoylov 72° 22.2' N 129° 28.5' E	soil sample, polygoncentre	15-20	microbiological
19	LD02-6972	07.08.2002	Samoylov 72° 22.2' N 129° 28.5' E	soil sample, polygoncentre	20-23	microbiological
20	LD02-6973	07.08.2002	Samoylov 72° 22.2' N 129° 28.5' E	soil sample, polygoncentre	23-30	microbiological
21	LD02-6974	07.08.2002	Samoylov 72° 22.2' N 129° 28.5' E	soil sample, polygoncentre	30-35	microbiological
22	LD02-6975	07.08.2002	Samoylov 72° 22.2' N 129° 28.5' E	soil sample, polygoncentre	35-40	microbiological
23	LD02-6976	07.08.2002	Samoylov 72° 22.2' N 129° 28.5' E	soil sample, polygoncentre	40-45	microbiological
24	LD02-6983	16.08.2002	Samoylov 414.860m 8.031.980m	soil sample, top of polygonborder, BS 1	0-3	geo chemical,microbiological, molecularbiological
25	LD02-6984	16.08.2002	Samoylov 414.860m 8.031.980m	soil sample, top of polygonborder, BS 1	3-7	geo chemical,microbiological, molecularbiological
26	LD02-6985	16.08.2002	Samoylov 414.860m 8.031.980m	soil sample, top of polygonborder, BS 1	7-15	geo chemical,microbiological, molecularbiological
27	LD02-6986	16.08.2002	Samoylov 414.860m 8.031.980m	soil sample, top of polygonborder, BS 1	15-23	geo chemical,microbiological, molecularbiological
28	LD02-6987	16.08.2002	Samoylov 414.860m 8.031.980m	soil sample, top of polygonborder, BS 1	23-29	geo chemical,microbiological, molecularbiological
29	LD02-6988	16.08.2002	Samoylov 414.860m 8.031.980m	soil sample, top of polygonborder, BS 1	29-34	geo chemical,microbiological, molecularbiological
30	LD02-6989	16.08.2002	Samoylov 414.860m 8.031.980m	soil sample, top of polygonborder, BS 1	34-40	geo chemical,microbiological, molecularbiological
31	LD02-6990	16.08.2002	Samoylov 414.860m 8.031.980m	soil sample, top of polygonborder, BS 1	40-55	geo chemical,microbiological, molecularbiological
32	LD02-6991	16.08.2002	Samoylov 414.860m 8.031.980m	soil sample, top of polygonborder, BS 1	55-65	geo chemical,microbiological, molecularbiological
33	LD02-6992	16.08.2002	Samoylov 414.860m 8.031.980m	soil sample, top of polygonborder, BS 1	>65	geo chemical,microbiological, molecularbiological
34	LD02-6993	19.08.2002	Samoylov 72° 23` 11.9 N 126° 28`54.0 E	soil sample, profile 2002-1	0-5	molecularbiological
35	LD02-6994	19.08.2002	Samoylov 72° 23` 11.9 N 126° 28`54.0 E	soil sample, profile 2002-1	5-9	molecularbiological
36	LD02-6995	19.08.2002	Samoylov 72° 23` 11.9 N 126° 28`54.0 E	soil sample, profile 2002-1	9-20	molecularbiological
37	LD02-6996	19.08.2002	Samoylov 72° 23` 11.9 N 126° 28`54.0 E	soil sample, profile 2002-1	20-35	molecularbiological
38	LD02-6997	19.08.2002	Samoylov 72° 23` 11.9 N 126° 28`54.0 E	soil sample, profile 2002-1	35-40	molecularbiological
39	LD02-6998	19.08.2002	Samoylov 72° 23` 11.9 N 126° 28`54.0 E	soil sample, profile 2002-1	40-52	molecularbiological
40	LD02-6999	19.08.2002	Samoylov 72° 23` 11.9 N 126° 28`54.0 E	soil sample, profile 2002-1	52-60	molecularbiological
41	LD02-7000	19.08.2002	Samoylov 72° 23` 11.9 N 126° 28`54.0 E	soil sample, profile 2002-1	60-65	molecularbiological
42	LD02-7001	20.08.2002	Samoylov 414.860m 8.031.981m	plant sample, polygonborder, BS 2	+4	
43	LD02-7002	20.08.2002	Samoylov 414.860m 8.031.981m	soil sample, polygonborder, BS 2	0-10	geo chemical,microbiological, molecularbiological
44	LD02-7003	20.08.2002	Samoylov 414.860m 8.031.981m	soil sample, polygonborder, BS 2	10-17	geo chemical,microbiological, molecularbiological
45	LD02-7004	20.08.2002	Samoylov 414.860m 8.031.981m	soil sample, polygonborder, BS 2	17-25	geo chemical,microbiological, molecularbiological
46	LD02-7005	20.08.2002	Samoylov 414.860m 8.031.981m	soil sample, polygonborder, BS 2	>25	geo chemical,microbiological, molecularbiological

Appendix 3-1. cont.

no.	sample ID	date	location	description	depth (cm)	planned analyses
47	LD02-7006	20.08.2002	Samoylov 414.858m 8031.987m	plant sample, polygoncentre, BS 3	+1	
48	LD02-7007	20.08.2002	Samoylov 414.858m 8031.987m	soil sample, polygoncentre, BS 3	0-15	geo chemical,microbiological, molecularbiological
49	LD02-7008	20.08.2002	Samoylov 414.858m 8031.987m	soil sample, polygoncentre, BS 3	15-34	geo chemical,microbiological, molecularbiological
50	LD02-7009	20.08.2002	Samoylov 414.858m 8031.987m	soil sample, polygoncentre, BS 3	>34	geo chemical,microbiological, molecularbiological
51	LD02-7016	28.08.2002	Samoylov 415.386m 8.032.421m	soil sample, top of polygonborder, BS 4	0-6	geo chemical,microbiological, molecularbiological
52	LD02-7017	28.08.2002	Samoylov 415.386m 8.032.421m	soil sample, top of polygonborder, BS 4	6-20	geo chemical,microbiological, molecularbiological
53	LD02-7018	28.08.2002	Samoylov 415.386m 8.032.421m	soil sample, top of polygonborder, BS 4	20-32	geo chemical,microbiological, molecularbiological
54	LD02-7019	28.08.2002	Samoylov 415.386m 8.032.421m	soil sample, top of polygonborder, BS 4	>32	geo chemical,microbiological, molecularbiological
55	LD02-7020	29.08.2002	Samoylov 415.382m 8.032.419m	soil sample, polygoncentre, BS 5	0-10	geo chemical,microbiological, molecularbiological
56	LD02-7021	29.08.2002	Samoylov 415.382m 8.032.419m	soil sample, polygoncentre, BS 5	10-26	geo chemical,microbiological, molecularbiological
57	LD02-7022	29.08.2002	Samoylov 415.382m 8.032.419m	soil sample, polygoncentre, BS 5	26-34	geo chemical,microbiological, molecularbiological
58	LD02-7023	29.08.2002	Samoylov 415.382m 8.032.419m	soil sample, polygoncentre, BS 5	>34	geo chemical,microbiological, molecularbiological
59	LD02-7024	26.07.2002	Kurungnakh 72° 20' 00.6 N 126° 17`09.2	plant sample	surface	C/N-content, 13C-content
60	LD02-7025	26.07.2002	Kurungnakh 72° 20' 00.6 N 126° 17`09.3	plant sample	surface	C/N-content, 13C-content
61	LD02-7026	26.07.2002	Kurungnakh 72° 20' 00.6 N 126° 17`09.4	plant sample	surface	C/N-content, 13C-content
62	LD02-7027	26.07.2002	Kurungnakh 72° 20' 00.6 N 126° 17`09.5	plant sample	surface	C/N-content, 13C-content
63	LD02-7028	26.07.2002	Kurungnakh 72° 20' 00.6 N 126° 17`09.6	plant sample	surface	C/N-content, 13C-content
64	LD02-7029	26.07.2002	Kurungnakh 72° 20' 00.6 N 126° 17`09.7	plant sample	surface	C/N-content, 13C-content
65	LD02-7030	26.07.2002	Kurungnakh 72° 20' 00.6 N 126° 17`09.8	plant sample	surface	C/N-content, 13C-content
66	LD02-7031	25.07.2002	Kurungnakh 72° 20' 00.6 N 126° 17`09.9	plant sample	surface	C/N-content, 13C-content
67	LD02-7032	25.07.2002	Kurungnakh 72° 20' 00.6 N 126° 17`09.10	plant sample	surface	C/N-content, 13C-content
68	LD02-7033	25.07.2002	Kurungnakh 72° 20' 00.6 N 126° 17`09.11	plant sample	surface	C/N-content, 13C-content
69	LD02-7040	02.09.2002	Samoylov 72° 23` 11.9 N 126° 28`54.0 E	soil sample, profile 2002-1	0-5	molecularbiological
70	LD02-7041	02.09.2002	Samoylov 72° 23` 11.9 N 126° 28`54.0 E	soil sample, profile 2002-1	5-9	molecularbiological
71	LD02-7042	02.09.2002	Samoylov 72° 23` 11.9 N 126° 28`54.0 E	soil sample, profile 2002-1	9-18	molecularbiological
72	LD02-7043	02.09.2002	Samoylov 72° 23` 11.9 N 126° 28`54.0 E	soil sample, profile 2002-1	20-35	molecularbiological
73	LD02-7044	02.09.2002	Samoylov 72° 23` 11.9 N 126° 28`54.0 E	soil sample, profile 2002-1	35-40	molecularbiological
74	LD02-7045	02.09.2002	Samoylov 72° 23` 11.9 N 126° 28`54.0 E	soil sample, profile 2002-1	40-52	molecularbiological
75	LD02-7046	02.09.2002	Samoylov 72° 23` 11.9 N 126° 28`54.0 E	soil sample, profile 2002-1	52-60	molecularbiological
76	LD02-7047	02.09.2002	Samoylov	soil sample	4-9	geo chemical,microbiological, molecularbiological

Appendix 3-2. List of sediment samples (total amount = 76), collected at central Lena Delta during the expedition Lena Delta 2002.

no.	sample ID	date	location	description	depth (cm)	planned analyses
1	LD02-6977	08.08.2002	Samoylov 415.290m 8.032.337m	sediment sample	0-2	geo chemical,microbiological, molecularbiological
2	LD02-6978	08.08.2002	Samoylov 415.290m 8.032.337m	sediment sample	2-4	geo chemical,microbiological, molecularbiological
3	LD02-6979 A	08.08.2002	Samoylov 415.290m 8.032.337m	sediment sample	4-7	geo chemical,microbiological, molecularbiological
4	LD02-6979 B	08.08.2002	Samoylov 415.290m 8.032.337m	sediment sample	7-10	geo chemical,microbiological, molecularbiological
5	LD02-6980A	08.08.2002	Samoylov 415.290m 8.032.337m	sediment sample	10-13	geo chemical,microbiological, molecularbiological
6	LD02-6980B	08.08.2002	Samoylov 415.290m 8.032.337m	sediment sample	13-16	geo chemical,microbiological, molecularbiological
7	LD02-6981A	08.08.2002	Samoylov 415.290m 8.032.337m	sediment sample	16-17	geo chemical,microbiological, molecularbiological
8	LD02-7010	23.08.2002	Samoylov 415.305m 8.032.350m	plant sample	~+15	microbiological, molecularbiological
9	LD02-7011	23.08.2002	Samoylov 415.305m 8.032.350m	sediment sample	0-2	geo chemical,microbiological, molecularbiological
10	LD02-7012	23.08.2002	Samoylov 415.305m 8.032.350m	sediment sample	2-4	geo chemical,microbiological, molecularbiological
11	LD02-7013A	23.08.2002	Samoylov 415.305m 8.032.350m	sediment sample	4-7	geo chemical,microbiological, molecularbiological
12	LD02-7013B	23.08.2002	Samoylov 415.305m 8.032.350m	sediment sample	7-10	geo chemical,microbiological, molecularbiological
13	LD02-7014A	23.08.2002	Samoylov 415.305m 8.032.350m	sediment sample	10-13	geo chemical,microbiological, molecularbiological
14	LD02-7014B	23.08.2002	Samoylov 415.305m 8.032.350m	sediment sample	13-16	geo chemical,microbiological, molecularbiological
15	LD02-7015	23.08.2002	Samoylov 415.305m 8.032.350m	sediment sample	16-19	geo chemical,microbiological, molecularbiological

Appendix 3-3. List of water samples (total amount = 19), collected at central Lena Delta during the expedition Lena Delta 2002.

no.	sample ID	date	location	description	depth (cm)	planned analyses
1	LD02-6955	14.07.2002	Samoylov 415.290m 8.032.337m, polygonal lake 1	filter (water sample)	surface	molecularbiological
2	LD02-6956	14.07.2002	Samoylov 415.290m 8.032.337m, polygonal lake 1	filter (water sample)	bottom	molecularbiological
3	LD02-6957	14.07.2002	Samoylov 415.305m 8.032.350m, polygonal lake 2	filter (water sample)	surface	molecularbiological
4	LD02-6958	14.07.2002	Samoylov 415.305m 8.032.350m, polygonal lake 2	filter (water sample)	bottom	molecularbiological
5	LD02-6959	14.07.2002	Samoylov 415.370m 8.032.350m, ice wedge lake	filter (water sample)	surface	molecularbiological
6	LD02-6960	14.07.2002	Samoylov 415.370m 8.032.350m, ice wedge lake	filter (water sample)	bottom	molecularbiological
7	LD02-6961	03.08.2002	Samoylov 415.370m 8.032.350m, ice wedge lake	filter (ice sample)	bottom	molecularbiological
8	LD02-6962	03.08.2002	Samoylov 415.290m 8.032.337m, polygonal lake 1	filter (water sample)	surface	molecularbiological
9	LD02-6963	03.08.2002	Samoylov 415.290m 8.032.337m, polygonal lake 1	filter (water sample)	bottom	molecularbiological
10	LD02-6964	03.08.2002	Samoylov 415.305m 8.032.350m, polygonal lake 2	filter (water sample)	surface	molecularbiological
11	LD02-6965	03.08.2002	Samoylov 415.305m 8.032.350m, polygonal lake 2	filter (water sample)	bottom	molecularbiological
12	LD02-6966	03.08.2002	Samoylov 415.370m 8.032.350m, ice wedge lake	filter (water sample)	surface	molecularbiological
13	LD02-6967	03.08.2002	Samoylov 415.370m 8.032.350m, ice wedge lake	filter (water sample)	bottom	molecularbiological
14	LD02-7034	31.08.2002	Samoylov 415.290m 8.032.337m, polygonal lake 1	filter (water sample)	surface	molecularbiological
15	LD02-7035	31.08.2002	Samoylov 415.290m 8.032.337m, polygonal lake 1	filter (water sample)	bottom	molecularbiological
16	LD02-7036	31.08.2002	Samoylov 415.305m 8.032.350m, polygonal lake 2	filter (water sample)	surface	molecularbiological
17	LD02-7037	31.08.2002	Samoylov 415.305m 8.032.350m, polygonal lake 2	filter (water sample)	bottom	molecularbiological
18	LD02-7038	31.08.2002	Samoylov 415.370m 8.032.350m, ice wedge lake	filter (water sample)	surface	molecularbiological
19	LD02-7039	31.08.2002	Samoylov 415.370m 8.032.350m, ice wedge lake	filter (water sample)	bottom	molecularbiological

Appendix 3-4: List of sediment and water samples.

No	Sample No.	Date	Site	Sedi-ment	Ostra-cods	Cat-ion	An-ion	Iso-topes	Resi-due
01	SAM-01	02.08.02	Samoylov	X	X	X	X	X	X
02	SAM-02	03.08.02	Samoylov	X	X	X	X	X	X
03	SAM-03	03.08.02	Samoylov	X	X	X	X	X	X
04	SAM-04	04.08.02	Amerika Khaya	X	X	X	X	X	X
05	SAM-05	06.08.02	Tit-Ary	X	X	X	X	X	X
06	SAM-06	06.08.02	Tit-Ary	X	X	X	X	X	X
07	SAM-07	07.08.02	Tit-Ary	X	X	X	X	X	X
08	SAM-08	07.08.02	Tit-Ary	X	X	X	X	X	X
09	SAM-09	14.08.02	Samoylov	X	X	X	X	X	X
10	SAM-10	14.08.02	Samoylov	X	X	X	X	X	X
11	SAM-11	14.08.02	Samoylov	X	X	X	X	X	X
12	SAM-12	15.08.02	Kurungnakh	X	X	X	X	X	X
13	SAM-13	15.08.02	Kurungnakh	X	X	X	X	X	X
14	SAM-14	18.08.02	Samoylov	X	X	X	X	X	X
15	SAM-15	19.08.02	Samoylov	X	X	X	X	X	X
16	SAM-16	19.08.02	Samoylov	X	X	X	X	X	X
17	SAM-17	19.08.02	Samoylov	X	X	X	X	X	X
18	SAM-18	20.08.02	Samoylov	X	X	X	X	X	X
19	SAM-19	20.08.02	Samoylov	X	X	X	X	X	X
20	SAM-20	20.08.02	Samoylov	X	X	X	X	X	X
21	SAM-21	21.08.02	Samoylov	X	X	X	X	X	X
22	SAM-22	21.08.02	Samoylov	X	X	X	X	X	X
23	SAM-23	21.08.02	Samoylov	X	X	X	X	X	X
24	SAM-24	21.08.02	Samoylov	X	X	X	X	X	X
25	SAM-25	25.08.02	Samoylov	X	X	X	X	X	X
26	SAM-26	25.08.02	Samoylov	X	X	X	X	X	X
27	SAM-27	25.08.02	Samoylov	X	X	X	X	X	X
28	SAM-28	26.08.02	Samoylov	X	X	X	X	X	X
29	SAM-29	26.08.02	Samoylov	X	X	X	X	X	X
30	SAM-30	27.08.02	Samoylov	X	X	X	X	X	X
31	SAM-31	27.08.02	Samoylov	X	X	X	X	X	X
32	SAM-32	27.08.02	Samoylov	X	X	X	X	X	X
33	SAM-33	29.08.02	Samoylov	X	X	X	X	X	X
34	SAM-34	29.08.02	Samoylov	X	X	X	X	X	X
35	SAM-35	30.08.02	Samoylov	X	X	X	X	X	X
36	SAM-36	30.08.02	Samoylov	X	X	X	X	X	X
37	SAM-37	30.08.02	Samoylov	X	X	X	X	X	X
38	SAM-38	31.08.02	Kurungnakh	X	X	X	X	X	X
39	SAM-39	31.08.02	Kurungnakh	X	X	X	X	X	X
40	SAM-40	01.09.02	Samoylov	X	X	X	X	X	X
41	SAM-41	01.09.02	Samoylov	X	X	X	X	X	X
42	SAM-42	02.09.02	Samoylov	X	X	X	X	X	X
43	SAM-43	02.09.02	Samoylov	X	X	X	X	X	X
44	SAM-44	03.09.02	Samoylov	X	X	X	X	X	X

Appendix 3-5: List of results of water investigations.

No	Sample No.	pH	Conductivity [μS/cm]	Temperature [°C]	O_2 [mg/l]	Total hardness [°dH]	Carb. hardness [°dH]	NH_4^+ [mg/l]	NO_3^- [mg/l]	NO_2^- [mg/l]	PO_4^{3-} [mg/l]
01	SAM-01	7.0	90.4	11.4	9.8	5.1	2.3	0	0	<0.025	<0.25
02	SAM-02	7.5	68.5	11.6	8.7	4.4	2.6	0	0	0	0.25
03	SAM-03	7.5	84.6	13.6	9.3	6.0	2.5	0	0	0	0
04	SAM-04	7.0	24.3	14.1	9.4	3.8	2.0	0	0	0	0
05	SAM-05	7.0	70.9	15.7	8.3	3.4	3.2	<0.2	0	0.025	0.25
06	SAM-06	7.0	66.8	16.9	8.6	4.6	2.4	0	0	0	0
07	SAM-07	7.5	117.9	19.4	7.2	4.8	3.6	0	0	0	0
08	SAM-08	7.5	136.0	18.9	8.4	4.0	3.8	<0.4	0	0	<0.25
09	SAM-09	7.0	44.5	15.5	7.2	5.0	2.4	0	0	0	0
10	SAM-10	7.5	45.3	14.2	6.8	3.2	1.6	0	0	0	0
11	SAM-11	7.0	92.7	12.4	7.3	5.0	3.2	<0.4	0	0	0
12	SAM-12	7.0	28.0	13.4	7.7	2.4	1.0	0	0	0	0
13	SAM-13	6.5	27.0	13.6	5.9	3.8	1.0	0	0	0	0
14	SAM-14	7.5	86.6	12.6	8.8	3.6	2.4	0	0	0	0
15	SAM-15	7.5	72.8	11.2	8.9	3.2	2.2	0	0	0	0
16	SAM-16	7.5	64.7	11.3	9.3	2.8	2.4	0	0	0	0
17	SAM-17	7.5	64.9	12.0	8.4	3.4	2.4	0.4	0	0	0
18	SAM-18	7.5	115.8	11.2	7.6	4.5	4.0	0	0	0	0
19	SAM-19	7.5	53.1	12.5	8.8	3.3	2.0	0	0	0	0
20	SAM-20	7.5	76.8	12.6	8.9	4.0	3.0	0	0	0	0
21	SAM-21	7.5	105.6	11.4	9.0	4.8	4.4	0	0	0	0
22	SAM-22	7.5	94.2	12.3	8.1	5.2	4.2	0	0	0	0
23	SAM-23	7.5	98.8	13.9	8.3	4.8	3.4	0.2	0	0	0
24	SAM-24	7.0	254.0	15.3	5.3	9.4	9.4	0	0	0	0
25	SAM-25	7.5	94.3	6.2	9.4	7.4	4.6	0	0	0	0
26	SAM-26	7.5	78.5	7.7	10.6	7.8	3.0	0	0	0	0
27	SAM-27	7.5	109.4	8.3	10.0	7.2	4.4	0	0	0	0
28	SAM-28	7.6	122.6	7.8	8.8	7.0	5.0	0	0	0	0
29	SAM-29	7.5	110.8	10.3	11.0	5.6	4.4	0	0	0	0
30	SAM-30	7.5	106.6	8.0	10.6	7.2	4.4	0	0	0	0
31	SAM-31	7.5	97.6	10.3	10.0	5.2	4.0	0.2	0	0	0
32	SAM-32	7.5	113.2	9.8	10.8	7.0	4.6	0	0	0	0
33	SAM-33	7.5	96.9	6.7	9.7	5.6	3.4	0	<10	0	0
34	SAM-34	7.5	107.7	6.1	9.5	6.3	4.4	0	0	0	0
35	SAM-35	7.0	44.8	7.8	9.8	5.2	2.2	0	0	0	0
36	SAM-36	7.0	48.7	10.2	11.4	4.8	2.4	0	0	0	0
37	SAM-37	7.0	93.3	9.3	11.3	6.0	3.8	0	0	0	0
38	SAM-38	7.5	109.2	7.8	9.8	7.0	4.2	0	<10	0	0
39	SAM-39	6.5	54.5	6.3	7.8	6.4	2.0	0	<10	0	0
40	SAM-40	7.5	77.8	5.9	11.2	5.0	2.6	0	<10	0	0
41	SAM-41	7.5	79.6	6.3	9.4	4.2	2.8	0	0	0	0
42	SAM-42	7.5	100.3	5.6	10.7	4.4	3.8	0	0	0	0
43	SAM-43	7.5	86.7	7.0	10.7	4.2	3.6	0	0	0	0
44	SAM-44	7.5	70.8	7.0	9.0	3.4	2.8	0	0	0	0

Appendix 3-6: List of environmental parameters.

No.	Sample No.	Vegetation	Ground	Type of lake	Remarks
01	SAM-01	Carex sp.	mouldy over sand	BPL	
02	SAM-02	Carex sp.	mouldy over sand	LPL	
03	SAM-03	Carex sp.	mouldy	BPL	
04	SAM-04	-	loamy	AL	
05	SAM-05	Hippuris vulgaris	mouldy	OB	
06	SAM-06	Arctophila sp., Hippuris vulgaris	mouldy over sand	?	
07	SAM-07	Arctophila sp.	mouldy over sand	OB	
08	SAM-08	Carex sp.	mouldy	BPL	
09	SAM-09	Carex sp.	mouldy	LPL	= SAM-35
10	SAM-10	Arctophila sp.	mouldy	LPL	= SAM-36
11	SAM-11	Carex sp., Potentilla palustris	mouldy	PTL	= SAM-37
12	SAM-12	Carex sp., Potentilla palustris	mouldy	AL	
13	SAM-13	Carex sp.	muddy	LPL	
14	SAM-14	Arctophila sp., Hippuris vulgaris	mouldy over sand	OB	
15	SAM-15	Arctophila sp., Hippuris vulgaris, Potentilla palustris	mouldy over sand	OB	
16	SAM-16	Carex sp.	mouldy over sand	OB	
17	SAM-17	Carex sp., Arctophila sp., Hippuris vulgaris	mouldy over sand	OB	
18	SAM-18	Carex sp., Potentilla palustris, Hippuris vulgaris	muddy	OB	
19	SAM-19	Arctophila sp.	mouldy over sand	OB	
20	SAM-20	Carex sp.	mouldy	BPL	
21	SAM-21	Hippuris vulgaris, Potentilla palustris, Caltha palustris	muddy over sand	LPL	= SAM-30
22	SAM-22	Hippuris vulgaris, Potentilla palustris, Caltha palustris	muddy over sand	BPL	
23	SAM-23	Carex sp., Potentilla palustris	mouldy	PTL	
24	SAM-24	Arctophila sp., Hippuris vulgaris	mouldy	OB	
25	SAM-25	Carex sp., Potentilla palustris, Arctophila sp.	plants	PTL	
26	SAM-26	Carex. sp., Potentilla palustris, Arctophila sp.	mouldy	BPL	
27	SAM-27	Carex. sp., Potentilla palustris, Arctophila sp.,	mouldy	BPL	
28	SAM-28	Potentilla palustris, Caltha palustris, Politricum alpinum	mouldy	BPL	
29	SAM-29	Potentilla palustris,	mouldy	BPL	

No.	Sample No.	Vegetation	Ground	Type of lake	Remarks
		Caltha palustris, Politricum alpinum			
30	SAM-30	Hippuris vulgaris, Potentilla palustris, Caltha palustris	muddy	LPL	= SAM-21
31	SAM-31	Hippuris vulgaris, Potentilla palustris, Caltha palustris	muddy	LPL	
32	SAM-32	Potentilla palustris, Arctophila sp., Carex sp.	muddy	BPL	
33	SAM-33	Potentilla palustris, Arctophila sp., Carex sp.	muddy	BPL	
34	SAM-34	Potentilla palustris, Arctophila sp., Carex sp.	muddy	BPL	
35	SAM-35	Carex sp.	mouldy	LPL	= SAM-09
36	SAM-36	Arctophila sp.	mouldy	LPL	= SAM-10
37	SAM-37	Carex sp., Potentilla palustris	mouldy	PTL	= SAM-11
38	SAM-38	Arctophila sp., Hippuris vulgaris	mouldy over sand	AL	
39	SAM-39	Arctophila sp.	mouldy	PTL	
40	SAM-40	Arctophila sp., Hippuris vulgaris	mouldy over sand	BPL	
41	SAM-41	Carex sp., Hippuris vulgaris, Politricum alpinum	mouldy	BPL	
42	SAM-42	Carex sp., Potentilla palustris, Caltha palustris, Politricum alpinum, Hippuris vulgaris	mouldy	BPL	
43	SAM-43	Carex sp., Potentilla palustris, Caltha palustris, Politricum alpinum, Hippuris vulgaris	mouldy	BPL	
44	SAM-44	Carex sp., Potentilla palustris, Politricum alpinum	mouldy	LPL	

Appendix 3-7. List of recent beetles collected in the Lena Delta in 2002.

No.	Species	Locality	Habitat	Date	Num-ber
Ord. Coleoptera **Fam. Carabidae**					
1	Carabus odoratus Motsch.	Tit-Ary	forest-tundra, south-facing slope, motley grass	06.08.02	4
				Total	**4**
2	Nebria nivalis Payk.	Samoylov	shrub tundra, river bank, sedge	18.08.02	2
				Total	**2**
3	Pelophila borealis Payk.	Samoylov	shrub tundra, river bank, sedge	01.09.02	4
		Tit-Ary	forest-tundra, near pool	06.08.02	1
				Total	**5**
4	Notiophilus aquaticus L.	Samoylov	shrub tundra, on sand	01.09.02	2
		Samoylov	shrub tundra, on sand	14.08.02	1
				Total	**3**
5	Elaphrus riparius L.	Samoylov	shrub tundra, stream bank	14.08.02	1
		Samoylov	shrub tundra, stream bank	01.09.02	4
		Sokol	rocky tundra, near water	23.08.02	1
				Total	**6**
6	Bembidion (Plataphus) sp.	Samoylov	shrub tundra, near stream, sandy soil	01.09.02	7
		Samoylov	shrub tundra, near stream, sandy soil	02.09.02	5
				Total	**14**
7	Pterostichus (Cryobius) brevicornis (Kirby)	Samoylov	shrub tundra, middle flood-plain, under driftwood	18.08.02	6
		Samoylov	shrub tundra, middle flood-plain, under driftwood	01.09.02	10
		Samoylov	shrub tundra, middle flood-plain, under driftwood	02.09.02	4
		Samoylov	shrub tundra, middle flood-plain, under driftwood	10.08.02	7
		Tit-Ary	forest-tundra, high flood-plain with small willow and alder	07.08.02	10
		Tiksi	wet tundra	06.09.02	7
				Total	**37**
8	Pterostichus (Cryobius) spp.	Samoylov	shrub tundra, middle flood-plain, under driftwood	18.08.02	36

		Samoylov	shrub tundra, middle flood-plain, under driftwood	25.08.02	9
		Samoylov	shrub tundra, middle flood-plain, under driftwood	01.09.02	27
		Samoylov	shrub tundra, middle flood-plain, under driftwood	02.09.02	10
		Samoylov	shrub tundra, middle flood-plain, under driftwood	10.08.02	10
		Samoylov	shrub tundra, middle flood-plain, under driftwood	01.08.02	62
		Samoylov	shrub tundra, middle flood-plain, under driftwood	02.08.02	16
		Sokol	rocky tundra	23.08.02	2
		Tit-Ary	forest-tundra, high flood-plain with small willow and alder	07.08.02	14
		Tiksi	wet tundra	06.08.02	13
				Total	**199**
9	P. (Stereocerus) haematopus Dej.	Samoylov	shrub tundra, middle flood-plain, under driftwood	25.08.02	20
		Samoylov	shrub tundra, middle flood-plain, under driftwood	01.09.02	9
		Samoylov	shrub tundra, middle flood-plain, under driftwood	03.08.02	13
		Samoylov	shrub tundra, middle flood-plain, under driftwood	18.08.02	29
		Samoylov	shrub tundra, middle flood-plain, under driftwood	01.09.02	19
		Samoylov	shrub tundra, middle flood-plain, under driftwood	03.08.02	13
		Samoylov	shrub tundra, middle flood-plain, under driftwood	01.08.02	17
		Tit-Ary	forest-tundra, high flood-plain with small willow and alder	07.08.02	20
				Total	**140**
10	P. (Steroperis) vermiculosus Men.	Tit-Ary	forest-tundra, high flood-plain with small willow and alder	06.08.02	10
				Total	**10**

11	P. (Steroperis) costatus Men.	Samoylov	shrub tundra, middle flood-plain, under driftwood	18.08.02	91
		Samoylov	shrub tundra, middle flood-plain, under driftwood	01.08.02	19
		Samoylov	shrub tundra, middle flood-plain, under driftwood	10.08.02	2
		Samoylov	shrub tundra, middle flood-plain, under driftwood	14.08.02	2
		Samoylov	shrub tundra, middle flood-plain, under driftwood	02.09.02	8
		Samoylov	shrub tundra, middle flood-plain, under driftwood	25.08.02	4
		Samoylov	shrub tundra, middle flood-plain, under driftwood	01.08.02	15
		Tit-Ary	forest-tundra, high flood-plain with small willow and alder	07.08.02	4
				Total	**145**
12	P. (Petrophilus) abnormis Sahlb.	Tit-Ary	forest-tundra, high flood-plain with small willow and alder	07.08.02	1
				Total	**1**
13	*Curtonotus alpinus* Payk.	Samoylov	shrub tundra, middle flood-plain, under driftwood	18.08.02	4
		Samoylov	shrub tundra, middle flood-plain, under driftwood	25.08.02	3
		Samoylov	shrub tundra, middle flood-plain, under driftwood	01.09.02	9
		Tiksi	rocky tundra	07.09.02	8
		Tit-Ary	forest-tundra, high flood-plain with small willow and alder	07.08.02	17
				Total	**41**
14	Amara glacialis Mnnh.	Samoylov	shrub tundra, middle flood-plain, under driftwood	01.08.02	2
		Samoylov	shrub tundra, middle flood-plain, under driftwood	18.08.02	1
		Samoylov	shrub tundra, middle flood-plain, under driftwood	25.08.02	2
		Samoylov	shrub tundra, middle flood-plain, under	14.08.02	1

			driftwood		
		Tit-Ary	forest-tundra, high flood-plain with small willow and alder	06.08.02	20
				Total	**26**
15	A. interstitialis Dej.	Samoylov	shrub tundra, middle flood-plain, under driftwood	18.08.02	1
		Samoylov	shrub tundra, middle flood-plain, under driftwood	10.08.02	1
				Total	**2**
Fam. Dytiscidae					
16	Hydroporus sp.	Tit-Ary	forest-tundra, small pool inside sphagnum bog	06.08.02	2
17	Agabus moestus (Curt.)	Tit-Ary	forest-tundra, in lake near bank	06.08.02	2
		Samoylov	shrub tundra, high flood-plain, in lake	18.08.02	1
				Total	**3**
18	Colymbetes dolobratus (Payk.)	Samoylov	shrub tundra, first flood-plain terrace, in lake	18.08.02	2
				Total	**2**
Fam. Silphidae					
19	Thanatophilus lapponicus Hbst.	Samoylov	shrub tundra, near camp	18.08.02	1
		Samoylov	shrub tundra, near camp	18.08.02	1
		Sokol	near house	23.08.02	1
		Tit-Ary	forest-tundra, in settlement	06.08.02	1
				Total	**4**
Fam. Staphylinidae					
20	Stenus sp.	Tiksi	rocky tundra, under driftwood	08.09.02	3
				Total	**3**
21	Lathrobium sp.	Samoylov	shrub tundra, sandy soil, under wood	18.08.02	1
		Samoylov	shrub tundra, sandy soil, under driftwood	01.08.02	4
				Total	**5**
22	Micralymma sp.	Samoylov	shrub tundra, sandy soil, under wood	01.08.02	1
		Tiksi	rocky tundra, under driftwood	07.08.02	9
		Tiksi	rocky tundra, under driftwood	08.08.02	1
				Total	**11**
23	Tachinus arcticus Motsch	Samoylov	shrub tundra, middle flood-plain, under driftwood	01.09.02	12
		Samoylov	shrub tundra, middle flood-plain, under driftwood	14.08.02	3

		Samoylov	shrub tundra, middle flood-plain, under driftwood	10.08.02	4
		Samoylov	shrub tundra, middle flood-plain, under driftwood	01.08.02	19
		Tiksi	rocky tundra, under a wood	08.09.02	1
		Tiksi	rocky tundra, under driftwood	07.09.02	2
				Total	**41**
24	Staphylininae gen.indet.	Samoylov	shrub tundra, sandy soil, under driftwood	14.08.02	2
		Samoylov	shrub tundra, sandy soil, under driftwood	10.08.02	2
		Samoylov	shrub tundra, sandy soil, under driftwood	01.08.02	2
		Tiksi	rocky tundra, under a wood	08.09.02	1
		Tiksi	rocky tundra, under a wood	08.09.02	1
				Total	**8**
Fam. Buprestidae					
25	Melanophila acuminata Deg.	Samoylov	shrub tundra, on a wood	25.08.02	2
				Total	**2**
FAM. COCCINELIDAE					
26	Hyppodamia arctica Schneid.	Samoylov	shrub tundra, on wood boards near camp	18.08.02	2
		Samoylov	shrub tundra, on a wood	01.09.02	1
		Sokol	rocky tundra, near a house	23.08.02	2
				Total	**5**
27	Coccinella spp.	Samoylov	shrub tundra, on wood boards near camp	18.08.02	10
		Samoylov	shrub tundra, on wood boards near camp	10.08.02	13
		Samoylov	shrub tundra, on wood boards near camp	01.08.02	11
		Samoylov	shrub tundra, on a wood	14.08.02	5
		Tiksi	rocky tundra, on a wood	07.08.02	1
				Total	**40**
Fam. Cerambycidae					
28	Monochamus sutor L.	Samoylov	shrub tundra, on a wood	14.08.02	2
		Samoylov	shrub tundra, on a wood	18.08.02	3
		Samoylov	shrub tundra, on a wood	02.08.02	1
		Sokol	bank of Lena, on a wood	23.08.02	1
				Total	**7**
29	Asemum striatum L.	Samoylov	on beach (dead)	10.08.02	1
				Total	**1**

Fam. Chrysomelidae					
30	Chrysolina septentrionalis Men.	Samoylov	shrub tundra, middle flood-plain, under driftwood	18.08.02	5
		Samoylov	shrub tundra, flood-plain, under driftwood	02.09.02	4
		Samoylov	shrub tundra, near camp	10.08.02	1
		Samoylov	shrub tundra, middle flood-plain, under driftwood	01.09.02	4
		Samoylov	shrub tundra, middle flood-plain, under driftwood	14.08.02	2
		Sokol	rocky tundra	23.08.02	1
		Tiksi	rocky tundra under driftwood	07.09.02	3
		Tiksi	rocky tundra under a wood	08.09.02	1
				Total	**21**
Fam. Curculionidae					
31	Lepyrus norden-skjoeldi Faust	Samoylov	shrub tundra, middle flood-plain, under driftwood	01.08.02	13
		Samoylov	shrub tundra, middle flood-plain, under driftwood	18.08.02	10
		Samoylov	shrub tundra, high flood-plain, under driftwood	01.09.02	3
		Samoylov	shrub tundra, high flood-plain, under driftwood	14.08.02	10
		Samoylov	shrub tundra, high flood-plain, under driftwood	02.09.02	1
		Tit-Ary	forest-tundra, high flood-plain with small willow and alder	06.08.02	1
				Total	**38**
				All	**828**

Appendix 3-8. Field description of the permafrost cores drilled on Kurungnakh Island, August 2002.

sampl e ID	**sample No**	**depth [cm]**	**description**	**date**
Island Kurungnakh-Sise, KUR-02R/3a N 72°20` / E 126°17` H=43 m, active layer 32 cm, 3 m off exposure				
LD-02	5007	28-48 (48 b.h.d.)	28-40 cm thawing peat, decomposed, dense, reddish-brown with silt and living roots 40-48 cm frozen, the same, lense-shaped structure, ice lenses ≈ 0,3 cm	13.07.02
LD-02	5008	48-66 (66 b.h.d.)	48-66 cm cryoturbate: silt, grey, ice-rich, transparent with chains of air babbles, and decomposed peat, reddish-brown, irregular reticulated: ice lenses > 1 cm	13.07.02
LD-02	5009	68-136 (136 b.h.d.)	3 parts 66-78 cm silt, ice-rich, grey, irregular reticulated, ice lenses up to 0.8 cm 78-86 cm ice-rich silt with peat, irregular reticulated, lenses ≈ 0.8 cm 86-110 cm peat, reddish-brown, with twigs (Salix?), lense-shaped structure, lenses: 0.4-0.5 cm 110-136 cm cryoturbate: silt with peat, like subvertical sublayer, reticulated, ice lenses ≈ 0.3 cm	13.07.02
			On the depth about 2 m equipment was lost	
KUR-02R/3b – the same polygon: 30 cm from KUR-02/3a				
LD-02	5010	106-162 (163 b.h.d.)	4 parts 106-129 cm cryoturbate: peat, reddish-brown, with silt sublayer, grey, ice-rich, reticulated (lenses 0.4-0.5 cm) 129-143 cm peat, reddish-brown, with twigs, thin-reticulated: 0,2-0,3 cm 143-162 cm silt with small amount of peat inclusions, grey, ice-rich, reticulated, ice lenses ≈ 0,4-0,5 cm	13.07.02
LD-02	5011	163-249 (249 b.h.d.)	6 parts 163-182 cm peat, reddish-brown, with shrub (?) roots-twigs, thin-reticulated 182-201 cm icing silt, grey, irregular reticulated, ice lenses ≈ 0.7-1.0 cm 201-249 cm cryoturbate: peat, decomposed, reddish-brown, thin-reticulated, with silt, grey, ice-rich, lenses up to 0.8 cm	13.07.02
LD-02	5012	249-320 (320 b.h.d.)	3 parts 249-266 cm peat, reddish-brown decomposed, with twigs (∅≈0.4 cm) of horizontal position, thin-reticulated 266-294 cm silt, ice-rich, irregular reticulated, lenses up to 1 cm 294-305 cm peaty silt, grayish-brown, thin-reticulated 305-320 cm silt, grey, ice-rich, lenses 1 cm	13.07.02
LD-02	5013	320-385 (385 b.h.d.)	320-342 cm silt, grey, ice-rich, irregular reticulated, lenses up to 1 cm 342-358 cm silt with m/sand, ice lenses ≈ 0.5 cm 358-369 cm silty peat, grayish-brown, lenses 0.3 up to 0.6 cm	13.07.02

			369-385 cm silty peat, thin-reticulated: 0.2 cm	
			Equipment was frozen on the depth about 4 m	
KUR-02R/3c – the same polygon				
LD-02	5014	344-384 (384 b.h.d.)	2 parts 344-372 cm f/sandy silt with peat, plant remnants (twigs), reticulated, ice lenses ≈ 0.3-0.4 cm 372-384 cm f/sandy silt with peat, thin-reticulated	19.07.02
LD-02	5015	384-425 (425 b.h.d.)	384-391 cm f/sandy silt with peat, reticulated, ice lenses ≈ 0.30 cm 391-425 cm silty peat, grayish-brown, thin-reticulated, ice lenses ≈ 0.2 cm with twigs of horizontal and subhorizontal position	19.07.02
LD-02	5016	425-485 (485 b.h.d.)	5 parts 425-460 cm silt, grey, ice-rich, alternation of reticulated texture, lenses ≈ 0.3 cm, and ice sublayer up to 1.0-1.2 cm 460-485 cm sandy silt, with peat and small amount of twigs, lenses 0.3-0.4 cm	19.07.02
LD-02	5017	485-544 (544 b.h.d.)	4 parts 485-495 cm the same 495-517 cm sandy silt, thin-reticulated, 500-503 cm – ice layer 517-544 cm sandy silt with peat, reticulated, with twigs of subhorizontal position	19.07.02
LD-02	5018	544-613 (613 b.h.d.)	3 parts 544-574 cm silt+f/sand, ice-rich, lenses 0.3-0.4 cm 574-607 cm silt+f/sand+twigs of vertical position 607-613 cm silt+f/sand, reticulated	19.07.02
LD-02	5019	616-647 (647 b.h.d.)	616-647 cm silt+f-m/sand, ice-rich, lenses 0.3 up to 0.6 cm; 640-645 cm with twigs	20.07.02
LD-02	5020	647-728 (728 b.h.d.)	3 parts 647-669 cm f/sandy silt, thin-reticulated, 0.1-0.2 cm 669-695 cm silt, grey, ice-rich with twigs of subvertical position, lenses 0.3-0.8 cm 695-728 cm f/sandy silt with twigs of subvertical position, thin-reticulated, 0.1-0.2 cm	20.07.02
LD-02	5021	728-798 (798 b.h.d.)	5 parts 728-744 cm f/sandy silt, grey, reticulated, lenses 0.2 cm 744-746 cm ice sublayer 746-763 cm f/sandy silt, greyish, thin-reticulated, 0.1 cm 763-798 cm silt with f/sand, grey, reticulated, 0.2 cm with more ice sublayer in the middle	20.07.02
LD-02	5022	798-847 (847 b.h.d.)	3 parts 798-832 cm sandy silt with sparse twigs (subvertical position), lense-like reticulated, lenses ≈ 0.2 cm 832-847 cm cm sandy silt with sparse twigs (subvertical position), reticulated, lenses ≈ 0.3 cm	20.07.02
LD-02	5023	847-900 (900 b.h.d.)	847-861 cm f/sandy silt, reticulated, lenses 0.2-0.3 cm with thin white roots (?) – 0.1-0.15 cm of vertical position 861-900 cm m/sandy silt, thin reticulated: lenses 0.1 cm	20.07.02

			882-887 cm – more ice sublayer	
LD-02	5024	902-934 (934 b.h.d.)	2 parts 902-934 cm m-f/sandy silt with thin white roots and twigs of horizontal position, reticulated: lenses 0.1 cm	20.07.02
LD-02	5025	934-990 (990 b.h.d.)	6 parts 934-956 cm m-f/sandy silt with plant remnants (twigs and white roots), lenses < 0.1 cm 956-990 cm f/sandy silt with thin white roots, reticulated, lenses 0.3-0.4 cm	20.07.02
LD-02	5026	990-1048 (1048 b.h.d.)	4 parts 990-1005 cm f/sandy silt, grey, reticulated; 996-998 cm 2 ice lenses ≈ 1.0 cm 1005-1024 cm silty f-m/sand and thin white roots, massive 1024-1048 cm f/sandy silt, reticulated, lenses 0.3-0.4 cm	22.07.02
LD-02	5027	1048-1091 (1091 b.h.d.)	5 parts f-m/sandy silt, ice-rich, ice layers 1.5-2.0 cm	22.07.02
LD-02	5028	1091-1153 (1153 b.h.d.)	7 parts f-m/sand with silt, ice-rich: irregular layers > 1 cm, with thin subvertical roots	22.07.02
LD-02	5029	1153-1204 (1204 b.h.d.)	1153-1169 cm the same lake 1091-1153 cm 1169-1199 cm silty f-m/sand with sparse plant remnants (moss?) 1195-1196 cm ice layer, transparent 1199-1201 cm sandy silt with peaty spot (on side) 1201-1204 cm peat, brown, slightly decomposed	22.07.02
Island Kurungnakh-Sise, KUR-02G/4 N 72°19' / E 126°17' The top of baydzherakh, H=31 m, active layer 62 cm				
LD-02	5505	62-107 (107 b.h.d.)	∅ = 76 mm 62-66 cm silt, grey, with m/sand, ice-rich: lenses ≈ 0.7 cm 66-67 cm ice layer 1.2 cm 67-107 cm silty sand, yellow-grey, with turbate of decomposed organic and plant remnants of chaotic position, inclined lenticular	15.07.02
LD-02	5506	107-169 (169 b.h.d.)	4 parts – all layers have angle ≈ 45° - NB! 107-111 (up to 113) cm ice layer with silt and f/sand 111(113)-147(150) cm – sandy silt with plant remnants, reticulated, 0.7-0.8 cm 147(150)-169 cm silty sand + plant remnants of subhorizontal position, yellow-greyish, cryogenic texture: subhorizontal lenticular with subvertical layered	15.07.02
LD-02	5507	169-200 (202 b.h.d.)	2 parts 169-**186** cm silty sand, yellow-brown, with plant remnants, lense-shaped **186**-200 cm silty-sandy-peat with plant remnants, reticulated	15.07.02
LD-02	5508	202-231 (231 b.h.d.)	3 parts (202-210; 210-223; 223-231 cm) 202-231 cm turbate(?): silty sand and peat with plant remnants, yellow-grey, reticulated	15.07.02
LD-02	5509	231-253 (253 b.h.d.)	3 parts: 231-238, 238-243, 243-253 231-247cm f/sandy silt, greyish, reticulated, with sand inclusions, yellow, with oxidized points, massive and plant remnants	15.07.02

			247-253 cm cm silty f-m/sand with silty organic matter, thin-reticulated	
LD-02	5510	257-296 (299 b.h.d.)	3 parts 257-296 cm f-m/sand, yellow, with gleyish vertically elongated inclusions of decomposed organic matter, thin-reticulated (<0.1 cm), in sand - massive	15.07.02
LD-02	5511	299-314 (314 b.h.d.)	2 parts 299-304 cm f/sandy silt with decomposed organic, brown-grey, loose frozen 304-310 cm m/sand, yellow, with grey silt spots 310-314 cm peat with sandy silt, dark grey, and twigs of chaotic position, massive	17.07.02
LD-02	5512	314-335 (335 b.h.d.)	2 parts 314-335 cm subvertical border between m/sandy, yellow-gray, massive and decomposed silty organic matter, brown, thin-reticulated with twigs of vertical position	17.07.02
LD-02	5513	335-355 (355 b.h.d.)	4 parts 335-343; 343-**347** (350)cm turbate: peat with twigs of chaotic position and silty sand, thin-reticulated, ≈0.2 cm **347**(350)-355 cm ice (ice wedge?), transparent with air babbles and m/sand, yellow	17.07.02
LD-02	5514	355-374 (374 b.h.d.)	4 parts – *looks like contact zone with ice wedge* 355-374 cm diagonal border between ice, milky-white, and silty-f-m/sand + twigs	17.07.02
LD-02	5515	374-404 (404 b.h.d.)	3 parts 374-**378** cm silty sand with lateral contact of ice **378-391** cm silt with sand, grayish-yellowish, plant remnants of chaotic position **391**-404 cm silt + sand, oxidized points, horizontal thin-reticulated, 0.1-0.2	17.07.02
LD-02	5516	404-424 (424 b.h.d.)	3 parts (404-415; 415-420; 420-424 cm) f-m/sandy silt, grey, thin-reticulated (0.1-0.15 cm) with twigs of horizontal position	17.07.02
LD-02	5517	425-440 (440 b.h.d.)	3 parts (425-433; 433-438; 438-440 cm) the same as above layer f-m/sand silt, dark grey with oxidized spots and plant remnants	17.07.02
LD-02	5518	440-476 (476 b.h.d.)	2 parts **440**-444 cm lost sediment 444-453(460) cm silty sand, greyish, with twigs, thin-reticulated (<0.1), close to massive 453(460)-**469** cm sandy silt, with twigs (0.15-0.2 cm), reticulated, 0.3-0.4 cm **469**-476 cm m/sand, yellow, with turbated layeres of decomposed organic matter, close to massive	18.07.02
		476-505	Lost material: probably it was m/sand, loose, massive, yellow, with oxidized points	
LD-02	5519	505-549 (549 b.h.d.)	505-549 cm silty f-m/sand, yellow-grey, twigs (0.2 cm), ice lenses ≈ 0.3 cm	18.07.02
LD-02	5520	549-571 (571 b.h.d.)	3 parts 549-556, 556-561, 561-571 cm silty-f/sand, grey, thin-reticulated, 0.3 cm, with twigs (0.15 cm)	18.07.02
LD-02	5521	571-579 (579 b.h.d.)	f-m/sand with twigs (0.2 cm) and brown spots of decomposed organic, loose frozen, thin-reticulated, grey-brown	18.07.02
LD-02	5522	579-601 (601 b.h.d.)	**579**-580 cm the same like above 580-595 cm f-m/sand with vertically elongated silt	18.07.02

			spots and twigs of vertical position, thin lense-shaped 595-601 cm more silty sand, grey, thin-reticulated (0.1-0.2 cm)	
LD-02	5523	601-610 (610 b.h.d.)	601-**605** cm the same like above **605**-610 cm turbate: m/sand with peat and plant remnants, massive	18.07.02
LD-02	5524	610-628 (628 b.h.d.)	3 parts - all layers have angle ≈ 40° ! 610-615(**617**) cm peaty sand with a lot of twigs and other plant remnants 615(**617**)-625; 625-628 cm silt with sand, lenses ≈ 0.2-0.3 cm up to ice sublayer of 0.8 cm	18.07.02
LD-02	5525	628-634 (634 b.h.d.)	silty sand, grey, with plant remnants, thin-reticulated 634 cm ice lens 0.5 cm	18.07.02
LD-02	5526	634-650 (650 b.h.d.)	2 parts 634-646 cm silt with f/sand, grey, thin-reticulated (0.2 cm) 646-**650**(652) cm the same + ice lenses ≈ 0.4 cm – angle = 40°	19.07.02
LD-02	5527	650-663 (663 b.h.d.)	f-m/sand with twigs of subvertical position, reticulated 0.3-0.4 cm	19.07.02
LD-02	5528	663-**669** (669 b.h.d.)	f-m/sand and silt, yellow-brown, with twigs of subvertical position, lenses ≈ 0.3 cm	19.07.02
LD-02	5529	669-701 (701 b.h.d.)	669-**690** cm silty sand, yellow-grey, thin-reticulated **690**-701 cm f-m/sand, yellow with small amount of twigs	19.07.02
LD-02	5530	701-716 (716 b.h.d.)	701-710 cm f-m/sand, yellow, with twigs 710-716 cm silty sand, grey, with twigs, thin-reticulated	19.07.02
LD-02	5531	716-734 (734 b.h.d.)	2 parts: 716-730, 730-734 cm f-m/sand, yellow, with grey strips and twigs (0.15-0.2 cm) of subvertical position, massive	19.07.02
LD-02	5532	734-745 (745 b.h.d.)	2 parts f-m/sand, grayish-yellow, thin-reticulated	19.07.02
LD-02	5533	745-**792** (792 b.h.d.)	2 parts – changed spoon! 745-**758** cm the same like above 758-**792** cm silt and f-m/sand, yellowish-grey, with twigs of chaotic position, reticulated	19.07.02
LD-02	5534	792-813 (813 b.h.d.)	**792**-811 cm the same 811-813 cm ice, transparent, with silt, angle ≈ 40°	19.07.02
LD-02	5535	813-827 (827 b.h.d.)	2 parts 813-817 cm broken ice layer 817-820 cm ice with f/sandy silt, grey 820-827 cm sandy silt, grey, with ice layer on the bottom 1.2 cm	19.07.02
LD-02	5536	827-847 (847 b.h.d.)	3 parts 827-830 cm f-m/sand with twigs of subhorizontal position 830-847 cm f/sand, grayish-yellow, with twigs of subhorizontal position, reticulated + ice lens ≈ 1 cm	20.07.02
LD-02	5537	847-867 (867 b.h.d.)	3 parts silty sand, ice-rich, lenses up to 0.8 cm, with big plant remnants and decomposed organic	20.07.02
LD-02	5538	867-**898** (898 b.h.d.)	2 parts f/sand and silt, grey, reticulated (0.1-0.2), with twigs of subhorizontal position and ice sublayer up to 1-1.2 cm	20.07.02
LD-02	5539	**898**-914	f/sand with silt, grayish-yellow, twigs of	20.07.02

		(914 b.h.d.)	subhorizontal position, reticulated ≈ 0.1-0.3 cm	
LD-02	5540	914-934 (934 b.h.d.)	f/sand with twigs and plant remnants, ice lenses 0.2 up to 1.4 cm	20.07.02
LD-02	5541	934-954 (954 b.h.d.)	934-943 cm f/sand, grayish-yellow, ice-rich, lenses ≈ 0.3 cm up to 1.4 cm 943-954 cm f-m/sand, yellow, with plant remnants of chaotic position, thin-reticulated	20.07.02
LD-02	5542	954-985 (985 b.h.d.)	4 parts 954-**958** cm f/sand, grey, ice-rich, thin-reticulated: 0.1-0.2 cm **958**-965 cm organic layer: decomposed peat 965-**985** cm m/sand, layered, yellow, near organic layer – slightly grey, massive from 979 with plant remnants	20.07.02
LD-02	5543	985-999 (999 b.h.d.)	2 parts **985**-990 cm f/sand and silt, grayish, reticulated: lenses 0.2-0.3 cm up to 1.5 cm 990-999 cm the same, but more yellow sand	20.07.02
LD-02	5544	999-**1012** (1012 b.h.d.)	3 parts f-m/sand and silt, yellowish-grey, thin-reticulated: ≈ 0.15 cm, nearly the bottom – ice lens 0.7 cm	20.07.02
LD-02	5545	1023-1050 (1050 b.h.d.)	2 parts 1023-1034, 1034-1039 cm peat consisting of twigs (horizontal and subhorizontal position) with silt and m/sand, brown-grey, thin-reticulated 1039-**1046** silt and m/sand, grey, thin-reticulated **1046**-1050 cm m/sand, grayish-yellow, massive	24.07.02
LD-02	5546	1050-1088 (1088 b.h.d.)	2 parts 1050-1080 cm m/sand, orange-oxidized, loose-frozen, massive – NB! The middle part of this layer was lost 1080-1088 cm m/sand, grayish-yellow, dense, massive	24.07.02
LD-02	5547	1088-**1108** (1108 b.h.d.)	4 parts m/sand, slightly layered, grayish-yellow, loose-frozen, massive	24.07.02

Appendix 3-9. List of general samples from the Buor-Khaya section, Kurungnakh Island.

No.	Sample No.	Date	Altitude [m,a.r.l.]	Depth [m]	Sediment	Bayd-zherakh (Point)	Ice con-tent [%]	Pol-len
01	Bkh2002 S01	10.08.02	42.75	0.25	grey silt with peat lenses	point 1	-	x
02	Bkh2002 S02	10.08.02	42.75	0.25	grey silt	point 1	100.0	x
03	Bkh2002 S03	10.08.02	42.0	1.0	peat	point 1	94.4	x
04	Bkh2002 S04	10.08.02	42.0	1.0	grey silt	point 1	56.8	x
05	Bkh2002 S05	10.08.02	42.2	0.8	grey silt with peat lenses	point 2	100.0	-
06	Bkh2002 S06	10.08.02	40.2	2.8	grey silt	point 2	73.1	x
07	Bkh2002 S07	10.08.02	39.8	3.2	grey silt	point 2	150.0	x
08	Bkh2002 S08	10.08.02	38.7	4.3	grey sandy silt	point 2	121.7	x
09	Bkh2002 S09	10.08.02	39.2	3.8	grey sandy silt	point 2	78.3	x
10	Bkh2002 S10	11.08.02	38.5	4.5	sandy silt, roots	M	58.1	x
11	Bkh2002 S11	11.08.02	38.0	5.0	sandy silt	M	59.3	x
12	Bkh2002 S12	11.08.02	37.5	5.5	sand	C	64.0	x
13	Bkh2002 S13	11.08.02	38.0	5.0	sandy silt	C	-	x
14	Bkh2002 S14	12.08.02	37.0	6.0	sand	C	55.2	x
15	Bkh2002 S15	12.08.02	36.5	6.5	sand, roots	C	60.0	x
16	Bkh2002 S16	12.08.02	36.0	7.0	sand with peat	C	133.3	x
17	Bkh2002 S17	12.08.02	39.5	3.5	grey silt	B	23.8	x
18	Bkh2002 S18	12.08.02	34.7	8.3	brown silt, roots	E	70.8	x
19	Bkh2002 S19	12.08.02	35.3	7.7	brown silt, roots	E	61.3	x
20	Bkh2002 S20	12.08.02	36.2	6.8	silt	E	63.4	x

No.	Sample No.	Date	Altitude [m,a.r.l.]	Depth [m]	Sediment	Baydzherakh (Point)	Ice content [%]	Pollen
21	Bkh2002 S20D	12.08.02	36.2	6.8	peat	E	-	-
22	Bkh2002 S21	13.08.02	34.8	8.2	silt, plants	F	106.3	x
23	Bkh2002 S22	13.08.02	33.1	9.9	peat	G	77.8	x
24	Bkh2002 S22D	13.08.02	33.3	9.7	peat	G	-	-
25	Bkh2002 S23	13.08.02	31.0	12.0	peat	G	108.7	x
26	Bkh2002 S24	13.08.02	32.0	11.0	grey silt, plants	G	86.4	x
27	Bkh2002 S25D	13.08.02	30.0	13.0	peat	P	-	-
28	Bkh2002 S26	13.08.02	31.5	11.5	silt, roots	G	104.3	x
29	Bkh2002 S27	16.08.02	41.7	1.3	grey silt with peat lenses	point 3	117.6	x
30	Bkh2002 S28	16.08.02	41.5	1.5	grey silt with peat lenses	point 3	48.4	x
31	Bkh2002 S29	16.08.02	41.0	2.0	grey silt with peat lenses	point 3	51.5	x
32	Bkh2002 S30	16.08.02	40.5	2.5	grey silt with peat lenses	point 3	58.8	x
33	Bkh2002 S30D	16.08.02	40.4	2.5	peat lenses in silt	point 3	-	-
34	Bkh2002 S31	16.08.02	32.5	10.5	brown silt, plants	H	100.0	x
35	Bkh2002 S32	22.08.02	20-24	-	peat		67.9	x
36	Bkh2002 S32D	22.08.02	20-24	-	peat		-	-
37	Bkh2002 S33	22.08.02	9.6	-	yellow sand with fine layers of silt		-	x
38	Bkh2002 S34	22.08.02	10.0	-	yellow sand, roots		-	x
39	Bkh2002 S35	22.08.02	10.5	-	alternation of yellow sand and dark silt layers, roots		-	x
40	Bkh2002 S36	22.08.02	11.0	-	yellow sand		-	x

No.	Sample No.	Date	Altitude [m,a.r.l.]	Depth [m]	Sediment	Baydzherakh (Point)	Ice content [%]	Pollen
41	Bkh2002 S37	22.08.02	11.5	-	yellow sand		-	x
42	Bkh2002 S38	22.08.02	11.7	-	peat		52.6	x
43	Bkh2002 S39	22.08.02	12.0	-	sand with fine dark layers		28.6	x
44	Bkh2002 S40	22.08.02	12.5	-	sand (fine layers)		26.1	x
45	Bkh2002 S41	22.08.02	13.0	-	sand		24.5	x
46	Bkh2002 S42	22.08.02	13.5	-	sand		23.9	x
47	Bkh2002 S43	22.08.02	14.0	-	sand (fine layers)		-	x
48	Bkh2002 S44	22.08.02	14.5	-	sand (fine layers)		23.1	x
49	Bkh2002 S45	22.08.02	17.5	-	brown silt with peat		74.1	x
50	Bkh2002 S45aD	22.08.02	17.9	-	peat		-	x
51	Bkh2002 S46	22.08.02	19.4	-	sandy silt with peat		78.3	x
52	Bkh2002 S46aD	22.08.02	19.8	-	peat		-	x
53	Bkh2002 S47	23.08.02	23.5	-	peat		38.3	x
54	Bkh2002 S48	23.08.02	24.0	-	grey silt, plants		56.8	x
55	Bkh2002 S49	23.08.02	9.0	-	sand		18.3	x
56	Bkh2002 S50	23.08.02	8.5	-	sand (fine layers)		-	x
57	Bkh2002 S51	23.08.02	8.0	-	sand (fine dark layers)		-	x
58	Bkh2002 S52	24.08.02	16.1	-	grey sand (fine layers)		-	x
59	Bkh2002 S53	24.08.02	15.3	-	sand (fine dark layers)		-	x

Appendix 3-10. List of permafrost samples from Samoylov Island.

No.	Sample No.	Date	Altitude [m, a.r.l.]	Sec-tion	Sample description	Remarks
1	Sam-1-S-1	02.08.02	7.55	1	greyish-yellow medium grained sand (upper ice wedge)	
2	Sam-1-S-1a	03.08.02	7.5	1	peat (to right from ice wedge top)	
3	Sam-1-S-2	02.08.02	7.35	1	yellow medium grained sand with reddish spots (upper ice wedge)	
4	Sam-1-S-2a	03.08.02	7.35	1	peat (to right from ice wedge top)	
5	Sam-1-S-3	02.08.02	7.2	1	peaty silt with plant detritus	
6	Sam-1-S-4	02.08.02	7.0	1	silt with plant detritus	
7	Sam-1-S-5	02.08.02	6.7	1	silt with plant detritus	
8	Sam-1-S-6	02.08.02	6.4	1	silt with peat spots	
9	Sam-1-S-7	02.08.02	6.1	1	silt with peat spots	
10	Sam-1-S-8	02.08.02	5.8	1	peat and peaty silt	
11	Sam-1-S-9	02.08.02	5.6	1	greyish-yellow sand with grass roots	
12	Sam-1-BOT-1	03.08.02	7.2	1	moss peat	for plant de-termination
13	Sam-1-BOT-2	03.08.02	6.0	1	grass roots	for plant de-termination
14	Sam-1-BOT-3	03.08.02	6.4	1	moss, grass, shrub roots	for plant de-termination
15	Sam-2-S-10	20.08.02	5.5	2	silt with woody twigs	
16	Sam-2-S-11	20.08.02	5.9	2	silt with woody twigs and roots	
17	Sam-2-S-12	20.08.02	6.2	2	silt and sand from sand lens	
18	Sam-2-S-13	20.08.02	6.6	2	sand with grass stems and roots	
19	Sam-2-S-14	20.08.02	7.0	2	sand with plant detritus	
20	Sam-2-S-15	20.08.02	7.3	2	sand with plant detritus	

No.	Sample No.	Date	Altitude [m, a.r.l.]	Sec-tion	Sample description	Remarks
					detritus	
21	Sam-2-S-16	20.08.02	7.6	2	sand	
20	Sam-2-S-17	20.08.02	7.9	2	modern soil	

Appendix 3-11. List of ice samples from Buor Khaya section on Kurungnakh Island.

No.	Sample No.	Date	Isotopes	Hydro-chemistry	Altitude [m, a.r.l,]	Depth [m]
01	Bkh IW I/01	17.08.02	X	-	-	0.7
02	Bkh IW I/02	17.08.02	X	-	-	0.7
03	Bkh IW I/03	17.08.02	-	X	-	0.7
04	Bkh IW I/04	17.08.02	X	-	-	0.7
05	Bkh IW I/05	17.08.02	X	-	-	0.7
06	Bkh IW I/06	17.08.02	X	-	-	1.0
07	Bkh IW I/07	17.08.02	X	-	-	1.0
08	Bkh IW I/08	17.08.02	X	-	-	1.0
09	Bkh IW I/09	17.08.02	-	X	-	1.0
10	Bkh IW I/10	17.08.02	X	-	-	1.0
11	Bkh IW I/11	17.08.02	X	-	-	1.3
12	Bkh IW I/12	17.08.02	X	-	-	1.3
13	Bkh IW I/13	17.08.02	X	-	-	1.3
14	Bkh IW I/14	17.08.02	X	-	-	1.3
15	Bkh IW I/15	17.08.02	X	-	-	1.3
16	Bkh IW II/01	28.08.02	X	-	16.1	-
17	Bkh IW II/02	28.08.02	X	-	16.1	-
18	Bkh IW II/03	28.08.02	X	-	16.1	-
19	Bkh IW II/04	28.08.02	-	X	16.1	-
20	Bkh IW II/05	28.08.02	X	-	16.1	-
21	Bkh IW II/06	28.08.02	X	-	16.1	-
22	Bkh IW II/07	28.08.02	X	-	16.1	-
23	Bkh IW II/08	28.08.02	X	-	16.1	-
24	Bkh IW II/09	28.08.02	X	-	16.1	-
25	Bkh IW II/10	28.08.02	X	-	16.1	-
26	Bkh IW II/11	28.08.02	-	X	16.1	-
27	Bkh IW II/12	28.08.02	X	-	16.1	-
28	Bkh IW II/13	28.08.02	X	-	16.1	-
29	Bkh IW II/14	28.08.02	X	-	16.1	-

Appendix 3-12: List of the samples for insect fossils from Kurungnakh and Samoylov Islands.

No.	Samples No.	Date	Altitude [m,a.r.l.]	Depth [m]	Site, Section	Bayd-zherakh (Point)	Sedi-ment
1	Bkh-02-B-1	10.08.02		1.0-1.3	Buor Khaya, 1	point 1	silt and peat
2	Bkh-02-B-2	11.08.02		6.0-6.3	Buor Khaya, 1	C	sand
3	Bkh-02-B-3	12.08.02		3.5-3.7	Buor Khaya, 1	B	silt
4	Bkh-02-B-4	13.08.02		5.0-5.3	Buor Khaya, 1	C	silt
5	Bkh-02-B-5	15.08.02		6.7-7.0	Buor Khaya, 1	E	silt
6	Bkh-02-B-6	15.08.02		9.2-9.5	Buor Khaya, 1	F	silt
7	Bkh-02-B-7	16.08.02		2.0-2.3	Buor Khaya, 1	point 3	silt
8	Bkh-02-B-8	17.08.02		10,7-11,0	Buor Khaya, 1	G	silt
9	Bkh-02-B-9	19.08.02	21.5-21.8		Buor Khaya, 2	block 1	silt
10	Bkh-02-B-10	19.08.02	23.5-23.8		Buor Khaya, 2	block 1	silt
11	Bkh-02-B-11	19.08.02	10.0-10.3		Buor Khaya, 2		silt and sand
12	Bkh-02-B-12	22.08.02	17.5-17.7		Buor Khaya, 2		silt and peat
13	Bkh-02-B-13	22.08.02	19.2-19.4		Buor Khaya, 2		silt
14	Bkh-02-B-14	25.08.02	22.7-23.0		Buor Khaya, 2	block 2	silt
15	Bkh-02-B-15	25.08.02	24.7-25.0		Buor Khaya, 2	block 2	silt
16	Sam-1-B-1	3.08.02	6.6-6.9		Samoylov, 1		silt and peat
17	Sam-1-B-2	3.08.02	7.0-7.3		Samoylov, 1		silt and peat
18	Sam-1-B-3	3.08.02	5.9-6.2		Samoylov, 1		silt
19	Sam-2-B-4	20.08.02	5.5-5.9		Samoylov, 2		silt
20	Sam-2-B-5	20.08.02	6.4-6.6		Samoylov, 2		sand
21	Sam-2-B-6	20.08.02	7.0-7.2		Samoylov, 2		sand

Appendix 3-13. List of mammal bones collected on Lena Delta in 2002.

No.	Sample No.	Taxon	Skeleton element	Notes	Preser-vation	Location	Locality
1	BKh2002 O-1	Rangifer (?)	Vertebra		Compl.	depth 8,5 m in mud flow	Buor Khaya
2	BKh2002 O-2	Rangifer tarandus (L.)	Horn	n/s	Frag.	depth 2 m in froz-en silt near contact with ice wedge	Buor Khaya
3	BKh2002 O-3	Ovibos sp.	Metatarsal		Comp.	depth 5,5 m in dry mud	Buor Khaya
4	BKh2002 O-4	Mammuthus primigenius (Blum.)	Femur (caput)	tra-shed	Frag.	Lena bank	Buor Khaya
5	BKh2002 O-5	Equus (Equus) sp.	Mandibula ramus dex		Frag.	height 19,5 m on the slope between two peat layers	Buor Khaya
6	BKh2002 O-6	Equus caballus L.	Atlas		Comp.	height 4,5 m. in dry mud	Buor Khaya
7	BKh2002 O-7	Equus caballus L.	Pelvis		Frag.	Lena bank	Buor Khaya
8	BKh2002 O-8	Equus caballus L.	Carpale III		Comp.	Lena bank	Buor Khaya
9	BKh2002 O-9	Equus caballus L.	Metatarsale		Comp.	height 19-20 m from the frozen silt between two peat layers	Buor Khaya
10	BKh2002 O-10	Mammuthus primigenius (Blum.)	Vertebra		Comp.	Lena bank	Buor Khaya
11	BKh2002 O-11	Equus caballus L.	Vertebris cervicale		Comp.	Lena bank	Buor Khaya
12	BKh2002 O-12	?	?	define	Frag.	Lena bank	Buor Khaya
13	BKh2002 O-13	Equus caballus L.	Mandibula	Same as Bkh 2002-O-5	Frag.	height 19,5 m on the slope between two peat layers	Buor Khaya
14	BKh2002 O-14	Mammuthus	Rib		Frag.	height 26,5 m in mud flow	Buor Khaya
15	BKh2002 O-15	Mammuthus primigenium (Blum.)	tooth lower		Frag.	height 26,5 m in mud flow	Buor Khaya
16	BKh2002 O-16	Equus caballus L.	Tibia		Comp.	Lena bank	Buor Khaya
17	BKh2002 O-17	Equus caballus L.	Tibia		Comp.	height 19-20 m from the frozen silt between two peat layers	Buor Khaya
18	BKh2002 O-18	Bison priscus	Mandibula	juv.	Frag.	Lena bank	Buor Khaya

No.	Sample No.	Taxon	Skeleton element	Notes	Preser-vation	Location	Locality
19	BKh2002 O-19	?	?	define	Frag.	height near 24 m from frozen peat	Buor-Khaya
20	BKh2002 O-20	Equus caballus L.	Femur		Comp.	height 19-20 m from the frozen silt between two peat layers	Buor Khaya
21	BKh2002 O-21	Mammuthus	Femur	tra-shed	Frag.		Buor Khaya
22	BKh2002 O-22	Equus caballus L.	Radius		Comp.		Buor Khaya
23	BKh2002 O-23	Rangifer tarandus (L.)	Tibia		Comp.		Buor Khaya
24	BKh2002 O-24	Ovibos sp.	vert. Thor.		Da-maged		Buor Khaya
30	BKh2002 O-30	Equus caballus L.	Ante-brachium		Comp.	Lena bank	Buor Khaya
31	AKh2002 O-1	Rangifer tarandus (L.)	Vertebrae cervic. (epi-stroph.+3)		Comp.	from Holocene terrace, in dry peat, height 6m, depth 1,5	Amerika Khaya
32	Sam2002 O-1	Rangifer tarandus (L.)	tibia		Frag.	Lena bank	Samoy-lov

Appendix 3-14. Species composition and distribution of zooplankton in the Lena Delta in summer 2002.

I - Samoilovskii Island: 1 – Olenekskaya channel, 2 - flood-plain lake, 3 – big thermokarst lake, 4 – polygons , 5 - crack between polygons.

II - Tit-Ary Island: 6 - terrace lake, 7 – big thermokarst lake, 8 - polygons

III - Buor-Khaya Island: 9 - polygons, 10 - alas

IV - America-Khaya Island: 11 - alas

Taxa	I					II			III		IV
	1	2	3	4	5	6	7	8	9	10	11
Rotatoria:											
Anuraeopsis fissa				+						+	
Asplanchna girodi?										+	
Asplanchna priodonta	+	+	+			+	+		+	+	
Bipalpus hudzoni	+	+				+	+			+	
Brachionus calyciflorus	+										
Brachionus diversicornis	+										
Brachionus quadridentatus	+					+					
Cephalodella gibba		+									
Collotheca sp.							+	+			
Colurella obtusa		+									
Colurella colurus		+									
Colurella uncinata										+	
Conochilus unicornis	+	+	+							+	+
Dicranophorus forcipatus		+					+				
Dicranophorus lutkeni										+	
Eosphora najas					+						
Euchlanis dapidula	+	+		+			+		+	+	
Euchlanis deflexa		+									
Euchlanis dilatata	+				+						
Euchlanis incisa										+	
Euchlanis lyra		+		+							
Euchlanis lucksiana	+	+		+	+	+	+		+		
Euchlanis myersi		+									
Euchlanis sp.							+				+
Filinia terminalis		+									
Filinia longiseta			+					+		+	
Keratella cochlearis	+	+	+	+		+	+		+	+	+
Keratella irregularis										+	
Keratella quadrata	+	+									
Keratella serrulata										+	
Keratella testudo		+									
Keratella sp.		+									
Kellicottia longispina	+	+	+			+	+		+	+	+
Lecane bulla							+			+	
Lecane brachydactyla										+	
Lecane cornuta										+	
Lecane luna						+	+				
Lecane lunaris		+			+	+	+				
Lecane sp.		+									
Lepadella ovalis		+					+				
Macrotrachella quadricornifera					+						

Appendix 3-14. continuation.

Taxa	I					II			III		IV
	1	2	3	4	5	6	7	8	9	10	11
Mytilina mucronata					+		+			+	
Mytilina ventralis		+						+			
Notholca acuminata	+	+	+	+	+		+	+	+		+
Notholca caudata	+	+			+	+	+			+	
Notholca squamula		+		+	+						
Polyarthra dolychoptera	+	+	+								
Polyarthra major	+	+							+		+
Polyarthra minor	+	+									
Testudinella patina		+									
Tretocephala ambiqua		+									
Trichocerca cylindrica	+			+							
Trichocerca brachyura	+										
Trichocerca elongata				+			+			+	
Trichocerca longiseta	+				+						
Trichotria pocillum		+		+		+				+	
Trichotria tetractis		+									
Trichotria truncata		+		+	+		+		+		
Synchaeta pectinata		+									
Synchaeta sp.	+	+	+				+			+	
Bdelloida	+	+	+	+	+		+		+	+	
Copepoda											
Cyclopoida:											
Acanthocyclops vernalis	+	+		+	+	+		+		+	
Acanthocyclops americanus		+			+	+					
Acanthocyclops capillatus						+					
Cyclops abyssorum		+		+				+			+
Cyclops kolensis	+		+								
Cyclops strenuus			+	+	+			+			
Cyclops vicinus			+								+
Diacyclops bicuspidatus	+		+	+	+			+			
Diacyclops bisetosus		+				+					
Diacyclops languidus				+				+			
Eucyclops serrulatus				+	+	+	+	+	+		
Megacyclops gigas								+			
Megacyclops viridis	+	+		+	+	+		+	+		
Mesocyclops leuckartii	+		+								
Calanoida:											
Arctodiaptomus acutilobatus				+							
Arctodiaptomus bacillifer	+										
Diaptomus glacialis				+							
Heterocope appendiculata	+	+				+					
Heterocope borealis				+	+			+	+		+
Eudiaptomus graciloides		+	+								
Eudiaptomus gracilis				+					+	+	
Eurytemora arctica					+						
Eurytemora bilobata		+				+				+	
Eurytemora gracilis		+				+					
Eurytemora sp.		+									

Appendix 3-14. continuation.

Taxa	I					II			III		IV
	1	2	3	4	5	6	7	8	9	10	11
Leptodiaptomus angustilobus				+	+			+	+		+
Limnocalanus johanseni		+									
Mixodiaptomus theeli				+	+			+	+		
Harpacticoida:											
Canthocamptus glacialis		+		+	+			+		+	
Mesochra sp.								+			
Cladocera:											
Alonopsis elongata	+	+		+	+			+	+		
Alonella sp.	+	+		+	+		+	+			
Bosmina longirostris	+	+				+				+	
Bosmina obtusirostris						+					
Bosminopsis deitersi	+	+									
Chydorus sphaericus	+	+	+	+	+	+	+	+	+	+	+
Daphnia cucullata	+					+				+	
Daphnia longiremis	+										
Daphnia pulex	+	+		+	+			+	+		
Eurycercus glacialis						+	+			+	
Polyphemus pediculus						+					
Pseudochydorus globosus					+						
Simocephalus serrulatus						+					
Phyllopoda											
Polyarthemia forcipata				+	+						
Artemiopsis bungei								+			

3.15 References

Abramova, E.N. (1996). Copepoda (Crustacea, Copepoda) of the Lena Delta Reserve. Hydrobiological investigations in natural reserves. Moscow, 8, 5-16. (in Russian).

Abramova, E.N., Sokolova, V.A. (1999). About findings and life cycle of Limnocalanus johanseni (Copepoda, Calanoida) in the Lena Delta. Zoologicheskii Zhurnal, 78, 11, 1360-1363. (in Russian).

AG Boden (1994): Bodenkundliche Kartieranleitung. 4th edition. Stuttgart. E. Schweizerbartsche Verlagsbuchhandlung. 392 p.

Akhmadeeva, I., Becker, H., Friedrich, K., Wagner, Pfeiffer, E.-M., D., Quass, W., Zhurbenko, M., Zöllner, E., Bojke, J., (1999). Modern processes in Permafrost Affected Soils. In: Rachold, V. and Grigoriev, M. (ed.) : Expeditions in Siberia 1998. Reports on Polar Research, 315: pp.19-21.

Akhmetshina, I., Abramova, E. (2002). Zooplankton abundance, biomass and production in the Lena Delta polygon lakes: preliminary results. Climate Driver of the North, Kiel, May 8-11, 20.

Aleksandrova, V. D. (1980): The Arctic and Antarctic: their division into geobotanical areas. Cambridge. University Press. 247 p.

Ammosov, Yu.N. (1961). Plankton of the tundra lake Raspadochnoe and its feeding importance for fishes and fry. Uchenye zapiski Yakutskogo universiteta, 2, 47-54. (in Russian).

Annual data on the regime and water quality of the seas and marine mouths of rivers, 1990-2001, part 2, Marine mouths of rivers, volume 5, Tiksi, 1991-2002.

Atlas of the Sardakh channel of 1949 // Sailing Directions. Tiksi Hydrographic Base.

Bening, A.L. (1942). About the Lena River plankton. Izvestiya Biol.-Geogr. NII pri Vostochno-Sib. Gos. Universitete, IX, 3-4, 217-230. (in Russian).

Bolshiyanov D.Yu., Tretiakov M.V. Investigation of Run off in the Sardakh-Trofimovsky Bifurcation Point of the Lena River Delta. Russian-German Cooperation SYSTEM LAPTEV SEA 2000: The Expedition LENA 2001, Reports on Polar and Marine Research, 426, 2002, pp.57-62

Botvinnik, E.F., N.V. Vershinin (1958). Some results of the Lower Lena River fishering expedition of 1957. Uchenye zapiski Yakutskogo universiteta, 4, 137-146. (in Russian).

Dereviagin A. Yu., Meyer H., Chizhov A. B., Hubberten H.-W., & Simonov E. F. (2000 (published 2002)). New data on the isotopic composition and evolution of modern ice wedges in the Laptev Sea Region. Polarforschung, 70, 27-35.

Elovskaya L.G. (1987): Classification and diagnostics of Yakutian permafrost soils. Yakutsk, 172 p. (in Russian).

FAO (Food and Agriculture Organization of the United nations) (1998): World Reference base for Soil Recourses. World Soil Recources Reports 84. Rom: FAO. 88 p.

French H. M. (1996). The Periglacial Environment, Longman Singapore Publishers, Singapore.

Grigoriev, M.N. (1993): Cryomorphogenesis of the Lena River mouth. Permafrost Institute Press Yakutsk 176 pp. (in Russian).

Grosse, G., Schirrmeister L., Krbetschek, M., Schwamborn, G, Oezen, D., Kunitsky, V., Kuznetsova, T., Kuzmina, S. (2002) New data on Late Quaternary terrestrial permafrost deposits of the Laptev Sea region by IR-OSL, radiocarbon and U/Th age determination. - In Terra Nostra (Climate drivers of the North, Program and Abstracts) pp. 47-47.

Gukov, A.Yu. (2001). Hydrobiology of the Lena River mouth region. M., Nauchnyi mir. 285 pp. (in Russian).

Ivanov, V.V., A.A. Piskun. Distribution of the River Water and Suspended Sediment Loads in the Deltas of Rivers in the Basin of the Laptev and East-Siberian Seas. In: H. Kassens, H.A. Bauch, I.A. Dmittrenko, H. Eicken, H.-W. Hubberten, M. Mellis, J. Thiede, L. A. Timokhov (eds.) Land-Ocean Systems in the Siberian Arctic: Dynamics and History. Springer-Verlag Berlin, 1999, p.239-250.

Kerer, E.F. (1968). Zooplankton of the flood plain lakes in the lower reaches of the Lena River. Uchenye zapiski Leningradskogo Gos. Ped. Instituta, 311, 1, 37-60. (in Russian).

Krbetschek, M.R., Gonser, G., Schwamborn, G., 2002. Luminescence dating results on sediment sequences of the Lena Delta. Polarforschung 70: pp. 83-88.

Kunitsky, V.V. (1989): Cryolithology of the lower Lena region. - Permafrost Institute Press, Yakutsk, 162 p. (In Russian).

Kuzmina, S., Korotyaev, B. (1987): New species of the pill beetle genus Morychus Er. (Coleoptera, Byrrhidae) from the North-West of USSR. Entomol. review, v. 66, N 2, pp. 342-344 (in Russian).

Kuznetsova, T., Kuzmina, S. (2001): Study area of the Eastern Olenyok-Channel – Kurungnakh Island (Buor Khaya), Paleontological study - In Rachold, V. and Grigoryev, M. N. (eds.): Russian-German Cooperation SYSTEM LAPTEV SEA 2000: The Expedition LENA 2000. Reports on Polar Research, 388: pp. 96-98.

Lungersgausen, G. F. (1961): Stratigraphy of Cenozoic deposits of the middle and lower Lena and Lena Delta. (In Russian).

Mackay J. R. (1993). Air temperature, snow cover, creep of frozen ground, and the time of ice-wedge cracking, western Arctic coast. Canadian Journal of Earth Sciences, 30, 1720-1729.

Manual for Hydrometeorological stations and posts. Issue 6, Part 1. Gidrometeoizdat. L., 1978.-384 p.

Meisch, C. (2000): Freshwater Ostracoda of Western and Central Europe. Springer Akademischer Verlag, Heidelberg Berlin, pp. 1-515.

Mostakhov, C.E. (1973). Lakes in the cryolithozone of the USSR. Ground waters of the cryolithozone. 2nd International Conference on Permafrost Studies. Yakutsk, vol. 5, 118-120. (in Russian).

Nikolaev V. I. & Mikhalev D. V. (1995). An oxygen-isotope paleothermometer from ice in Siberian permafrost. Quaternary Research, 43 (1), 14-21.

Nüchterlein, H. (1969): Süßwasserostracoden aus Franken. Ein Beitrag zur Systematik und Ökologie der Ostracoden. In: Int. Revue ges. Hydrobiol. 54/1: pp. 223-287.

Pavlova, E., Dorozhkina, M. (2000): Geological-geomorphological studies in the western and central part of the Lena Delta - In Rachold, V. and Grigoriev, M. N. (eds.): Russian-German Cupertino SYSTEM LAPTEV SEA 2000: The Expedition LENA 1999. Reports on Polar Research, 354: pp. 75-90.

Pfeiffer, E.-M., Akhmadeeva, I., Becker, H., Friedrich, K., Wagner, D., Quass, W., Zhurbenko, M., Zöllner, E., Boike, J. (1999): Modern Processes in Permafrost Affected Soils. In: Rachold V. and M.N. Grigoriev (ed.) Expeditions in Siberia 1998. Reports on Polar Research 315. pp 19-80

Pfeiffer, E.-M., Wagner D., Kobabe, S., Kutzbach L., Kurchatova A., Stof, G., Wille, C. (2002): Modern processes in permafrost affected soils.- In Pfeiffer, E.-M., and Grigoryev, M. N. (eds.): Russian-German Cooperation SYSTEM LAPTEV SEA 2000: The Expedition LENA 2001. Reports on Polar Research, 426: pp. 21-41.

Pirozhnikov, P.L. (1958). About the area of distribution and ecology of copepoda Senecella calanoides Juday. Zoologicheskii Zhurnal, 37, 4, 625-629. (in Russian).

Pirozhnikov, P.L., Shulga, E.L. (1957). The main characterishes of zooplankton from the Lower Lena River. Trudy Vsesoyuznogo gidrobiologicheskogo obshestva, 8, 219-230. (in Russian).

Polunin, N. (1959): Circumpolar Arctic Flora.Oxford. University Press. 514 p.

Post, W.M., Emanuel, W.R., Zinke, P.J., Stangenberger, A.G. (1982): Soil carbon pools and world life zones. Nature 298, 156-159.

Report on the hydrological studies in the Lena delta. 1985 // Report. TTUGMiKPS, Hydrographic party, Head – P.V. Seleznev. Tiksi, 1986, 88 p.

Rylov, V.M. (1928). Materials on the fauna of freshwater copepods (Copepoda, Calanoida) of the Northern Siberia. Trudy komissii po izucheniyu Yakutskoi ASSR, 11, 1-32. (in Russian).

Schirrmeister, L., Kunitsky, V., Grosse, G., Kuznetsova, T. (2001): Kurungnakh Island (Buor Khaya), Geological-cryological survey - In Rachold, V. and Grigoryev, M. N. (eds.): Russian-German Cooperation SYSTEM LAPTEV SEA 2000: The Expedition LENA 2000. Reports on Polar Research, 388: pp. 94-96.

Schirrmeister, L. , Kunitsky, V. , Grosse, G. , Schwamborn, G. , Andreev, A.A., Meyer, H., Kuznetsova T., Bobrov, A., Oezen, D. (submitted): Late Quaternary history of the accumulation plain north of the Chekanovsky Ridge (North East Yakutia).- Polar Geography.-

Schlesinger ME, Mitchell JFB (1987): Climate model simulations of the equilibrium climatic response to increased carbon dioxide. Rev Geophys 25: 760-798.

Schwamborn, G, Schneider, W., Grigoryev, M., Rachold, V., Antonow, M. (1999): Sedimentation and environmental history of the Lena Delta. - In Rachold, V. and Grigoryev, M. N. (eds.): Russian-German Cooperation SYSTEM LAPTEV SEA 2000: The Lena Delta 1998 Expedition. Reports on Polar Research, 315: pp. 94-111.

Schwamborn, G., Andreev, A.A., Rachold, V., Hubberten, H.-W., Grigoriev, M.N., Tumskoy, V., Pavlova, E.Yu., Dorozhkina, M. V., 2002. Late Quaternary sedimentation history of the Lena Delta. Quaternary International, 89: 119-134.

Serkina, R.A. (1969). Plankton and benthos of the Lena Delta and adjacent coastal waters. Trudy Yakutskogo otdeleniya Sibirskogo NII rybnogo khozyaistva, Yakutsk, 3: 188-196. (in Russian).

Siegert, C., Schirrmeister, L, Kunitsky, V, Tumskoy, V., Derevyagin, A., Meyer, H., Kuznetsova, T., Kuzmina, S., Sher, A, Syromyatnikov I, (1999): Paleoclimate Signals of ice-rich permafrost. - In Rachold, V. and Grigoryev, M. N. (eds.): Russian-German Cooperation SYSTEM LAPTEV SEA 2000: The Lena Delta 1998 Expedition. Reports on Polar Research, 315: pp. 145-259.

Sher, A, Kuzmina, S., Lisitsyna, O., Parmuzin, I., Demmyankov, S. (2002): Paleoecological and permafrost studies of Ice Complex in the Laptev Sea area (Bykovsky Peninsula) - In Pfeiffer, E.-M., and Grigoryev, M. N. (eds.): Russian-German Cooperation SYSTEM LAPTEV SEA 2000: The Expedition LENA 2001. Reports on Polar Research, 426: pp. 94-107.

Sher, A, Parmuzin, I., Bortsov, A. (2000): Ice Complex on Bykovsky Peninsula. - In Rachold, V. and Grigoryev, M. N. (eds.): Russian-German Cooperation SYSTEM LAPTEV SEA 2000: The Expedition LENA 1999. Reports on Polar Research, 354: pp. 169-182.

Soil Survey Staff (1998): Keys to Soil Taxonomy. 8th edition. Lincoln, Nebraska: USDA-The National Recources Conservation Sevice. 599 p.

Sokolova, V.A. (1984). Composition of zooplankton in the Lower Lena River. Byulleten' nauchno-tekhnicheskoi informatsii, Yakutsk, 16-19. (in Russian).

Stepanova, L.A., Abramova, E.N. (1997). Historical-faunistic analysis of copepoda from the Lena Delta Reserve. Abstracts of the Conference "Facvtors of taxonomic and biochorological diversity". St.Petersburg, 77. (in Russian).

Urban, V.V. (1949). Hydrobiologycal investigations in the Lena Delta. Izvestiya VNIORKH. Leningrad, Volum 29. 75-95. (in Russian).

Van Everdingen, R.O. (ed.)(1998): Multi-Language Glossary of Permafrost and Related Ground-Ice Terms. International Permafrost Association, p. 31 (definitions).

Vasil'chuk Yu. K. (1992). Oxygen isotope composition of ground ice. - Application to paleogeocryological reconstructions, Moscow, Russia. pp. 420.

Viehberg, F. (2000): Faunistische und ökologische Untersuchungen zur Ostracodenfauna ausgewählter Kleingewässer der Stadt Greifswald (diploma thesis). University of Greifswald. pp. 1-141.

Vtyurin, B. I. (1956): About some geomorphological terms in geogeokryology (O nekotorykh geomorfologicheskikh terminakh v geokriologii). In: Meyster, L.A. (ed.) Materials of basic knowledge about permafrost zones of the Earth crust (Materialy k osnovam ucheniya o merzlykh zonakh zemnoy kory), Academy of Science USSR, Moscow, pp 126-134 (In Russian).

Wagner, D., Kutzbach, L., Becker, H., Vlasenko, A. and Pfeiffer, E.-M. (2000): Seasonal variability of trace gas emission (CH4, CO2) and in situ process studies In: Rachold V. and M.N. Grigoriev (ed.) The Expeditions Lena 1999. Reports on Polar Research 354. pp 28-36.

Zhang T, Barry RG, Knowles K, Heginbotton JA, Brown J (1999): Statistics and characteristics of permafrost and ground-ice distribution in the northern hemisphere. Polar Geography 23, 2:132-154.